The Production of Non-Methane Hydrocarbons by Marine Plankton

Stephanie Lyn Shaw

Center for Global Change Science
Department of Earth, Atmospheric and Planetary Sciences
MIT, Cambridge, MA 02139-4307 USA

Report No. 66
September 2001

The Earth's unique environment for life is determined by an interactive system comprising the atmosphere, ocean, land, and the living organisms themselves. Scientists studying the Earth have long known that this system is not static but changing. As scientific understanding of causal mechanisms for environmental change has improved in recent years there has been a concomitant growth in public awareness of the susceptibility of the present environment to significant regional and global change. Such change has occurred in the past, as exemplified by the ice ages, and is predicted to occur over the next century due to the continued rise in the atmospheric concentrations of carbon dioxide and other greenhouse gases.

The *Center for Global Change Science* at MIT was established to address long-standing scientific problems that impede our ability to accurately predict changes in the global environment. The Center is interdisciplinary and involves both research and education.

This report is one of a series of reports and preprints from the Center intended to communicate new results or provide useful reviews and commentaries on the subject of global change. See the inside back cover of this report for a complete list of the titles in this series.

Ronald G. Prinn, *Director*
Rafael L. Bras, *Associate Director*
MIT Center for Global Change Science

For more information contact the Center office.

LOCATION:
Center for Global Change Science
Massachusetts Institute of Technology
Building 54, Room 1312
77 Massachusetts Avenue
Cambridge, MA 02139-4307 USA

ACCESS:
Tel: (617) 253-4902
Fax: (617) 253-0354
E-mail: cgcs@mit.edu
World Wide Web: http://web.mit.edu/cgcs/

Printed on recycled paper

The Production of Non-Methane Hydrocarbons by Marine Plankton

by

Stephanie Lyn Shaw

B.S. Chemical Engineering
Massachusetts Institute of Technology, 1995

Submitted to the Department of Earth, Atmospheric, and Planetary Sciences
in partial fulfillment of the requirements for the degree of

Doctor of Philosophy in Atmospheric Chemistry
at the
MASSACHUSETTS INSTITUTE OF TECHNOLOGY

September, 2001

Author.....
Department of Earth, Atmospheric, and Planetary Sciences
July 27, 2001

Certified by.....
Ronald G. Prinn
TEPCO Professor of Atmospheric Chemistry
Thesis Supervisor

Accepted by.....
Ronald G. Prinn
Head, Department of Earth, Atmospheric, and Planetary Sciences

The Production of Non-Methane Hydrocarbons by Marine Plankton

by

Stephanie Lyn Shaw

Submitted to the Department of Earth, Atmospheric, and
Planetary Sciences on July 27, 2001 in partial fulfillment
of the requirements for the Degree of Doctor of Philosophy in
Atmospheric Chemistry

ABSTRACT

The oceans are a small source of non-methane hydrocarbons (NMHC), a suite of volatile organics whose chemical destruction mechanism by reaction with hydroxyl radical can significantly affect the oxidation capacity of the atmosphere. Little is known about the water column cycling processes that constrain this source; previous work has established a photochemical source for many alkenes, and a phytoplanktonic source for isoprene. The focus of this thesis was to gain further insight on marine microbiological cycling of NMHC. This included investigations on two main themes. The first was the effect of different physiological conditions on phytoplanktonic isoprene production. A variety of phytoplankton were examined for the ability to produce isoprene. All were found to have constant isoprene production rates per cell during exponential growth, with decreasing rates as the populations senesced. A positive allometric relationship between isoprene production rate and cell volume was found; highest production rates were found for the largest cell tested, *Emiliania huxleyi*, and lowest rates for *Prochlorococcus*, the smallest. Isoprene production in *Prochlorococcus* was found to be a function of light intensity and temperature, with patterns similar to the relationships between growth rate of this species and these environmental parameters. The second theme investigated was the effect that heterotrophic marine plankton might have on NMHC cycling. We detected no clear production or consumption of any NMHC, except isoprene, from any of the phytoplankton or other organisms tested. The heterotrophic bacteria examined had no detectable effect on

isoprene production per *Prochlorococcus* cell in a dual-species culture, but a temporary production of isoprene was detected from bacterial cultures grown in organically-enriched media. Nanoflagellate grazing by *Cafeteria roenbergensis* on *Prochlorococcus* had no detectable effect on NMHC cycling except to control the total phytoplankton counts, and thus total isoprene production. Besides controlling phytoplankton counts, phage lysis of *Prochlorococcus* had no detectable effect on NMHC cycling except to decrease isoprene production per *Prochlorococcus* cell during the latent period of infection. Any other effect these particular organisms may have on NMHC cycling likely involves other processes, such as photochemistry.

Thesis Supervisor:	Ronald G. Prinn
Title:	Head, Department of Earth, Atmospheric, and Planetary Sciences
	TEPCO Professor of Atmospheric Chemistry

ACKNOWLEDGEMENTS

I owe a sincere thank you to my advisors, Ron Prinn and Penny Chisholm, for their part in this thesis. Ron gave me the encouragement to pursue a research interest somewhat outside of the mainstream, and the support and resources to achieve it. Thank you for the independence you afforded me, for freely giving of your time, and for great group meeting dinners! Penny was instrumental during the last several years - her guidance and constructive criticism were just what I needed, at just the right time. You were right, I learned a lot! I've also gained a greater appreciation for the importance and individuality of those tiny 'bugs' in the ocean. Overall I feel very lucky to have experienced two very different research styles and perspectives on science… thank you both for your patience with the iterations in communication!

I would also like to thank my other committee members - John Dacey, Mario Molina, and Glenn Flierl - for their time and insightful comments over the last 6 years. They have allowed this work to change and grow as I moved further into a new field, realizing the complexities inherent in biological research. I'm grateful for the opportunities I've had with each of you, from interesting discussions to T.A. opportunities.

John Graham and Gary Kleiman in the Prinn lab taught me most of what I know about laboratory atmospheric chemistry – thanks for putting up with my unending questions (even after you both left the lab!). The UROP students I've worked with - Karla Maguire, Brad Olsen, Cynthia Randles, Amalia Londono, and David Hsu - helped me carry out that knowledge day-to-day during my experiments. Without you all, I would have been lost. Other Prinn lab members – Jin Huang, Yuhan Chen, Don Lucas, Donnan Steele, Arnico Panday, Chien Wang, and Monika Mayer – graciously shared their perspectives and company over the years. Chisholm lab members – particularly Lisa Moore, Gabrielle Rocap, Liz Mann, and Matt Sullivan - put up with my attempts to prove I know a little

something about phytoplankton… with your help I learned more about the microbial food web than I ever would have in a classroom.

I can't forget the support staff who made my time here infinitely easier - Linda Kubrick, Mark Pendleton, Anne Slinn, Fran Goldstein, Rosemary Hanlon, Charlotte Peed, and Leontyne Bynoe. Thanks also to Sheila Frankel for sharing her instrumentation (and life!) wisdom. My dancing friends also made my years here much more enjoyable by providing a great outlet for thesis stress, and just having a great time. Without the… antics… of several Molina lab members, namely Geoff Smith and Keith Broekhuizen, the day-to-day would have been terribly boring. Thanks for your friendship, and the occasional cup of coffee.

I owe deep thanks to all my family and friends (who always knew just when to call) for their unwavering support through these past six years. Without my parents' love, continual support, and overwhelming belief in my ability, I never would have made it through to the end. (I'm no longer a student anymore, I swear!)

No one can get through as difficult an experience as a PhD alone. One needs constant affirmation, a shoulder to lean on, and someone to cook for you every once in a while. Simanta, I am indebted to you for your faith in me, your encouragement, your open and willing ear, and your determination to help me achieve my goal. This thesis is as much yours as it is mine.

The work for this thesis was supported by NASA, NSF, and the MIT Kerr Graduate Fellowship. Additional funding was supplied by the PAOC Houghton Fund and the TEPCO Research Fund.

TABLE OF CONTENTS

CHAPTER ONE

MARINE ORGANISMS AND TRACE GAS PRODUCTION

1.1 TRACE GASES IN THE OCEAN

The ocean surface layer and boundary layer troposphere are inextricably linked through the energy, momentum, and chemical exchanges that occur across their boundary. Net transfer of carbon dioxide into the global oceans results in a huge storage in the deep waters, which acts as a buffer on the increasing anthropogenic carbon emissions. This carbon is then available for biological use in the surface waters before transformation and storage in the deep waters and ocean sediments. Methane and nitrous oxide are also exchanged across the sea-air interface, and dust can be deposited and contribute phytoplanktonic nutrients to the water column. Other trace gases such as dimethylsulfide (DMS), halocarbons, and hydrocarbons are also exchanged across the ocean surface. All of these exchanged chemicals can influence the composition and reactivity of the atmosphere in very different ways. As a result, an understanding of the sources, sinks, and transformation of these chemicals is necessary to fully describe the atmospheric system.

1.1.1 Dimethylsulfide

Take dimethylsulfide (DMS) as one example: it is oxidized by hydroxyl radical (OH) to sulfur dioxide (SO_2) and other species in the marine atmosphere, which can then convert to sulfuric and methanesulfonic acids and form aerosol particles. These aerosols can act to scatter light and reflect incoming solar radiation back to space (Pandis et al., 1994), or as cloud condensation nuclei (Ayers et al., 1997), and are thought to result in a cooling effect on climate. Approximately 15-25 Tg of sulfur in DMS is estimated to be emitted from the global oceans each year (Seinfeld & Pandis, 1998). It is the largest biogenic source of sulfur

to the atmosphere and is derived from biological degradation of biologically-produced dimethylsulfoniopropionate (DMSP) (Keller et al., 1989).

Phytoplankton in the oceans produce DMSP, which may be a cellular osmoregulatory compound (Keller & Korjeff-Bellows, 1996). Its formation is physiologically dependent upon environmental factors such as light, temperature, salinity, and nutrient availability (Keller & Korjeff-Bellows, 1996), but the primary release mechanism is through cellular lysis. Once in the water column, DMSP is converted to DMS by a lyase that is primarily produced by heterotrophic bacteria (Kiene & Bates, 1990). Some grazers/protozoa and a few algae (Wolfe & Steinke, 1996; Stefels and Van Boekel, 1993) have also been shown to contain this lyase, and a few phytoplankton species directly emit DMS to the water column.

The main loss of DMS is uptake by bacteria (Kiene and Bates, 1990), a portion is photooxidized to DMSO in the water column (Brimblecombe and Shooter, 1986), and a portion is lost to the atmosphere. Any action that can put DMSP and its lyase in proximity to react, such as grazing (Dacey & Wakeham, 1986) or phage lysis (Malin et al., 1998), will enhance DMS production, and most likely emission to the atmosphere assuming constant winds and temperatures. It is therefore quite a spatially and temporally heterogeneous process. Such complicated cycling patterns mean there are no clear, systematic relationships of DMS with environmental parameters that can be used for integrated global climate modeling.

1.1.2 Halocarbons

The situation is similar for halocarbons - chemicals with a hydrocarbon backbone and one or more halogen atoms. The ocean has in the past been thought to be a significant source of many halocarbons, although the methyl halide budgets are currently under revision (Butler 2000). Other sources include terrestrial fungi and estuary plants (Wever et al., 1993; Saini et al., 1995). While iodine-containing halocarbons are photolyzed in the troposphere and interact with the photo-oxidant cycle (Solomon 1994), chloride- and bromide-containing halocarbons have long enough lifetimes to reach the stratosphere. There they are

photolytically destroyed to produce halide free radicals, which can then participate in ozone destruction through the following, or similar, mechanisms.

$$Cl + O_3 = ClO + O_2$$
$$ClO + O = Cl + O_2$$
$$\text{sum: } O + O_3 = 2\ O_2$$

Macroalgae (Manley & Dastoor, 1987, Gschwend et al., 1985), ice algae and other phytoplankton (Scarratt & Moore, 1996, 1998; Saemundsdottir & Matrai 1998, Tokarczyk & Moore 1994), have been shown to form both poly- and mono-halocarbons. The first through peroxidases (Moore et al., 1996; Wever et al., 1993), and the second through an s-adenosyl methionine transfer mechanism (Wuosmaa & Hager, 1990). These occur primarily in the stationary growth phase, and are also physiologically dependent on light, temperature, nutrients, and species. Production of halocarbons may be a form of oxidative stress relief (Mtolera, et al. 1996), a chemical defense mechanism again grazing organisms, or have other uses. It has been shown that some of these chemicals, such as methyl iodide, can also be produced photochemically (Moore and Zafiriou 1994). Potential loss processes in the water column include halide substitution and hydrolysis (Elliot & Rowland, 1995), photolysis (Zafiriou et al., 1984) as well as biological processes (King & Saltzman 1997, Goodwin et al., 1998) and loss to the atmosphere. But overall much less is known for the halocarbons than for DMS.

These complicated formation and transformation pathways involving biology and chemistry are interesting because what begins as a small scale process becomes effective on a large scale. Interest in this concept, as well as a realization that so little was known of the oceanic cycling of hydrocarbons, led to a hypothesis that similar processes may occur for these gases.

1.1.3 Non-Methane Hydrocarbons

The class of chemicals entitled non-methane hydrocarbons (NMHCs) is a loose grouping of both natural and anthropogenic alkyl and aromatic species, typically of low molecular weight (C_1 - C_{10}), and occurring in the gaseous phase. Methane is not included with the other carbonaceous species due to its large emissions, low reactivity (especially with OH), and important radiative role. NMHCs are considered trace gas species because their mole fractions are generally at parts per billion (ppb) levels (in gaseous dry mole fraction units), except in polluted urban areas. They are short-lived because of their strong tendency to become oxidized in the lower troposphere by OH and O_3.

OH is an extremely reactive oxidant, with a lifetime of only seconds at maximum. It drives the daytime atmospheric photochemistry in both polluted and clean atmospheres. OH is primarily removed by CO and CH_4 (~60 - 70 %), but organics such as NMHC, written below as RH, can account for significant portions as well.

$$OH + CO \rightarrow HO_2 + CO_2$$
$$OH + CH_4 \rightarrow CH_3 + H_2O$$

$$OH + RH \rightarrow R + H_2O$$
$$CH_3 \text{ (or other R)} + O_2 + M \rightarrow RO_2$$

In atmospheric regions where nitrogen oxide (NO_X) concentrations are quite low, a combination of radical-radical reactions ensues. The result is peroxide formation and net ozone destruction.

$$HO_2 + HO_2 \rightarrow H_2O_2 + O_2$$
$$RO_2 + HO_2 \rightarrow RO_2H + O_2$$
$$HO_2 + O_3 \rightarrow OH + 2O_2$$

If NO_X concentrations are above the 10-50 parts per trillion (ppt) range, the above reactions are overwhelmed by radical-NO cycling. The oxidation of NO to NO_2 provides for

photolysis of NO_2 which forms $O(^3P)$. This species adds to O_2 to form O_3 . Photolysis of NO_2 is also an ozone source, resulting in a net photochemical ozone production.

$$RO_2 + NO = RO + NO_2$$
$$NO_2 + h\nu \ (< 420\ nm) \rightarrow NO + O(^3)P$$
$$O(^3)P + O_2 \rightarrow O_3$$

Additional loss of NMHC can occur to ozone, nitrate radical (NO_3) during nighttime, or to chlorine free radicals in the marine boundary layer (Keene et al., 1996). Tropospheric chemistry modeling studies have shown that including NMHC chemistry can account for up to a 40-60% increase in CO production, a doubling of net O_3 photoproduction (20-30% increase in the remote atmosphere), and a net decrease in OH (10-20% over both oceans and continents) as compared to excluding NMHC chemistry (Poisson et al. 2000). Some fundamental properties of common NMHC are given in Table 1.

The atmosphere acts as a primary reservoir for NMHCs, but the sources are various: terrestrial biota, combustion, biomass burning, other anthropogenic sources, and the oceans all contribute. Table 2, modified from Singh & Zimmerman (1992), presents the global emissions of NMHC by source. The sources are subdivided into formation processes which indicate that the natural isoprene/terpene source is the most abundant. It also indicates that the oceanic source of light hydrocarbons is rather small compared to the other categories. At best, only approximately 1% of the total annual emissions are due to oceanic light NMHC. However it is their strong reactivity with OH (lifetimes on the order of hours to days) that secures their importance. If NMHC are destroyed more quickly than the time scale for long range transport out from or into continental regions, light NMHC of oceanic origin may be relevant in remote marine boundary layer photochemistry as the only significant hydrocarbon source there. (Plass-Dulmer et al., 1995; Donahue & Prinn, 1990).

Table 1: Physical/Chemical Data for Selected NMHC

	HENRY'S CONSTANT	**T_{BOIL} (°C)**	**T_{MELT} (°C)**	**$(K_{OH})^*$ 10^{-12}**	**(K_{OZONE}) $*10^{-17}$**	**LIFETIME (DAYS)**
ethane	20.4	-88.6	-182.8	0.27		30.6
ethene	8.8	-103.7	-169.2	8.52	0.18	0.9
propane	28.9	-42	-187.7	1.15		7.2
propene	8.6	-47.7	-185.3	26.8	1.13	0.3
cyclopropane	3.5	-32.8	-127.4	0.08		103.3
2-me-propane	48.5	-11.7	-159.6	2.34		3.5
n-butane	38.7	-0.495	-138.4	2.54		3.3
t-2-butene	~7.8	0.88	-105.6	64	20	0.1
1-butene	10.3	-6.2	-185.4	31.4	1	0.3
2-me-propene	8.7	-6.9	-140.4	51.4	1.2	0.2
c-2-butene	~5.8	3.72	-138.9	56.4	13	0.1
cyclopentane						
2-me-butane	48.4					
pentane	50.4					
isoprene	7.3	34.1	-146	92.6		0.1
hexane	69.1					
1-hexene	418	63.5	-139.8	37.5		0.2
3-me-hexane	98.7					
benzene	5.5	80.1	5.5	1.2		6.9
toluene		110.6	-95			

Reaction rates with OH and O_3 given as cm^3 $molecule^{-1}$ sec^{-1} at 298 K from Atkinson (1989), and Atkinson and Carter (1984). Henry's Law constants are non-dimensionalized air/water ratios and are from MacKay & Shiu (1981), Donahue & Prinn (1990), and Sander (1996). Note that isoprene + OH is a diffusion-controlled reaction (requires rates ~ 10^{10} cm^3 $molecule^{-1}$ sec^{-1}) (Finlayson-Pitts & Pitts, 2000)) at typical tropospheric temperatures and pressures.

Using a detailed photochemical model and published observations from Pacific marine boundary layer, equatorial Atlantic, and STRATOZ missions, Donahue & Prinn (1990) found that NMHC could be responsible for anywhere from a majority (30%) to a minority (10%), but still important, amount of OH loss in the remote marine atmosphere. They noted that there was a disparity between the ocean and atmospheric observations (ocean concentrations measured were too low to explain atmospheric concentrations), but not all

Table 2: NMHC Emission Estimates *(From Singh & Zimmerman (1992))*

SOURCE TYPE	**U.S. 1988 ($Tg\ yr^{-1}$)**	**WORLD ($Tg\ yr^{-1}$)**
ANTHROPOGENIC		
Transportation	6.1	22
Stationary source combustion	0.9	4
Industrial process (incl. Natural gas production)	8.5	17
Forest fires/incineration	1.4	45
Organic solvents	2.4	15
Subtotal	*19.3*	*103*
NATURAL		
Oceans		
Light hydrocarbons	-	5-10
C_9-C_{28} n-alkanes	-	1-26
Dimethyl Sulfide (for comparison)	-	20-40
Microbial production	1	6
Isoprene	7-20	350-450
Terpenes/ other biogenics	25-50	480
Subtotal	*33-71*	*862-1012*
TOTAL EMISSIONS	52-90	965-1115

measurements were concurrent. Those oceanic and atmospheric measurements that were concurrent matched their expected concentration ratios based on their Henry's Law constants (Table 1) fairly well. Model calculations were also performed on SAGA field measurements during 1990 in the equatorial Pacific (Donahue & Prinn 1993). These confirm that primary NMHC loss alone, as opposed to any reaction of OH with hydrocarbon oxidation products, can be important. NMHC reactions accounted for 10% of OH removal during baseline conditions, with occasional larger spikes to 20% or higher. With a photochemical model/field measurement study, Carslaw et al. (1999) also estimated that about 10% of the OH loss in the clean marine troposphere near Mace Head, Ireland was due to NMHC chemistry, with the balance being 53% CO, 21% CH_4, 6% NO_x, 4% O_3, and 6% H_2. The ACE I campaign in 1999 included a Pacific transect and focused on the area near

Tasmania and New Zealand. It was found that NMHC reported by Pszenny et al. (1999) accounted only for a negligible removal of OH (generally ~ 1% or less). However, the suite of 9 compounds did not include ethane, ethene, propene, or isoprene - the primary NMHCs expected to contribute to OH loss (Plass-Dulmer et al., 1995) This emphasizes the likely importance of the lightest NMHC to photooxidant processes as compared to the larger molecular weight compounds, probably due to their typically higher oceanic flux. However, Lewis et al. (2001) also determined the impact of oceanic alkenes on local OH concentrations at Cape Grim, Tasmania, and found them to be negligible, only responsible for about 1 - 1.5% of the total OH loss. Additionally, isoprene in particular may be a significant source of formaldehyde in clean marine air (Ayers et al., 1997).

Another reason the oceanic NMHC source is interesting is the possible parallel to biogenic emissions from terrestrial vegetation. Production rates of many NMHC have been measured from leaves, individual trees, and forests (Fehsenfeld et al., 1992). Of particular interest are isoprene and ethene. Vegetative emission of the former is the largest global source of any single NMHC. The enzymatic production mechanisms of isoprene are fairly well understood (Fall & Wildermuth 1998), and the short term environmental controls such as light, nutrient, and temperature dependence have been well-established by many researchers. However, despite two decades of dedicated research, many other aspects of isoprene formation are still unknown. Particularly, why do plants lose a non-trivial amount of their fixed carbon to this chemical? Several hypotheses, such as thermoregulation (Singsass et al., 1997), oxidative stress (Harley et al., 1999), release of excess reductive power (Fall, 1991), or defense are yet unproven. Perhaps an examination of NMHC production from other photosynthetic organisms may help our understanding of isoprene's functionality. This work may also provide additional data points for examining the phylogenetic relationships between isoprene-producers, as was begun by Harley et al (1999). Different species can produce isoprene at very different rates, ranging over several orders of magnitude. It would be reasonable to expect the same effect holds for various species of marine plants. Another interesting biogenic NMHC is ethene, a growth hormone which can hasten both growth and senescence (Abeles, 1973). A variety of stresses, such as

mechanical, thermal, insect-induced, and drought can lead to its formation (Yang & Pratt, 1978). Many molds and bacteria, soil and pathogenic, are also ethene producers (Fukuda et al., 1993). Perhaps comparative work between the terrestrial and marine photosynthates can lead to a better understanding to the physiology of ethene production as well.

Finally, it's important to understand the quantitative dependence of NMHC production and emission on environmental variables. Take as an example the case of terrestrial organic hydrocarbons: Isoprene and monoterpene production and emission depend strongly on temperature. As the troposphere warms due to greenhouse gas accumulation and other changes, hydrocarbon emissions may dramatically increase (Fuentes et al., 2001). Increased anthropogenic nutrient deposition observed in many areas could also serve to increase hydrocarbon emission through potential plant productivity increases. Similar dependencies may exist in phytoplanktonic hydrocarbon production. As oceanic primary production accounts for approximately half of global productivity (Falkowski & Raven, 1997), these effects could be significant on a global scale.

1.2 OCEANIC EMISSION OF NMHC

1.2.1 Seawater Measurements

Evidence for a marine source of NMHC was first presented by Swinnerton & Linnenbon (1967) and Swinnerton & Lamontagne (1974) who measured dissolved C_2 and C_3 species in the tropical oceans and found significant supersaturation as compared to equivalent atmospheric concentrations. Many others later confirmed the oceanic source of reactive NMHC, including Rudolph & Ehhalt (1981) in the Atlantic, Singh & Salas (1982), Greenberg & Zimmerman (1984), Bonsang et al. (1988) with the first simultaneous air and water measurements, Donahue & Prinn (1993), Plass-Dulmer et al. (1995), and Broadgate et al. (1997).

A large range of global sea-to-air fluxes has been estimated, from 5-50 Mtons $year^{-1}$ (Guenther et al., 1995; Bonsang et al., 1988; Ratte et al., 1998), with approximately 90% of the variability within 1 order of magnitude (Plass-Dulmer et al., 1995). A database of over 1000 C_2-C_4 NMHC measurements from about 40 field campaigns shows average extrapolated global emissions of about 2 Tg $year^{-1}$, with about 85% due to alkene species, and 40% due to ethene alone (Plass-Dulmer et al., 1995). Highest emissions for the lowest molecular weight compounds were found in this compiled database, and are usually found during individual measurement campaigns as well. Seawater concentrations average between 10-200 pmol L^{-1} for C_2-C_4 chemicals, with ethane at about 60 pmol L^{-1} and ethene at about 134 pmol L^{-1} (Plass-Dulmer et al., 1995).

The geographical distribution of available seawater concentration measurements is quite biased. There is fairly even coverage in the Atlantic from 60 °N to 30 °S, and heavy coverage in the Gulf of Mexico and Caribbean. The eastern Pacific (Pszenny et al., 1999; Yokouchi et al., 1999) and Southern Ocean (Broadgate et al., 1997) have been sampled only recently. The compilation of 40 datasets shows no clear trend with latitude for alkanes or alkenes, and there are not enough data to get a reliable picture for longitude (Plass-Dulmer et al, 1995). There do not appear to be any systematically enhanced emission rates near the equator for ethane and ethene from the 6 relevant datasets in the compilation (Plass-Dulmer et al., 1995), although some individual campaigns did find higher NMHC in the Northern Hemisphere than the Southern Hemisphere (Plass et al., 1992). Virtually nothing is known of coastal versus open ocean NMHC concentrations, although air and water measurements in Boston Harbor, MA, USA and several freshwater lakes in the area during spring of 1995 also show a supersaturation in the water for approximately 15 NMHCs (Shaw, data available by contacting the author).

In regards to a seasonality, Plass-Dulmer et al. (1995) had available only three datasets taken in the same geographical region that span a three month period. Surface water ethene concentrations were higher in summer as compared to spring in the east Atlantic and Gulf of Mexico. Broadgate et al. (1997) showed a distinct seasonal cycle in nearshore water NMHC

concentrations in the North Sea. Ethane, ethene, propane, propene, and isoprene, among others, were almost always supersaturated, and varied over 2 orders of magnitude with maxima in June and July. A notable exception is isoprene's peak in May, concurrent with the spring phytoplankton bloom in that region.

Diurnal cycles of NMHC have also been observed in air parcels backtracked to remote origins. Lewis et al. (1999) observed clear patterns for isoprene, ethene, propene, 1-butene, and 2-methyl-propene at Mace Head, Ireland with maxima around solar noon. Similar measurements at Cape Grim, Tasmania (Lewis et al., 2001) also show midday maxima for ethene, propene, and isoprene, although the profile shapes differed. Isoprene concentrations had a much sharper peak at midday, dropping below detection limit at night. Other alkenes had broader daytime peaks, and dropped at night, but to still detectable levels. In comparison, in terrestrial forest atmospheres the isoprene diurnal cycle peaks in mid afternoon, at about 2-4 p.m. Note these measurements would be influenced by any net sources from the local environments, as well as any chemical processes occurring during air parcel movements.

The few water column depth profiles available (Bonsang et al., 1988; Milne et al., 1995) show NMHC subsurface concentration maxima in the upper 150 m; this may be due to water column production processes occurring faster than physical mixing. The only known loss at the present time is transfer to the atmosphere (Plass-Dulmer et al., 1995; Ratte et al., 1995), but only slight anti-correlations of NMHC concentrations to transfer velocity and wind speed have been found (Plass-Dulmer et al., 1995; Pszenny et al., 1999). Reimer et al. (2000) estimated lifetimes of NMHC due to a variety of losses: air-sea exchange, microbial consumption, aqueous chemistry, and physical mixing/dilution. The primary loss mechanism in this calculation was air-sea exchange, which has a time constant of 5-20 days.

In summary, based on all the published studies, the temporal and spatial variations in seawater NMHC concentrations and sea-to-air fluxes are quite large, emphasizing the importance of local and heterogeneous cycling processes.

1.2.2 Possible Sources

Despite the lack of synthesis of global seawater NMHC measurements, interesting results have been found on smaller time and space scales, in regions that may be termed more homogeneous. These often take the form of correlations between NMHC and environmental variables, and have lead to two major hypothesis for oceanic sources of these chemicals: a direct biological production, or a photochemical production from dissolved organic matter (DOC) in the water column.

The first linkage to photosynthetic organisms was made by Bonsang et al. (1992) who featured depth profiles of ethene, propene, and isoprene at two South Pacific sites and the Mediterranean Sea. Subsurface maxima in all of these species at all locations appeared slightly shallower than maxima in the water column chlorophyll fluorescence, leading these authors to conclude a likely biotic source. Milne et al. (1995) and Baker et al. (2000) also saw subsurface maxima in isoprene that correlated broadly with the deep chlorophyll fluorescence maxima in measurements taken in the Gulf Stream off of Florida, and the eastern Atlantic Ocean, respectively. However, measurements in the North Atlantic and North Sea by Ratte et al. (1995) in the spring of 1991 showed more complex profiles. Most of the time ethene, propene, and 1-butene concentrations within 1 meter of the surface were slightly elevated in comparison to those at the 1% light intensity depth and below. One sunny and calm day there was a distinct vertical gradient. If loss to the atmosphere is the only water column sink, this is consistent with a light-induced production of alkenes which was not able to be quickly vented. The proximity to the water surface may make biological mediation unlikely, as compared to a purely photochemical one, due to low cell concentrations. The alkanes showed concentration maxima at or just below the 1% light level depth, although no clear correlation with bulk chlorophyll concentrations or phytoplankton counts was found. While the bottom of the euphotic zone typically has high plankton counts, it may also have numerous bacteria, zooplankton, or other organisms which can potentially contribute to NMHC production. Virtually nothing is currently known about these potential sources.

Correlations of NMHC with bulk chlorophyll concentrations in surface waters also give conflicting results. Ratte et al. (1995) found very weak anti-correlations of ethane, ethene, propane, propene, 1-butene, and n-butane with chlorophyll-a concentrations and phytoplankton densities at the 99% confidence level in the North Atlantic and North Sea. Broadgate et al. (1997) also found low- or not-significant correlations of ethene, propane, 2-me-propane, and 2-me-butane with chlorophyll-a concentrations in measurements made in the North Sea and Bellinghausen Sea (Southern Ocean). However, there is an excellent positive relationship between isoprene and chlorophyll-a concentrations seen at both sites that is > 99% significant. Winter isoprene concentrations tend to be a bit smaller than the overall linear regression line, and summer ones larger, which is consistent with a dependence on sea-to-air transfer velocity which maximizes in the winter. May/June data nearshore in the North Sea showed very high chlorophyll-a concentrations due to a *Phaeocystis* bloom, but lower isoprene levels than expected. It was postulated that the mucus-forming colonies of this organism may be less likely to produce or emit isoprene as compared to a more typical single-celled phytoplankton. More than 75% of the plankton in the Bellinghausen Sea were diatoms, which appeared to be correlated with the highest isoprene concentrations. Interestingly, if data points corresponding to a phytoplankton bloom in the North Atlantic are excluded from the Ratte et al. (1995) study, a highly significant positive correlation is found between all NMHC, except ethane, and biological activity. This bloom was dominated by *Chaetoceros*, *Nitzschia*, and *Thalassiosira* cells, and may imply these species (or perhaps diatoms in general) do not produce NMHC. No positive or negative correlations between cell and NMHC abundances were found during a dinoflagellate bloom detected during the same study.

In their summary of approximately 40 datasets of field measurements, Plass-Dulmer et al. (1995) found no significant correlation of any C_2-C_4 NMHC with bulk chlorophyll concentrations. However, it was necessary to supplement most hydrocarbon datasets with climatological chlorophyll concentration data from the Coastal Zone Color Scanner remote sensing satellite. Because of the heterogeneous nature of NMHC production and loss, it is not surprising that no relationship was found. Most recently, measurements from the ACE

I campaign in the Southern Ocean in 1995 by Pszenny et al. (1999) show significant positive correlations of butane, propane, and 2-me-propene with chlorophyll-a concentrations, but only in a subset of the many biogeographical regions sampled. It should be noted that ethane, ethene, propene, and isoprene were not measured by these authors. Yokouchi et al. (1999) sampled surface air on several cruise tracks in the western Pacific, eastern Indian Ocean, Southeast Asian Sea, and Southern Ocean and found weakly correlated atmospheric levels of isoprene, DMS, and bromoform that cannot be attributed to terrestrial vegetation sources. These concentration measurements would be governed by both the net water column production and the sea-to-air transfer.

Links between NMHC and photochemically-related parameters can also be found. Ratte et al. (1993) performed on-deck incubation experiments in the North Atlantic spring and found increasing alkenes in sunlight-illuminated bottles, and constant concentrations in darkened bottles. Incubations of water filtered to remove algae also showed alkene increases, but at a lower rate. Additionally, during periods of low transfer velocity, and thus low loss of NMHC to the atmosphere, surface water concentrations were observed to increase during the day and remain constant during darkness. The authors suggest that some portion of the DOC emitted by phytoplankton is the photochemical precursor for the detected NMHC, but they can not exclude a direct biological production. Pszenny et al. (1999) found associations of higher NMHC concentrations with higher DOC levels for the very limited number of available DOC data obtained in the ACE-I campaign. Ratte et al. (1995) report significant linear correlations between NMHC concentrations and photochemically-reactive DOC in surface measurements from the Mediterranean Sea to the North Sea. They note the data set of simultaneous measurements is quite small, primarily due to the difficulty of obtaining accurate DOC measurements. It is important to note there no relationship was found between NMHC and total DOC. Additionally, their depth profiles show a rapid decrease in ethene concentration from the surface to 50 meters depth, consistent with photochemical formation.

Other relationships examined during field work have included NMHC versus temperature, seawater nitrate concentration, and solar radiation. Plass-Dulmer et al. (1995) found no relationships of any C_2-C_4 NMHC with solar radiation or temperature, but once again these datasets were supplemented with a combination of climatological and calculated data. Pszenny et al. (1999) found negative correlations of various NMHC with temperature, and positive correlations with nitrate in a majority of biogeographical regimes sampled, but very few significant relationships with solar radiation. Baker et al. (2000) show a strong correlation of ethene with sea surface temperature (SST) in the eastern Atlantic ocean during the spring. The authors explain these results with a photochemical source: their SST data also correlate well with PAR, which would act to increase phytoplankton biomass and thus the putative phytoplankton-derived DOC precursors of alkenes, which would then be available to be transformed by UV.

The incomplete picture painted by the field measurements is supplemented by the results of controlled laboratory experiments. Wilson et al. (1970) were the first to propose an alkene dependence on DOC. Incubations of dilute algal culture filtrates from the diatom *Chaetoceros galvestonesis* were determined to produce ethene and propene when exposed to light. Darkened incubations produced few, if any, hydrocarbons. Lee and Baker (1992) found a light- and particle-dependent ethane and ethene production in estuarine river water incubations. They postulated both a direct phytoplanktonic source, and an abiotic one due to extracellular poly-unsaturated fatty acid (PUFA) decomposition. Also commonly referred to as lipids, these are organic chemicals containing a carbonyl group attached to an electronegative atom. When exposed to oxidants they have been shown to degrade to a variety of products including NMHCs. PUFA are common constituents of the oceanic DOC reservoir, as well as intracellular components of marine phytoplankton. It is proposed that these lipids would be protected by anti-oxidants within the cells, and only transform during exposure from cell lysis.

Schobert and Elstner (1980) found light-dependent production of ethane, ethene, and hexanal in cultures of the diatom *Phaeodactylum tricornutum* that was correlated with

pigment bleaching and fatty acid oxidation. They proposed a non-enzymatic, light-dependent formation of radical intermediates which may induce a series of oxidative reactions for the fatty acids, producing the NMHC. Axenic culture incubations of the diatom *Skeletonema costatum* and the dinoflagellate *Scripsiella troichoidea* by McKay et al. (1996) produced ethane, ethene, propane, propene, hexane, and isoprene. The first four chemicals were found to have elevated fluxes anti-correlated with chlorophyll-a concentrations. Their source was assumed to be decomposition of organics emitted during cellular degradation. Hexane and isoprene fluxes peaked during chlorophyll-a concentration peaks; the authors concluded a direct emission of these chemicals. Other organisms found to produce ethene and the occasional other alkene include soil and pathogenic bacteria, yeasts, and molds (Fukuda et al., 1993, Fujii et al., 1987).

Incubations of water from Florida's Shark River by Reimer et al. (2000) irradiated with a high intensity Xe lamp produced a variety of alkenes through an oxygen-inhibited process. These include ethene, propene, trans-2-butene, 1-butene, cis-2-butene, and 2-me-propene. Light was required for the samples to emit significant NMHC, but the authors allow the possibility that dark reactions, such as a metal mediated redox mechanism or enzymatic processes, may also occur. Vigorous filtration, expected to lyse many microorganisms in the samples, resulted in enhancements of NMHC emissions. Unusually, the authors found no measurable increase in DOC during this process, but they speculate the magnitude of the increase was less than the instrument precision. NMHC emission rates slowed after only an hour of irradiation, but continued until the end of the experiment (about 500 minutes), at which time the rates were approximately half the initial values. The authors speculate that irradiation converts the initial DOC to chemicals which are less likely to degrade to NMHC. UVB wavelengths were determined to be the most important for the absorption and quantum yields, but loss of energy in this band in seawater would increase the importance of slightly longer wavelength light to this process *in situ*. Ratte et al. (1998) also found this spectral range to photoproduce ethene and propene from DOC incubations. After 10 days of irradiation with UV in the 300-420 nm range, concentrations of several thousand pmol L^{-1} were reached, while concentrations in incubations exposed to visible light (320-800 nm or

410-540) only reached several hundred pmol L^{-1} or showed no increase, respectively. Fulvic and humic acid additions increased production rates, which were on the order of several pmol L^{-1} hr^{-1} $(mg\ DOC)^{-1}$. Oxygen did not affect the production rates, although these rates did taper off after long time exposure to UV 300-420nm. Ethene production rates were always about twice that of propene, and DOC-induced alkene production rates were all much higher than those from one non-axenic diatom culture of *Thalassiosira rotula*. The authors estimate the total natural alkene production from this DOC-induced mechanism to be at most 5 Mtons $year^{-1}$. Other experiments indicate possible precursor compounds that would be rapidly produced photochemically from biologically-derived DOC may include long chain isoprenoids such as methionine, phytol (pigment component), pristane(fatty acids, lipids), and other sterols which contain, or easily convert to, carbonyl structures (Rontani, 1991). Reimer et al. (2000) hypothesize that a carbonyl photofragmentation mechanism which releases alkenes could account for the oxygen dependence.

Interestingly, there is little alkane production rate data that shows clear relationships to either biological or chemical processes. McKay et al. (1996) found ethane and propane production in axenic cultures, at approximately half the rates of alkenes. However, Schobert and Elstner (1980) found ethane production more substantial than ethene for one diatom. UV and short wavelength visible photochemical incubations by Ratte et al. (1998) were inconclusive with either a biological or photochemical source of alkanes, and virtually no *in situ* correlations were found with any parameters tested. Currently it is assumed that the alkane formation pathway is different from that of the alkenes, but its exact nature is not known.

Isoprene production has been detected in about 15 various phytoplankton species grown under significantly different conditions, at rates ranging over several orders of magnitude. Production occurred in concert with bulk chlorophyll concentration increases, but not with lag phase cultures, or those at the end of senescence. In addition to the McKay et al. (1996) study already mentioned, Moore et al. (1994) found isoprene production by three unialgal

diatom species, *Nitzschia sp*., *Porosira glacialis*, and *Ondontella mobiliensis*. Milne et al. (1995) detected isoprene in 9 out of 10 different cultures of diatoms, coccolithophores, dinoflagellates, and cyanobacteria. Note that in all three studies, cultures began as uni-algal, but no check was made to see if they remained that way. Isoprene levels rapidly declined as the cultures senesced. However, non-axenic *Thalassiosira rotula* incubations by Ratte et al. (1998) had only a very small biological production that was close to that of a cell-free control. This particular study also showed a slight photochemical isoprene production in cell-free seawater blanks, but at several orders of magnitude smaller than other light hydrocarbons in the study.

To summarize, there is reasonable evidence for multiple mechanisms of NMHC production. One is a direct production and cellular release from phytoplankton, which appears to be the primary source of oceanic isoprene. Another is the photochemical degradation of phytoplankton-derived organic matter in the surface ocean. This appears to be the primary source of alkene species. There is no proposed mechanism for production of oceanic alkanes at this time.

1.3 UNANSWERED QUESTIONS AND THESIS GOALS

In summary, the current state of knowledge about oceanic NMHC leaves the following questions still wide open:

- What is the physiology of NMHC production in a given phytoplankton species?
  - Is there a growth rate dependence?
  - Does isoprene production vary with light, temperature, or nutrient limitation in the same way as for higher plants?
  - What percentage of fixed carbon is converted to NMHC, and how does this compare with higher plants?
  - Do isoprene production rates vary from species to species?

- Do other plankton (such as bacteria, grazers, phage) affect NMHC cycling?
    - By direct production or consumption?
    - By affecting the magnitude or distribution of phytoplankton?

In this thesis the results of a methodology which was developed in order to examine some of these questions are presented and discussed. Several phytoplankton and cyanobacterial species were chosen for culture in laboratory experiments. NMHC production rates were measured under a variety of physiological conditions, and compared against the limited available data from marine organisms and the numerous data from terrestrial plants. An appropriate method was also developed to scale laboratory measurements up to ocean regions with the help of *in situ* data.

The cyanobacteria chosen include *Prochlorococcus marinus* (Chisholm et al., 1988) and *Synechococcus sp.* (Waterbury et al, 1986). Both dominate the oligotrophic mid-ocean gyres, and tropical regions in general. Both have also been extensively studied, and much of that information is within reach. Their genomes are currently being sequenced and interpreted (http://spider.jgi-psf.org/JGI_microbial/html/index.html). Information is known about their comparative physiology, including light, temperature, and nutrient dependencies, and metal toxicity. Also, their ecological role is quite significant. The cyanobacterium *Prochlorococcus* appears to be the dominant oxygenic phototroph in the tropical and subtropical oceans (Chisholm et al., 1992; Olson et al., 1990; Binder et al., 1995; Partensky et al., 1999), and contributes significantly to primary production in those regions (Liu et al., 1997; Goericke & Welschmeyer, 1993). *Synechococcus* are also extremely abundant in the euphotic zone of these waters, although they can also be found at the high latitudes and in coastal areas where *Prochlorococcus* are not (Waterbury et al., 1986). Two picoeukaryotic species typical of the oligotrophic oceans (Simon et al., 1994; Andersen et al., 1996) were also studied: *Micromonas pusilla* (Zingone et al., 1999), and *Pelagomonas calceolata* (Andersen et al., 1993). *Emiliania huxleyi* was the representative larger eukaryote. This coccolithophore forms huge blooms (1000s of km in extent) and appears from the

subtropics to the subarctic Atlantic and Pacific (Cortes et al., 2001; Haidar et al., 2001). Additionally, *E. huxleyi* has been determined as one producer of large quantities of dimethylsulfide (DMS) (Keller et al., 1989).

The eventual goal is to be able to determine whether we can we detect changes in remote atmospheric boundary layer photochemistry due to plankton blooms. At a minimum this requires the development of an analytical model that can be used for marine production and sea-to-air transfer of NMHCs. But currently the fraction of biological versus chemical/ photochemical production, the portion ventilated versus lost/stored in the water column, and the dependence of these upon environmental parameters are almost wholly unknown. In particular, our lack of understanding of what controls the source and sink processes in the water column prevents an accurate assessment of potential impacts of phytoplankton blooms on marine boundary layer atmospheric processes. Thus, the focus of this thesis is to gain insight on the marine microbiological cycling of NMHC.

CHAPTER TWO

INSTRUMENT & PROTOCOL DEVELOPMENT

2.1 NMHC ANALYSIS

2.1.1 Instrumentation

The experimental system consists of a Hewlett-Packard 5890 Series II gas chromatograph (GC) with a Flame Ionization Detector (FID) installed. It is depicted in Figure 1. The column is a 50 m × 0.32 mm i.d. Chrompack PLOT fused silica column of Al_2O_3/Na_2SO_4 stationary phase (Varian, Inc.). A ~ 2 m pre-column of the same type is also in place to guard the primary column through backflushing. Ultra high purity (UHP) nitrogen is the make-up gas (30 cc min^{-1}), with UHP hydrogen as a carrier gas (40 cc min^{-1}). UHP hydrogen (40 cc min^{-1}) and zero-air (333 cc min^{-1}) are the flame gases. Data collection and analysis is performed with the Hewlett-Packard GC Chemstation Ver. A.04.02 software on a Pentium personal computer. This software is capable of controlling the GC and detector, as well as actuating online valves.

Because of their trace quantities in ambient air, it is almost always necessary to pre-concentrate hydrocarbon samples before GC analysis. This multi-step process begins with an initial cryogenic collection from a sample tank in a stainless steel sample loop of ~ 1 cc volume. Liquid argon (BP. -185.7 °C) is used as the cryogen so ambient oxygen and nitrogen in the samples are not trapped. After a sufficient volume of sample has passed through the loop, as measured by a controlled flow meter and pre-determined collection time, a boiling water bath induces sample re-volatilization. The gas lines are then switched to bring the collection loop inline with a pre-column to allow for separation of unwanted, larger molecular weight hydrocarbons from the chemicals of interest by backflushing. A second cryogenic collection of the lighter fraction occurs in a 'cryofocus' loop of i.d. 0.32

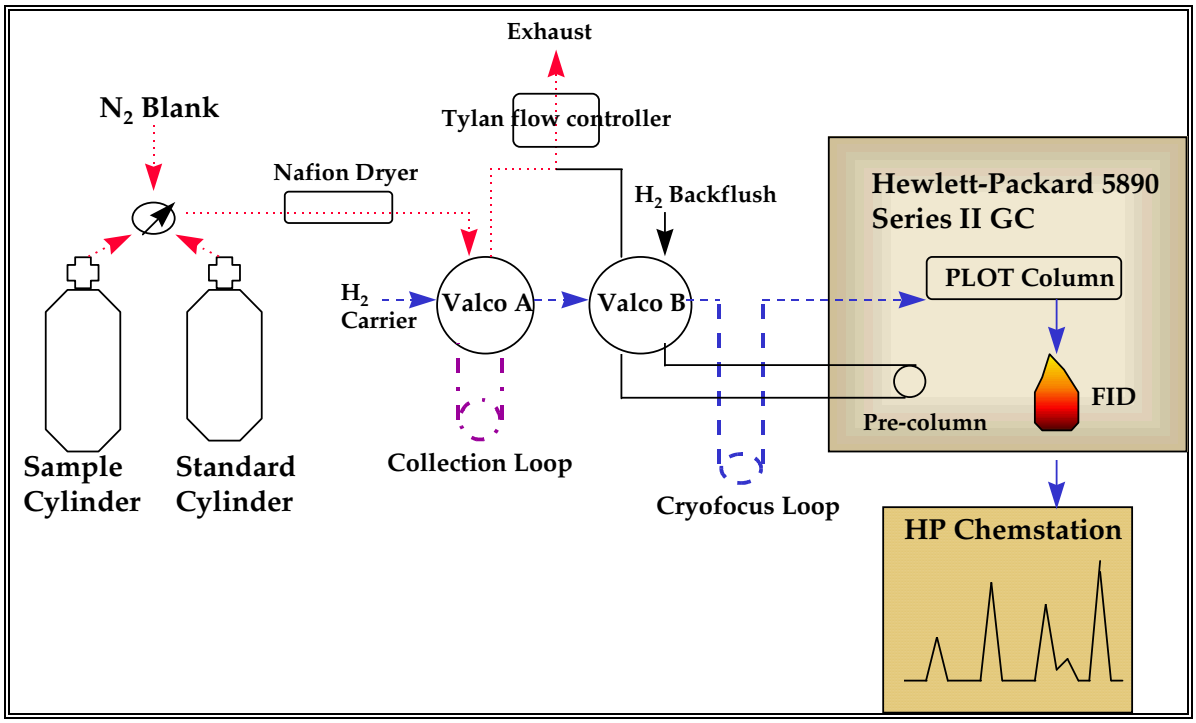

Figure 1: Injection System & Gas Chromatograph *Adapted from Kleiman (2000).* Typical configuration of culturing/sampling system. The red (dotted) pathway highlights sample collection through the cryogenic collection loop. The blue (dashed) pathway highlights the transfer of sample from the cryogenic loop to the cryofocus loop and transfer into the GC. Purple (dot-dash) indicates overlapping region of the 2 paths (collection loop).

mm diameter fused silica tubing downstream from the pre-column. Because this loop volume is approximately an order of magnitude smaller than the sample loop, we once again have a concentrating effect. This 'focuses' the hydrocarbons into a very small slug for injection into the column upon re-volatilization by a boiling water bath; this improves the final eluting peak shapes. The gas line switching necessary for these pre-concentration steps is performed by 6 port, dual-position actuated valves (Valco Instruments, Inc.).

The gas chromatograph oven is then programmed to begin at 35 °C and hold for 1.2 minutes. Then a 12 °C $minute^{-1}$ rise occurs until the oven reaches 65 °C, with a hold of 1 minute. A 10 °C $minute^{-1}$ rise until 150 °C is next, then a hold of 3 minutes, followed by a final rise of 15 °C $minute^{-1}$ to 200 °C, with an 8.7 minute hold. Under these conditions, this system can resolve on the order of 16 identified chemicals, and 10 un-identified chemicals, within 30 minutes.

The system has the option of receiving ambient air samples (typically ~ 500 to 1000 cc), or gas aliquots purged from aqueous samples. The purge chamber consists of a 60 ml glass vessel with a borosilicate fiber frit through which ~ 50-100 cc minute^{-1} of UHP nitrogen flows for 10 minutes. As the inert gas is bubbled through the water sample, the concentration difference between the two phases drives a mass transfer of the hydrocarbons to the nitrogen stream. This "aqueous" sample can then be analyzed in the same way as ambient air samples. Both analyses require a drying method due to column performance degradation with samples at ambient humidity levels. Water is potentially damaging to the system because it binds to the stationary column phase and limits separation capability (Donahue, 1991). It can also form ice plugs during the collection process, decreasing trapping efficiency, and in general increasing retention time variability (McClenny, 1984). Another interferent, carbon dioxide, is removed from the gas stream by Ascarite II ™ since it exists in large enough concentrations to cause a pressure surge in the system which can blow the FID flame out. Removing these chemicals also helps eliminate the possibility of reactions occurring within the sample loop during the collection period. Traditionally, chemical or physical dryers, such as Nafion® membranes (Perma-Pure, Inc.), have been used. Nafion® is a semi-permeable fluorocarbon polymer membrane which allows mass transfer of the water and other highly polar species from the sample stream into a counterflow of dry purge gas without loss of any NMHC from the samples.

A sample chromatogram produced on the analytical system is depicted in Figure 2 to demonstrate the current separation, resolution, and identification capabilities. As a check on our analytical method, a 5972A Hewlett-Packard Quadropole Mass Spectrometer (MS) was also temporarily installed on the model 5890 Series II Hewlett-Packard Gas Chromatograph. MS traces that appear similar to chromatograms can be produced, allowing quantitative sample concentration measurements. As the traces record a sample peak eluting, the corresponding mass spectra for that substance is simultaneously stored. With run

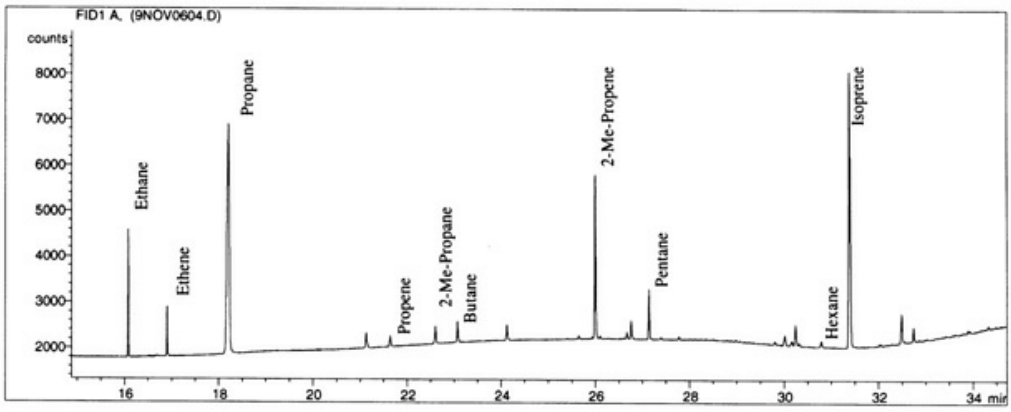

Figure 2: Identified Sample Chromatogram Relative detector counts are plotted versus species retention time for a typical experimental sample. A subset of peak identifications are shown.

completion, the spectra for each peak can then be compared to the installed library to confirm identification of all chemicals detected. Routine identification is achieved by matching retention times in the sample and standard analyses using the FID detector as discussed in Section 2.1.3.

2.1.2 Instrument Diagnostics

Analytical statistics are always important in experimental work, but they are more so here because of the high degree of sensitivity necessary to discern small changes in NMHC responses. System cleanliness and detection limits, as well as precision and accuracy, need to be calculated.

Cleanliness is determined by the amount of chemical contamination in a baseline run of UHP nitrogen. Such analyses were performed at the beginning of each day of measurements, and the chromatograms were almost always totally clean. If contamination peaks do exist, complete removal may not be possible. This is acceptable if they are of consistent size and significantly smaller than the sample response because they can then be simply subtracted from the sample data.

An estimate of analytical precision can be calculated from multiple identical runs of a calibrated hydrocarbon standard. Precision is defined here as the percent coefficient of variation (% CV) of these multiple standard runs. (A % CV is the ratio of one standard deviation to the mean, expressed as a percentage). The % CV on this system for all NMHC is less than 10% within a several week period except for ethene and pentane. This compares favorably to Reimer et al. (2000)'s 10% (3% single day), Broadgate et al.'s (1997) 11%, and Donahue and Prinn's (1993) 13%. The latter is the system we have modified for use in this work. For much longer time scales, such as a year, this variability is larger due to drift of the flame ionization detector (e.g. from variations in the detector gas flow rates). This is one reason calibration of the system through standard runs is performed daily during the experiments. A summary of these diagnostics appears in Table 3.

Detection limits can be calculated with a variety of methods. Kirchmer (1988) states that it is the variability of the blank response that establishes the minimum sample amount that can be detected and calibrated as above the blank. Assuming a normal distribution of results and a 95% confidence limit, the detection limit is defined as 4.65 times the standard deviation of the blank response. Because this chromatography system is quite clean, most NMHC do not appear in the blank runs, and thus a detection limit cannot be calculated from the blank response. In these cases, we use the smallest peak response able to be detected by our peak integration software. Our values are presented in Table 4 and are somewhat higher than those of other researchers with similar GC/FID analytical systems. McKay et al. (1996), and Rudolph and Johnen (1990) report 10 ppt, and 5-20 ppt, respectively for air samples. However, they do not define their detection limits; they likely assume the detection limits to be merely the standard deviation of multiple blank runs. We present our corresponding values in Table 4 for comparison. For liquid samples measured with some form of stripping or purging apparatus, Baker et al. (2000) and Reimer et al. (2000) report 0.28 picomoles and 0.1 picomoles, respectively. Our liquid sample detection limits are also presented in Table 4, and are about one order of magnitude higher than theirs. However, we use approximately 2 orders of magnitude less liquid volume for the analysis than these other authors use. All data reported in this thesis were calculated from original measurements that

Table 3: GC/FID System Diagnostics

	Standard, t ~ weeks			**Standard, t ~ years**			Blank, t ~ weeks		
	Mean n=15	SD	%CV	**Mean n=82**	**SD**	**%CV**	Mean n=10	SD	%CV
ethane	60.8	3.3	5.4	**58.4**	**8.9**	**15.2**	0.3	0.2	53.4
ethene	50.5	9.2	18.2	**53.2**	**13.7**	**25.8**	0.2	0.1	70.1
cyclo-propane	76.9	5.5	7.1	**76.3**	**16.8**	**22.0**	0.0	0	NA
propene	66.1	5.8	8.8	**61.6**	**15.7**	**25.5**	0.2	0.2	88.3
2me-propane	82.1	6.7	8.2	**80.8**	**14.2**	**17.6**	0.0	0	NA
butane	85.5	7.7	9.1	**82.1**	**17.2**	**21.0**	NA	NA	NA
2me-propene	84.2	6.9	8.2	**80.9**	**13.6**	**16.9**	0.1	0.2	144.8
cyclo-pentane	108.7	9.9	9.1	**106.8**	**19.2**	**17.9**	NA	NA	NA
pentane	97.8	27.9	28.6	**101.2**	**21.5**	**21.2**	0.1	0	NA
hexane	110.7	11.3	10.2	**115.5**	**21.8**	**18.9**	0.0	0	NA
isoprene	92.4	8.0	8.6	**94.8**	**17.1**	**18.0**	NA	NA	NA
3me-hexane	96.5	11.6	12.0	**106.4**	**25.6**	**24.0**	NA	NA	NA

Mean, standard deviation (SD), and % CV of the (peak area) (sample volume)$^{-1}$ responses for multiple identical standard and blank runs. NMHC with standard deviations of zero appeared in only one sample; NA indicates no peaks were found.

were above our detection limits. In some cases reported data may appear smaller; this is because of the subtraction of a blank (and other) corrections made to the data (see Section 2.5), where the difference of two numbers above the detection limits results in a number seemingly below them.

Further detailed diagnostics on the NMHC sampling system can be found in Appendix A.

Table 4: GC/FID System Detection Limits

	Air Detection Limit (following Kirchmer)	Air Detection Limit	Liquid Detection Limit (following Kirchmer)	Liquid Detection Limit
ethane	**115**	**24.7**	**9.9**	**2.1**
ethene	**87.9**	**18.9**	**10.1**	**2.2**
cyclo-propane	24.6	5.3		
propene	**71.4**	**15.4**	**6.6**	**1.4**
2-me-propane	24.1	5.2		
butane	22.7	4.9		
1-butene	24.4	5.2		
2me-propene	**21.7**	**4.7**		
cyclo-pentane	17.2	3.7		
pentane	18.9	4.1		
hexane	13.7	2.9	**4.3**	**0.9**
isoprene	18.6	4		

Detection limits following Kirchmer (1988) are calculated as 4.65 times the standard deviation of the blanks in ppt for air samples (~580 cc sample at room temperature, pressure) or picomoles for liquid samples (10 mL sample). Detection limits are calculated as simply the standard deviation of the blanks. Only selected values are reported for liquid detection limits as the original files containing this data have been lost. Detection limits in regular (not bold) face type indicate they were calculated using the integration software lower limit of peak response as explained in the text.

2.1.3 Identification and Quantification

The GC FID analysis is not a specific or absolute one; therefore, hydrocarbon sample identifications and concentrations must be determined by comparison against known composition standards. Initial identification of all peaks in all standard mixtures was performed with both permeation tubes following Donahue (1991) and mass spectrometer analyses. Identified and calibrated standard tanks were then used for identification and quantification of hydrocarbons in all samples run.

Standard tanks are commercially cleaned and electropolished 34 L stainless steel containers (Electromatic, Inc.). The standard gases are produced gravimetrically with a gas mixture of nitrogen, water, and the hydrocarbons of interest by a procedure developed by Michele Sprengnether (1992). The dilution of a standard tank is static, and the concentrations should remain stable over time. Over the course of this work several standards produced 'in-house' were used: Tank 5145 with C_2-C_7 compounds, Tank 5199 with C_2-C_8 compounds, and Tank 5138 with C_2-C_7 compounds. The latter was created as a diluted daughter of a commercially produced mix by Scott Specialty Gases using a modified Sprengnether (1992) method. Standards are often created with concentrations of hydrocarbons several orders of magnitude higher than in natural air. Subsequent dilution by Tylan mass flow controllers allows a calibration range that covers several orders of magnitude, including ambient levels. These high hydrocarbon levels ensure long-term stability/validity of the calibrations because small changes in compound amounts (e.g. due to wall loss) won't significantly affect the standard concentrations. Alternatively, a daughter of one high concentration standard mixture can be made by diluting the original into a new tank with UHP nitrogen. An advantage of standard tanks at the same order of magnitude concentration as the samples is simplicity of discovering any systematic errors associated with sample acquisition and storage. It also eliminates problems associated with repeated dynamic dilutions.

Previous work in the laboratory has shown this process produces C_2-C_6 standard tanks whose compositions are stable for several years (Graham, 1997). Figure 3a shows identical runs of the same standard tank as performed over a 6 week period. These measurements illustrate the generally good combined stability of the detector and standard mixture, as well as the smallness of the detector drift with time. Figure 3b shows similar data for about a 13 month period. There is more variability here, but most compounds vary together, signifying it is detector drift and not the standard composition that is changing. Variations in standard tank concentrations are negligible over any given two to three week experiment. We expect that over two years of experiments standard tank variations are still much less than biological variation. Means and standard deviations for the entire database were calculated

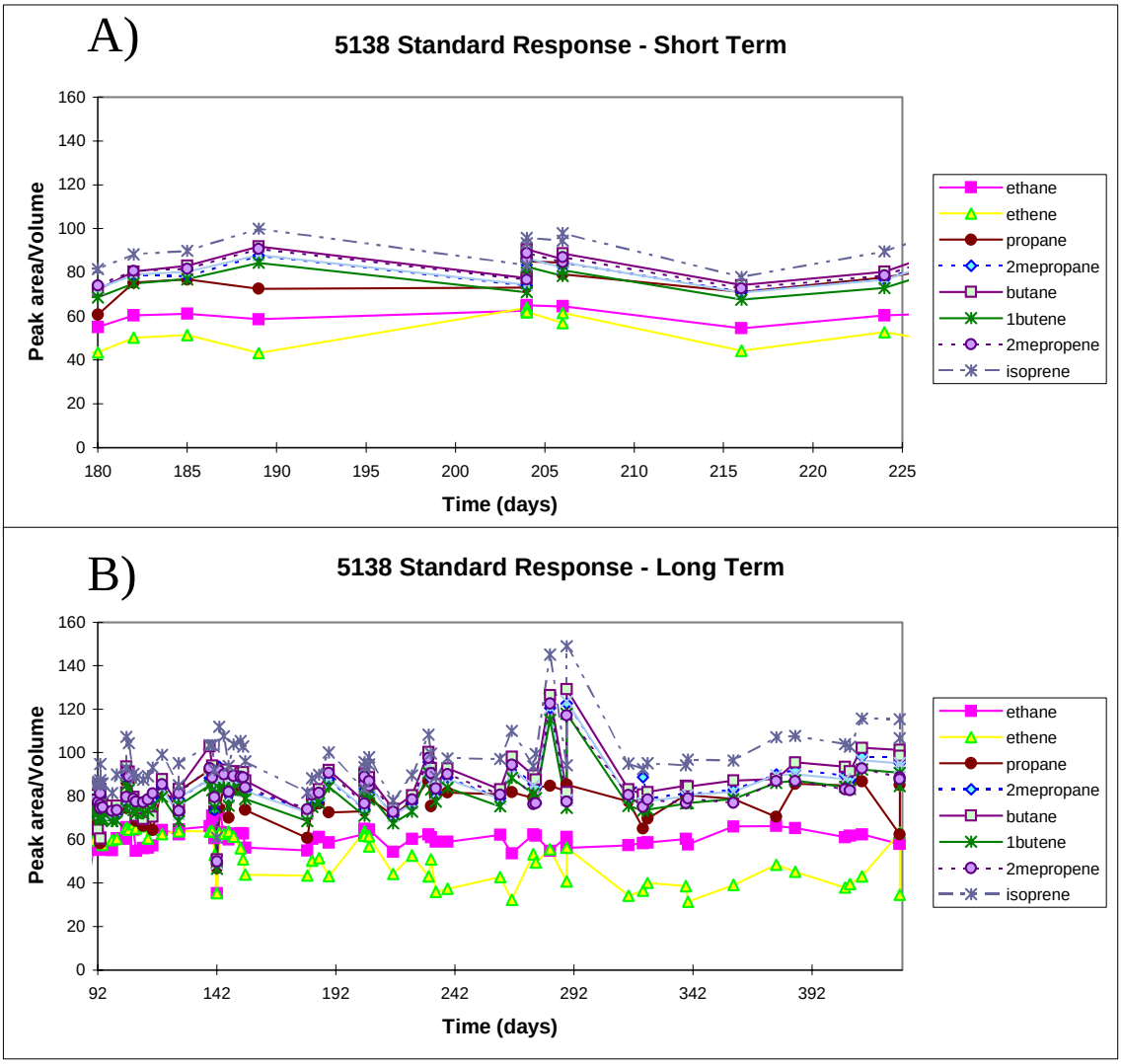

Figure 3: FID/Standard Tank Stability A) (Peak area) (sample volume)$^{-1}$ ratios for selected NMHC in standard tank 5138 over a six week period. Some detector drift is apparent; most species mirror the variability patterns. B) Similar, but for a 13 month period.

for each chemical. Any standard runs outside of 3σ error bars were not used for calibration purposes. As can be seen in Figure 4, there is an excellent fit of the calibration standard database within even the 1σ error bars for ethane and isoprene. Although ethene appears to be decreasing in the tank over time, there is still a fit within one σ.

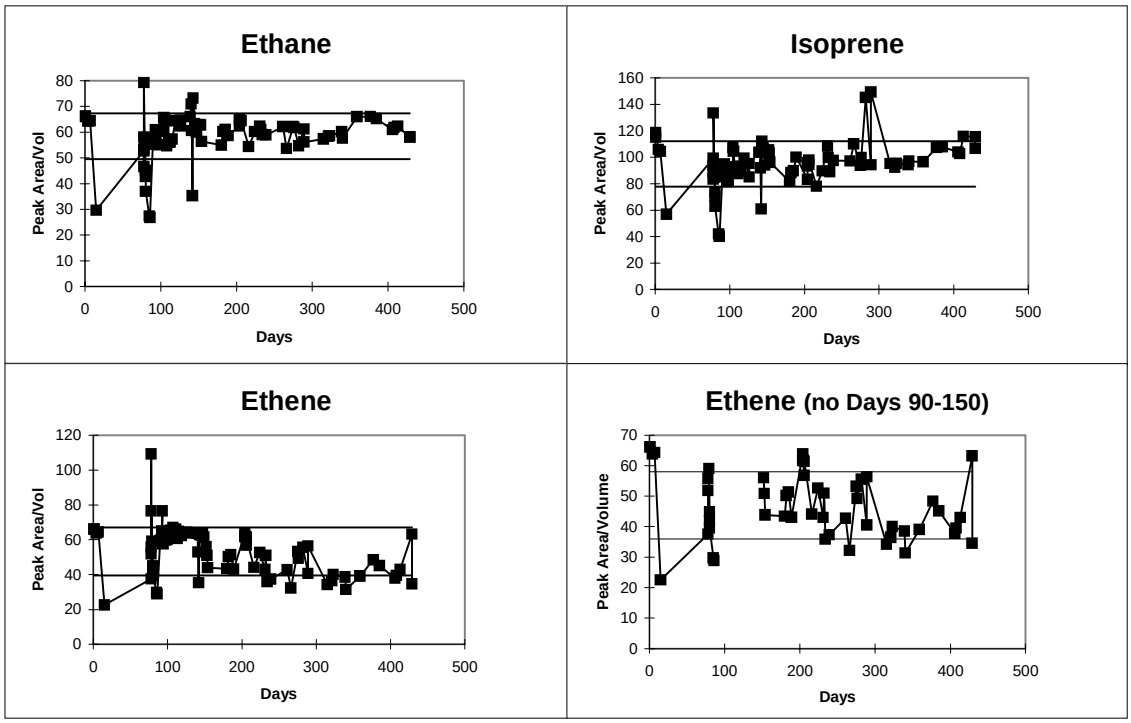

Figure 4: Standard Tank Drift for Selected NMHC. All data replotted from Figure 3. A) Ethane (peak area) (sample volume)$^{-1}$ response for the standard Tank 5138 over a 13 month period. Also plotted as straight lines are the +/- 1σ value of the mean of all points. B) As in A, but isoprene. C) As in A, but ethene. D) As in C, but with the runs from days 90-150 removed, and the 1σ value recalculated. The standard response for ethene on days 90-150 were deemed irregular due to the coherence of the high magnitude of response, and thus were not used for calibration purposes.

Analytical accuracy was assessed by comparison of our 'in-house' tanks against the Non-Methane Hydrocarbon Intercomparison Experiment (NOMHICE) sponsored by the International Global Atmospheric Chemistry Project (IGAC) (Apel et. al., 1994). It was determined during previous work by the author and by Kleiman (1999) that static dilution of a standard tank resulted in a daughter whose components had different dilution factors from each other. This is most likely due to the different chemical and physical adsorption characteristics of the chemicals (i.e. adsorption to the tank or tubing walls), and from analytical error in measuring very small pressure differentials in the tank production process (Kleiman, 1999). To account for this, each chemical must be calibrated separately against an external standard. As tanks 5199 and 5145 had been calibrated against the NOMHICE

scale in the past, these tanks were used to assign mixing ratio values to Tank 5138. All results reported in this thesis are on the Tank 5138 scale.

2.2 INCUBATION EQUIPMENT AND METHODOLOGY

The sensitivity study of planktonic NMHC production was achieved through monitoring of laboratory plankton monocultures, representing both prokaryotic and eukaryotic cells, in 1 liter glass vessels allowing a purge flow. Tests of the hydrocarbon content of the flasks were performed as a function of time by sampling the output gas purge stream. We observed ethane, ethene, propene, butane, all isomeric forms of butene, isoprene, and hexane, since these NMHCs have been often found by previous researchers to be potentially produced by phytoplankton (McKay et al., 1996; Milne et al., 1995; Ratte et al., 1993). The complete setup allowed for experimental studies over various ranges of light, temperature, and nutrient levels.

The incubating vessel was designed to enable the biological culturing to be as flexible as possible, yet remain leak-tight and contaminant-free for NMHC analysis. There are many commercially made incubation flasks available, but unfortunately none were acceptable for use in these experiments. The combination of cell culture and hydrocarbon measurements has many incompatibilities. For example, most biological vessels depend on plastics because of their ease of cleaning, low toxicity, durability, and design flexibility. However, most plastics are permeable to light hydrocarbons, and several have been shown to actively absorb these chemicals, and then sometimes re-emitting them at a later time. Contamination due to plastics is sufficient that researchers working with volatile organics generally constrain their fabrication material to glasses and stainless steels in their apparatus.

To reconcile these issues, a custom system was designed; a photograph is provided in Appendix B. 1 liter borosilicate glass Erlenmeyer flasks were modified with a ¼ inch outer diameter side port, and two #7 threaded ports at the top and side of the vessel by ACE Glass Inc. (NJ). A 27 cm long, ¼ inch outer diameter, porosity C dispersion tube was held in

place in the top thread by a nylon bushing and Viton o-ring. Both this inlet line and the outlet on the side were outfitted with PFA stopcocks for flow control, and 25 mm Delrin filter holders (Cole Parmer, Inc.) with 0.2 μm pore size hydroscopic filters (Millipore) for particulate and aerosol trapping. The additional side port is outfitted with a 3-way syringe valve (OSGE) with luer-lock connectors; this allows injection or withdrawal of liquid samples while keeping the system air-tight. The amount of plastic was minimized in the system, and confined to regions that were not in direct contact with the liquid phase.

The system is intended to be used as a purging as well as incubating vessel. A mixture of CO_2/air (BOC Gases) at roughly ambient levels (~350 parts per million (ppm)) mixed to a tolerance of <0.5 ppm total hydrocarbon contaminants is used as a purge gas. Two Supelpure™ hydrocarbon traps (Supelco, Sigma-Aldrich Co.) were installed to minimize hydrocarbon contamination from this mixture. As seen in Figure 5A, the typical configuration allows purging of the culture by this air mixture through the dispersion tube. Gas flows through the outlet directly to the clean, evacuated gas sample cylinder by a pressure differential of ~ 35 psi; the sample cylinder is outfitted with a pressure gauge to measure the amount collected. The adjustable height of the dispersion tube allows us to flush the entire system or just the flask headspace.

Internally passivated stainless steel 0.8 L gas cylinders (Electromatic, Inc., Goleta, CA) outfitted with Nupro SS-4H4 valves are used for sample collection. High humidity in the gas samples acts to preserve their integrity by preferentially adsorbing to cylinder walls as compared to NMHC, thus reducing NMHC loss to the walls (Pate et al., 1992). In-house tests also show these humidified experimental samples hold their composition stable longer than dry samples.

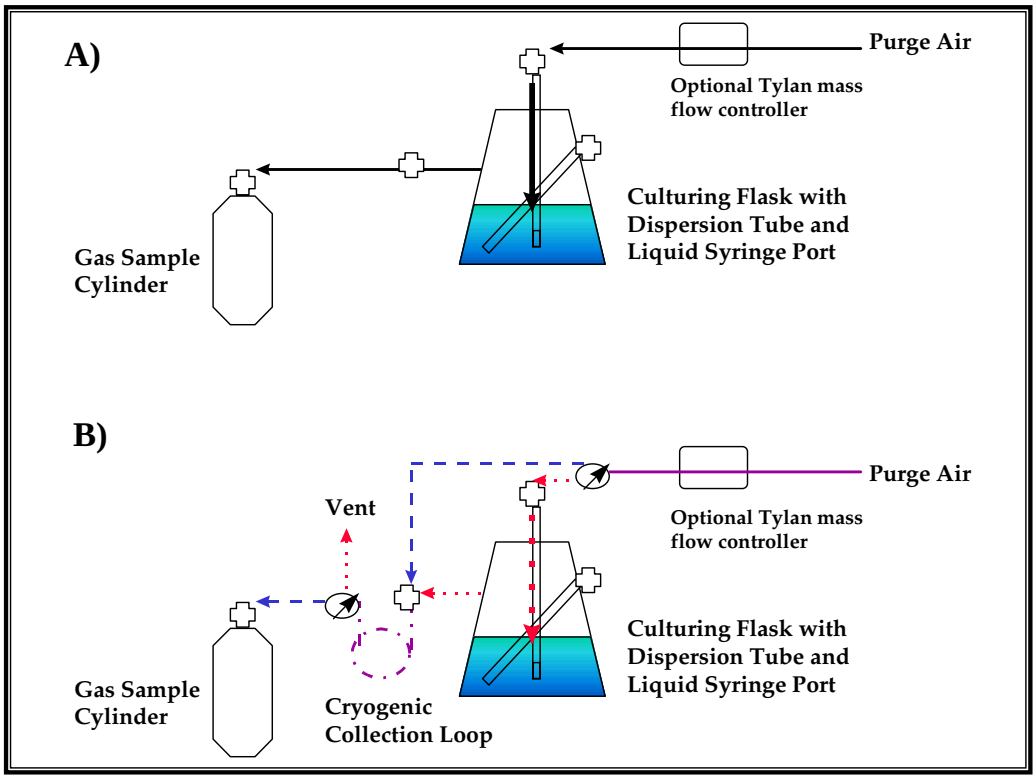

Figure 5: Culturing Incubation System A) Typical flow configuration. Crosses represent multi-way valves. B) Trial configuration for testing of larger sample collection volumes. The red (dotted) pathway highlights sample collection through the cryogenic loop. The blue (dashed) pathway highlights the transfer of sample from cryogenic loop to sample cylinder. Purple (dot-dash) indicates overlapping region of the 2 paths (collection loop).

The overall goal of the gas sampling is to have as complete a removal as possible of hydrocarbons within a reasonable time frame. Typically two methods have been used: equilibration and purging. Equilibration requires a clean, inert gas to recycle in contact with the water sample for a sufficient time to allow the system to equilibrate. The resulting gas stream can then be analyzed and the equivalent water concentrations calculated using headspace volume, fluid flowrates, and published Henry's Law constants. Purging requires a chamber to hold the water sample, with a glass frit through which to bubble clean, inert gas. With sufficient time, near complete mass transfer of volatile chemicals can occur into the gas stream, which can then be analyzed. Normalization to the known water volumes produces the needed sample concentrations. The benefits of a purging procedure are that equipment is minimized, no recirculating pump is necessary (which may be harmful to the

cells), and shorter sampling times. The primary drawback is that an incomplete purging process is likely with the short purging time necessary to process all samples in a reasonable amount of time. Fortunately the efficiency of this process can be quantitatively determined from multi-step purging experiments and effectively used in a data correction scheme.

The best time interval between sampling points was determined to be approximately one day. This interval must balance the requirements of obtaining enough hydrocarbon material to be reliably quantified on the GC, and resolving the interesting cellular dynamics in the experiments. Additionally, the relatively long analysis time (~ 1 hour) for the hydrocarbon samples limits the total number of samples that can reasonably be analyzed.

Sample chromatograms from this system using the sampling protocol outlined in Appendix C.1 are shown in Figure 6. Purge air alone (A) is reasonably clean, with the exception of three peaks from the purge gas mix despite two hydrocarbon traps online: ethane, ethene, and a large unidentified peak. The unidentified peak normally co-elutes with propane, making that compound non-quantitative in these experiments. Purged air from the culturing flask, incubated for two days (B) has similar or somewhat higher peak areas as for the purge gas alone. Additionally, the nominal propane peak has split (or multiple species have been resolved). Comparison of this plot with a sample taken from the temperature-controlled room (C) where all flasks are kept shows the system is leaktight. Room air has many small, unidentified peaks, almost all of which are absent in the flask sample. Those that do appear in the flask incubation have much lower peak areas per injection volume as compared to room air.

Sample chromatograms of a typical experimental media blank flask and cell culture flask appear in Figure 6D and 6E. Comparison to Figure 6A shows the system is not contributing a significant amount of contamination to any compound except propane, 2-me-propene, and pentane. A sense of the biological effects in the experiments can be determined by comparison of Figures 6D and

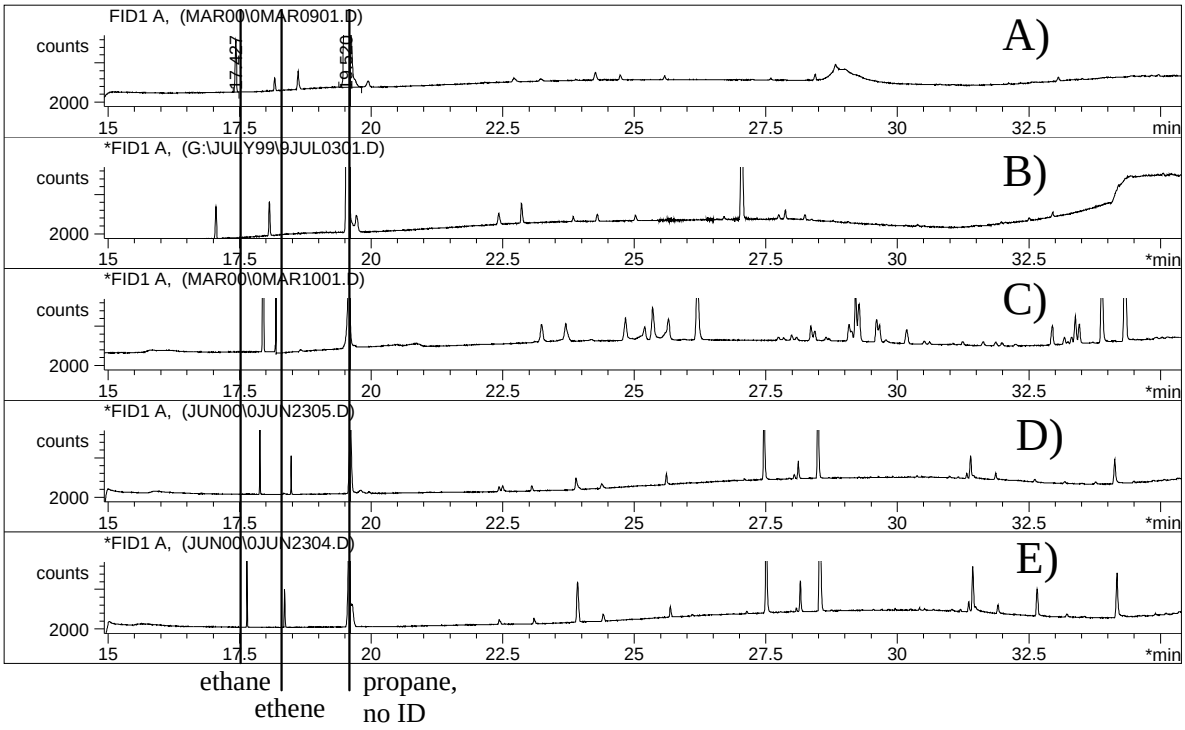

Figure 6: Sample chromatograms from the incubation system. A) Purge air mixture only. B) Purge air through empty flask with 2 day incubation. C) Incubator room air. D) Incubation flask sample with media only. E) Incubation flask sample with culture. Note that isoprene elutes at retention time of 32.7 minutes.

6E. Concentrations of NMHC in the media blanks are directly subtracted from culture sample concentrations as explained in Section 2.5. Resulting differences can be assumed to be due to biological effects.

2.3 PURGING AND ANALYSIS

Tests of the system's purging efficiency were performed. Successive gas samples were withdrawn at each step from individual incubation flasks and analyzed (Bullister & Weiss, 1988). (Peak area)(sample volume)$^{-1}$ ratios for the successive steps are expected to follow an exponentially decreasing pattern with purging time, as illustrated in Figure 7 for a *Prochlorococcus* culture. The (peak area) (sample volume)$^{-1}$ signal detected at each step

can be calculated as a percentage of the total signal (e.g. sum of all steps). This gives us the efficiency attributed to each step. As each individual step sampled here is taken using our experimental protocol, the optimal response would be to maximize efficiency in the first step, which represents the typical sampling time.

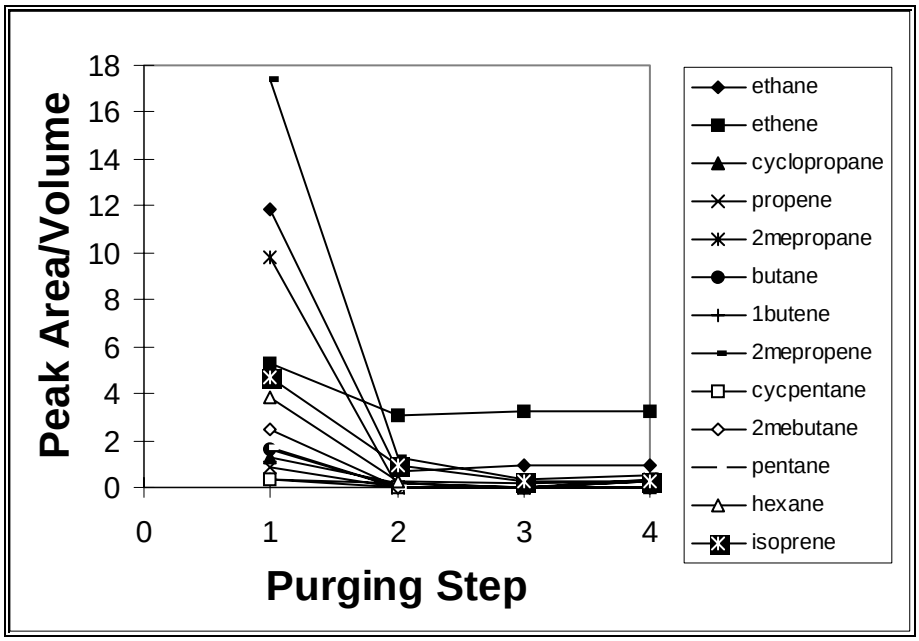

Figure 7: Multi-Step Purging (Peak area) (sample volume)$^{-1}$ ratios for successive step sampling. Four steps were analyzed and for all compounds shown to be near constant for the 3rd and 4th steps. This was true for all purging tests. The last three steps were also near constant for those experiments which used five individual steps.

A summary of purging efficiencies is shown in Table 5. Entries are organized from smallest to largest dimensionless air/water Henry's Law constants, H. The purging efficiencies show the expected general trend of more efficient purging with more volatile NMHC (e.g. As H increases, a higher percentage is attributed to the first step). However variations do occur because of the temperature functionalities and measurement errors in the Henry's Law constants, which are not taken into account here, as well as because of random sampling variations.

Table 5: Purging efficiencies

	Jan. 2000 B (4)	**May 2001 (4)**	**Average**	**Henry's Constant**
cyclopropane	NA	79,12,9	79,12,9	3.5
isoprene	NA	80,16,4	80,16,4	7.3
cyclopentane	43,0,57	100,0,0	72,0,28	7.5
propene	45,0,55	87,0,13	66,0,34	8.6
2-me-propene	63,18,19	91,7,2	77,13,10	8.7
ethene	39,37,23	46,27,28	43,32,25	8.8
1-butene	NA	64,36	64,36	10.3
ethane	94,3,3	88,5,7	91,4,5	20.4
butane	100,0,0	100,0,0	100,0,0	38.7
2-me-propane	100,0,0	98,0,2	99,0,1	48.4
2-me-butane	100,0,0	100,0,0	100,0,0	48.4
pentane	100,0,0	100,0,0	100,0,0	50.4

(Peak area)(sample volume)$^{-1}$ signal attributed to each stripping step (1st, 2nd, 3rd) out of the total signal, expressed as a percentage. For experiments in which more than three steps have been sampled, the last few steps (whose values have been determined to be approximately constant) have been averaged and that average value used as the third step. Total number of steps for each test is reported in parentheses (e.g. steps 3 and 4 from May 2001 were averaged to be step 3). Ethene efficiencies are smaller than expected on the first step because their values were already near the detection limit. Henry's constants are non-dimensional air/water as in Table 1.

Several NMHC have purging efficiencies well below 90%, generally considered to be sufficient efficiency. More rigorous purging would be necessary to ensure more complete hydrocarbon removal. This can be achieved through a longer purge time or higher flow rate. Unfortunately for this incubation system neither is possible. Higher flow rates can not be used because that would require purge gas head pressures likely to damage the glass flask. Longer purge times are not possible as they are is defined by the pressure differential between the purge gas head pressure and the evacuated sample cylinder (also see below). However it is possible to correct our NMHC measurements for this incomplete purging during the data analysis (see Section 2.5). We chose to use the average values from Table 5 and apply them to all experiments. For comparison, purging parameters from published papers and this work are reported in Table 6.

Table 6: Purging Parameters

Reference	Purge Efficiency	Flowrate & Purge Time	Incubation Volume	# of Flushings
Plass et al., 1992	> 90%	100, 30 min	0.87 L	3.4
Bonsang et al., 1992	97-99%	100, 60 min	1.5 L	4
Broadgate et al., 1997	> 90%	60, 30 min	1.4 L	1.3
Ratte et al., 1998	94-99%	100, 30 min	1 L	3
Reimer et al., 2000	> 95%	100, 30 min, 100, 10 min	300 mL, 110 mL	10, 9.1
This work (flasks)	see Table 4	1600, 1st min; mean 400, 3mins	0.5 L	5.6
This work (external purging chamber)	> 95%	60, 10 min	10 mL	60

Summary of purge efficiencies and number of complete 'flushings' for a variety of sample incubation apparati described in the recent literature. One 'flushing' is the passing of an equivalent volume of purge gas through a given liquid volume. Flow rates are all in cc/min.

Part of the experimental preparation is an initial overnight purge of the media broth, typically greater than 12 hours, before both cell inoculation and hydrocarbon measurement. This is intended to remove any background NMHC of interest from the incubation flask (Ratte et al., 1998). Occasionally the first few days of analysis have significantly elevated NMHC as compared to the following days. This behavior is used to determine that the media purge was incomplete and extra purging time (e.g. those first few days of sampling) was necessary to remove all background NMHC. Individual samples exhibiting this effect were removed from the datasets.

A variety of gas sampling methodologies were investigated during the development of the sampling protocol to ensure accuracy and consistency in the measurements. These include adding a mass flow controller on the purging line, utilizing a collection loop at the culturing

flask for larger volume collection, and removing liquid aliquots instead of purging gaseous samples.

The effect of installing a Tylan © Mass Flowmeter (Millipore Corporation) on the sample line between the purge air cylinder and the culturing flasks was tested following the method depicted in Figure 5A. Replicate flasks inoculated with equal volumes of *Prochloroccus* were allowed to grow past the lag phase. From this point on, the samples from one flask were collected with, and from the other without, a flowmeter on the line, set to an approximate average of 598 cc minute^{-1}. The effect was to slow the initial purging rate of the culturing vessel, and even it out over the entire collection period. Isoprene production rates are shown in Figure 8 for both collection methods.

There is no significant difference in the measured rates between sample collection methods. The metered flowrate was further lowered to approximately 577 cc minute^{-1} at and past hour 359, yet there is still no change in the NMHC production rates. In conclusion, there is no discernible difference between collecting the gas sample with a metered flow or a pressure differential method, and thus no reason to use the more cumbersome flowmeter approach.

One drawback to the pressure differential method of sample collection is the upper bound on the sample collection volume. NMHC analyses typically require sample volumes of several hundred cc's of gas, as well as cryogenic pre-concentration, because the quantities in ambient air are so small. However, each of the culturing system components has a maximum pressure rating, the lowest being the glass flask itself at approximately 10 psi. Working safely below that at 8psi allows an approximate sample volume of 1.2 L to be stored in the gas sample flasks at room temperature (21 °C). This is sufficient for one to two runs on the chromatograph, although it would be preferable to have further replicates. Additionally, the sample purging efficiency (Table 5) is directly dependent on the amount of sample volume pulled through the culture and into the gas flask. A larger sample volume, and thus longer purge time, would allow for a more complete removal of hydrocarbons and less carryover from one sampling time to the next.

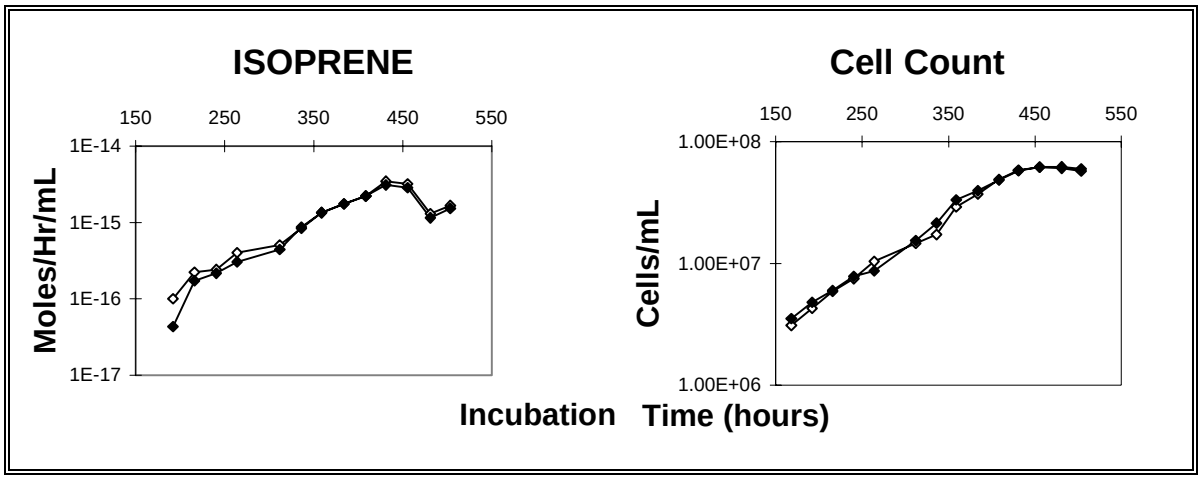

Figure 8: Isoprene Production with and without a Flowmeter Isoprene production rates calculated from the pressure differential method with (filled diamonds) and without (open diamonds) a mass-flow controller online.

In an attempt to collect larger sample volumes, a cryogenic trap was installed after the culturing flask. In this configuration (red-dotted pathway , Figure 5B) the purge gas sweeps the culturing volume before entering the trap. Flowrates are the same as in the method depicted in Figure 5A. Liquid argon is used to condense the chemicals of interest over an eight minute collection period, during which the gaseous remainder of the purge gas is vented. The cryogen is then removed and replaced with a boiling water bath. The contents of the cryogenic trap are swept into a sample gas cylinder by the purge gas through a bypass line (blue-dashed pathway, Figure 5B) which is routed around the culturing flask. This cylinder is analyzed as normal on the chromatograph with two cryogenic pre-concentration steps.

A chromatogram resulting from testing this method on a media blank can be seen in Figure 9A & 9B. Chromatographic quality and resolution is notably decreased, as evidenced by the misshapen and split peaks throughout the plot, compared to the original sampling method (e.g. Figure 9C). This was not attributed to an improved peak separation with the new method because the sum of the (peak area)(sample volume)$^{-1}$ ratios for the two halves

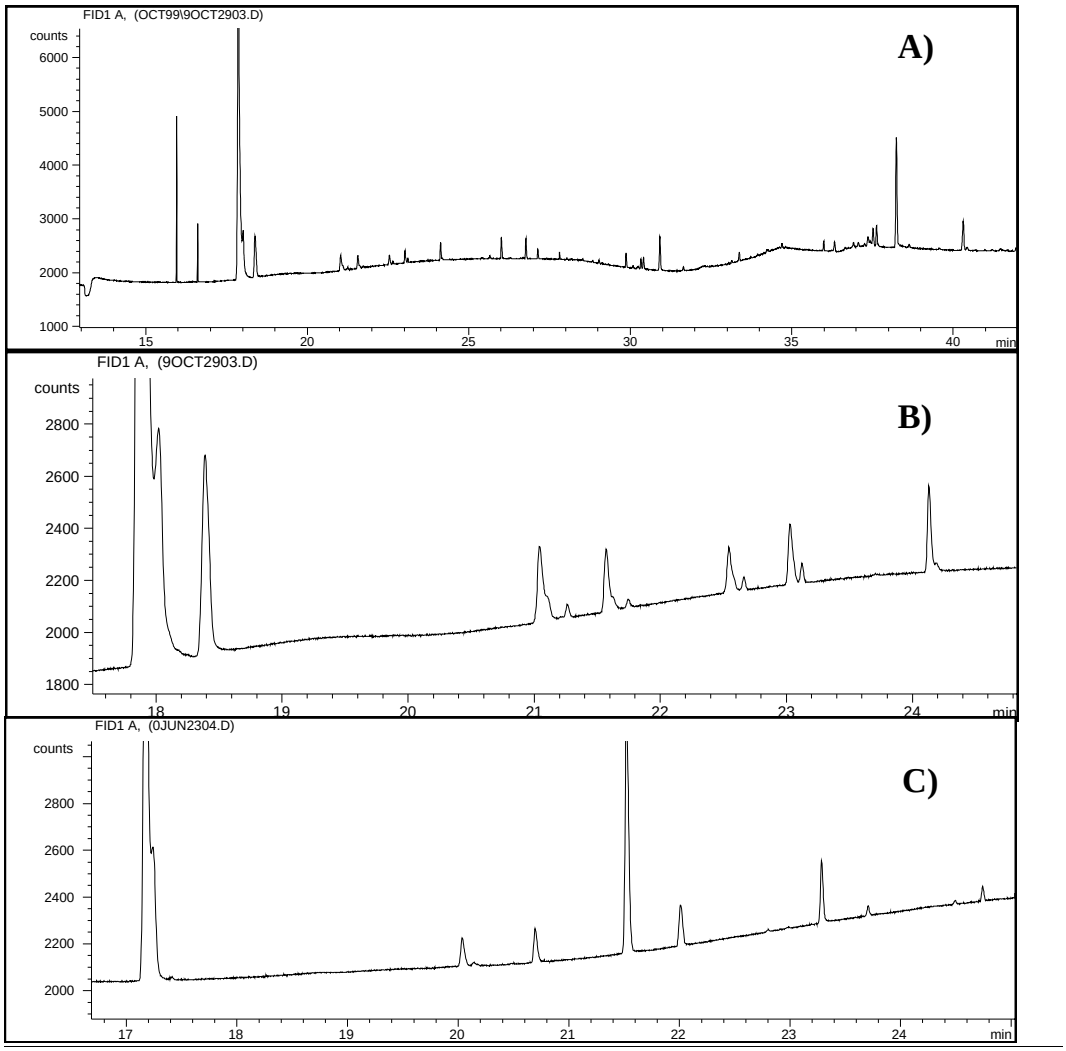

Figure 9: Chromatograms from Alternative Sampling Method A) Chromatogram from a sample withdrawn as per Figure 5B. Note large unidentified peak at RT 18 min, and misshapen peaks with splitting from RT 20-32. B) A close-up of the chromatogram in A. C) A close-up of the chromatogram in Figure 6E for comparison. Note the smoother peak shapes with smaller half-widths.

of the split peaks are equal to the (peak area)(sample volume)$^{-1}$ ratios of the corresponding peak in the original method chromatogram. Such peak splitting is often the result of excessive humidity in a sample. Adding the third cryogenic trap at the culturing flask itself would be expected to condense much of the water vapor out of the gas sample before it enters the cylinder. Assuming the re-volatilization by the boiling water bath is not 100% complete, it is reasonable to expect the humidity in the cylinder would be less than, or at

most equal to, that from the original sampling method. The expected result would be a similar or improved resolution, which is not the case. We currently have no explanation for this. Additionally, the presence near the retention time of 18 minutes of an unidentified large, broad peak, as well as a substantial increase in the 2-methyl-propene peak at the retention time of 27 minutes is unexplained. There may be a possibility of reactions occurring within the flasks as the sample gas is concentrated, due to the cryogenic collection, as compared to the original method. These puzzling results, compounded with the logistical difficulty of preparing this sampling procedure, led us to prefer the original protocol. Although the purging efficiency is thus lower than desired, it can be reliably quantified and can thus be used as an accurate correction factor.

A final option is to remove liquid aliquots from the incubation flasks at each sampling point for analysis with an external purging chamber. We have been able to reach much higher efficiencies with the latter system - approximately 95% removal in one step for all compounds (Table 6). This method would change the meaning of our measurement since we are no longer removing all NMHC produced in the flask. Instead we would be measuring the cumulative concentration of NMHC, assuming equilibrium between the liquid and air phases. This method required a minimization of the liquid volume removed each day to avoid changing the equilibrium dynamic in the flasks significantly over the course of the experiment, which we were not able to accomplish.

2.4 BIOLOGICAL PARAMETERS & ANCILLARY DATA

The primary source of cellular information, including counts, chlorophyll fluorescence per cell, DNA content, and general population health, was flow cytometry. The Becton-Dickinson FACScan instrument utilized is outfitted with a 15 mW 488 nm laser, and optics modified for optimal detection of picoplankton (Dusenberry & Frankel, 1994). The flow path is such that single cells pass through the laser beam at any given time, and the incident light is scattered as a function of their size and structure. Data are collected as forward and side (90° incident to light beam) scatter intensity. The argon laser also induces a

characteristic auto-fluorescence from the cellular pigments. The various chlorophylls emit a red fluorescence, phycoerythrin (a cyanobacterial pigment possessed by *Synechococcus)* emits an orange fluorescence, and various DNA stains, such as SYBR-Green (Molecular Probes, Inc.), emit green fluorescence. Photomultiplier tubes collect data from each of these channels. Each data point represents a single cell, and the bulk populations are shown as a density plot. Cellular data is always compared to that from small 0.474 μm diameter yellow-green polystyrene beads (Polysciences, Inc.) added to the samples as an internal standard against instrument drift. Different organisms can be identified by their unique combination of size and fluorescence properties. For example, *Synechococcus* are slightly larger than *Prochlorococcus*, resulting in a larger side scatter signal, and have more chlorophyll fluorescence per cell, as in the density plot Figure 10. *Synechococcus* also have phycoerythrin, and thus an orange fluorescence, but *Prochlorococcus* do not.

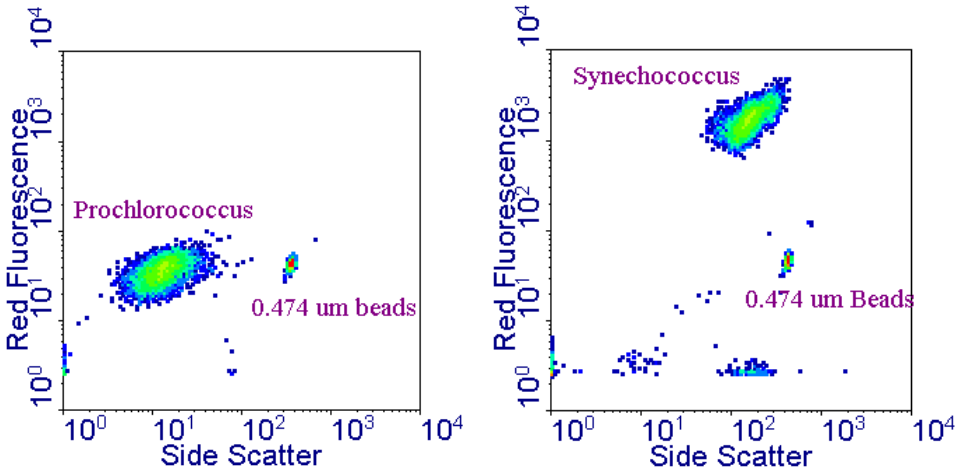

Figure 10: Flow Cytometry Plots of Two Phytoplankton Species Two dimensional histogram of side scatter per cell versus red fluorescence per cell. A) *Prochlorococcus* culture sample relative to internal bead standard (0.474 mm fluorescent microspheres). Lighter colors represent higher cell numbers. B) As in A, but for *Synechococcus*. Note the higher red fluorescence and side scatter for this species than in A, reflecting its larger size.

Additional cell counts and size estimations for some eukaryotes have been performed with Coulter Counter® (Model ZF from Coulter Electronics, Inc). Cells that have been DNA stained with SYBR-Green or 4',6 Diamidino-2-Phenylindole (DAPI) (see Appendix C.2)

can also be viewed and counted on a Zeiss Axiscope 2 epifluorescent microscope (Carl Zeiss, Inc.).

Chlorophyll-a, and divinyl chlorophyll-a (which is specific to *Prochlorococcus* in these experiments), were measured with a Model 650 Beckman-Dickson spectrophotometer as described in Appendix C.3. Relative chlorophyll concentrations were also monitored with a Turner Designs 10-AU Digital Field Fluorometer. It has been shown that in vivo fluorescence of clonal cultures acclimated to constant conditions accurately reflects the exponential cell abundance increase (Brand, 1981).

Bacterial contamination in phytoplankton cultures was determined with a Marine Purity Test Broth as described in Appendix C.4. Finally, an Orion Model 420A pH meter was used for pH measurements.

2.5 CALCULATION OF PRODUCTION RATES

Raw data obtained by the sampling methods just explained is in the form of a production rate: moles of hydrocarbon per air sample withdrawn per sampling time interval. This production rate is not the final form, as it does not account for the efficiency of the purging process. As previously discussed (Section 2.3), each sampling of the incubation flasks is intended to detect all of the hydrocarbon present by complete removal. Realistically, this is an incomplete process whose efficiency varies per chemical measured. The number of moles detected in the culture or blank is lower than the actual number in the incubation flask, and can be divided by this fractional efficiency to obtain a 'corrected' value as follows:

$$\text{'corrected' production rate} = \frac{[(moles_{culture_i} / E_i)]_T}{\Delta t}$$

with $moles_{culturei}$ representing the moles of hydrocarbon i detected in the culture at sampling time point index T, detected over the incubation time, Δt. E_i represents the purging efficiency of hydrocarbon i. This results in the estimated number of moles of a given hydrocarbon, i, that were present in the incubation flask over the time interval since the last sample.

We also wish to see the effect of the cellular incubations as compared to the media blanks, so we 'blank adjust' by subtracting the corrected blanks from the corrected cultures for each sampling point as follows:

$$\text{'blank adjusted' and 'corrected' production rate} = \frac{[(moles_{culture_i} / E_i) - (moles_{blank_i} / E_i)]_T}{\Delta t}$$

with $moles_{blanki}$ representing the moles of hydrocarbon i detected in the blank at sampling time point index T. This difference is the estimated number of moles of hydrocarbon i that were produced in the incubation flask *as a result of cellular activity* over the time interval since the last sample. This rate can be positive or negative, depending on a production or uptake of the chemicals by the cells.

The final correction also stems from the fact that the purging efficiency is < 100%. Not only does this mean we are not detecting all of the hydrocarbon in the incubation flask at a given time point, but also that there will be a small 'carryover' of that retained hydrocarbon from one sampling time point to the next. This 'carryover' for any time step, Δt, can be described as the fractional efficiency of *retaining* the hydrocarbon ($1- E_i$) at the previous time step (T-1), multiplied times the 'blank adjusted' and 'corrected' moles of new production at the previous time step (T-1), or

$$\text{'carryover'} = \frac{[(1 - E_i) \cdot ((moles_{culture_i} / E_i) - (moles_{blank_i} / E_i)]_{(T-1)}}{\Delta t}.$$

At any sampling point this carryover should be subtracted from the 'blank adjusted' and 'corrected' moles of new production. The final equation for production rate is as follows:

$$\frac{[(moles_{culture_i} / E_i) - (moles_{blank_i} / E_i)]_T - [(1 - E_i) \cdot ((moles_{culture_i} / E_i) - (moles_{blank_i} / E_i)]_{(T-1)}}{\Delta t}$$

These final NMHC production rates can then be normalized to incubation liquid volume or biological parameters such as cell count, biomass, or pigment content.

CHAPTER THREE

ISOPRENE PRODUCTION BY *PROCHLOROCOCCUS*, A MARINE CYANOBACTERIUM, AND OTHER PHYTOPLANKTON

Terrestrial photosynthesis is the dominant global source of isoprene to the atmosphere. Marine phytoplanktonic photosynthesis is thought to be a small global source of isoprene, but no consistent assessment has been performed of the dependence of isoprene production on light, temperature, and organism size. In this work, laboratory cultures of five different marine phytoplankton species (including *Prochlorococcus, Synechococcus, Micromonas pusilla, Pelagomonas calceolata*, and *Emiliania huxleyi*) were examined for isoprene production capabilities. All species were found to produce isoprene; rates ranged from $1x10^{-21}$ to $4x10^{-19}$ moles $cell^{-1}$ day^{-1} over all cell species and growth conditions tested. Isoprene production rates per cell were found to be constant during the balanced exponential growth phase, and decreased after entry into stationary phase. No consistent difference in production rate was detected between axenic and bacterized cultures. There was an apparent positive allometric relationship between isoprene production rate and cell volume; highest production rates were found for the largest cell, *E. huxleyi*, and lowest rates for *Prochlorococcus*, the smallest. Isoprene production was found to be a function of light intensity and temperature in *Prochlorococcus*, with patterns that are similar to the relationships between growth rate of these species and these environmental variables. The maximum production with light intensity was at the highest irradiance tested, 283 $\mu E\ m^{-2}s^{-1}$, and the maximum with temperature was at the maximum of growth rate for this species, near 23 °C. With certain assumptions, scaling the measured isoprene production rates with

observed water column phytoplankton counts, or bulk chlorophyll concentrations, resulted in a maximum sea-to-air flux of isoprene that was on the same order of magnitude as previously reported values determined using *in situ* marine sea and air measurements.

3.1 INTRODUCTION

Isoprene is the primary volatile organic compound emitted by most terrestrial higher plants to the atmosphere (Fehsenfeld et al., 1992). Its oxidation by hydroxyl radical can significantly affect the oxidative capacity of the lower atmosphere (Poisson et al., 2000; Fehsenfeld et al., 1992) and is a significant global source of CO (Granier et al., 2000). However, the physiological function, if any, of biogenic isoprene is still not known. Isoprene has also been detected in small amounts in the oceans and marine atmosphere (Bonsang et al., 1992). Current estimates indicate a small oceanic flux to the atmosphere on the order of 1 Tg C yr^{-1} globally (Broadgate et al., 1997; Milne et al., 1995; Bonsang et al., 1992). Although this is a very small amount of the total global flux to the atmosphere (Singh & Zimmerman, 1992), it could still be influential to remote marine boundary layer atmospheric processes due to isoprene's short lifetime and high reactivity (Carlslaw et al., 1998; Donahue & Prinn, 1993; Donahue & Prinn, 1990). Isoprene may also be a significant source of formaldehyde in clean marine air (Ayers et. al., 1997). However, the spatial and temporal variation of isoprene in seawater is poorly understood, and great uncertainties still exist in ocean-atmosphere flux estimates. Seawater concentrations range from 0 to 60 pmol L^{-1} (Baker et al., 2000; Broadgate et al., 1997; Milne et al., 1995), and are seasonally dependent in the North Sea with an abrupt maximum in May, and a smaller, second maximum in July (Broadgate et al., 1997). Independent of any relevance to atmospheric chemistry, it is also of interest to compare and contrast the isoprene production by simple aquatic organisms and terrestrial higher plants, given the lack of understanding of isoprene's functionality to the plants that produce it.

The only currently known source of oceanic isoprene is from phytoplankton (Moore et al., 1994; Milne et al., 1995; McKay et al., 1996; Broadgate et al., 1997; Ratte et al., 1998). Depth profiles from the Mediterranean, North Atlantic, Pacific, and North Sea show correlations between concentration peaks in the isoprene profiles and the subsurface bulk chlorophyll maxima (Baker 2000; Bonsang et al., 1992). Data from the North Sea and Southern Ocean also exhibit positive correlations between isoprene and bulk chlorophyll concentrations in surface waters over diverse geographical conditions (Broadgate et al., 1997; Baker et al., 2000), with R^2 values as high as 0.87 in the North Sea if a *Phaeocystis* algal bloom is excluded (Broadgate et al., 1997). Several laboratory studies have demonstrated that various species of diatoms, dinoflagellates, and coccolithophores grown under significantly different conditions can all produce isoprene, at rates ranging over several orders of magnitude. Production was always in concert with bulk chlorophyll concentration increases; low or zero isoprene production was found during lag or senescent phases (Moore et al., 1994; Milne et al., 1995; McKay et al., 1996). However, *Thalassiosira rotula* cultures had only a very small biological production of isoprene that was close to that of a cell-free control (Ratte et al., 1998). Irradiated samples of filtered seawater showed a slight photochemical isoprene production, several orders of magnitude smaller than for the other light hydrocarbons in the study (Ratte et al., 1998). However, other researchers with similar incubations found no evidence of a photochemical source of isoprene (Riemer et al., 2000).

While it is now known that phytoplankton can produce isoprene, no assessment has been performed of production as a function of light and temperature, which are two factors critical to the development of pelagic communities and to isoprene production by terrestrial plants. In this paper we report the results of a detailed multi-species incubation study which includes these light and temperature dependencies. We chose a variety of phytoplankton species for these laboratory studies, with the goal of broadly representing the

microorganisms populating the oligotrophic open oceans (e.g. Equatorial Pacific or Sargasso Sea). The atmospheric boundary layer above these regions is most likely to be affected by oceanic isoprene as it is most isolated from air masses of continental origin, has the lowest NMHC concentrations, and encompasses a net photochemical ozone destruction region (Evans et al., 2000). The cyanobacterium *Prochlorococcus* appears to be the dominant oxygenic phototroph in the tropical and subtropical oceans (Chisholm et al., 1992; Olson et al., 1990; Binder et al., 1995; Partensky et al., 1999), and contributes significantly to primary production in those regions (Liu et al., 1997; Goericke & Welschmeyer, 1993). *Synechococcus* are also extremely abundant in the euphotic zone of these waters, although they can also be found at the high latitudes and in coastal areas where *Prochlorococcus* are not (Waterbury et al., 1986). Two picoeukaryotic species typical of the oligotrophic oceans (Simon et al., 1994; Andersen et al., 1996) were also studied: *Micromonas pusilla* (Zingone et al., 1999), and *Pelagomonas calceolata* (Andersen et al., 1993). *Emiliania huxleyi* was the representative larger eukaryote. This coccolithophore forms huge blooms (1000s of km in extent) and appears from the subtropics to the subarctic Atlantic and Pacific (Cortes et al., 2001; Haidar et al., 2001). Additionally, *E. huxleyi* has been determined as one producer of large quantities of dimethylsulfide (DMS) (Keller et al., 1989).

3.2 METHODS

Our study included characterization of the phytoplankton and their environments, pigment and isoprene analyses, and genomic searching. The approaches used are described below.

3.2.1 Culturing, flow cytometry, and pigment analysis. *Prochlorococcus* (MIT 9401, SS120, axenic and xenic MED4 (CCMP 1378) strains) and *Synechococcus* (axenic WH 8103) were grown on a 0.2 μm filtered seawater-based media enriched with 800 μM NH_4Cl, 50 μM NaH_2PO_4, 11.7 μM EDTA, and the following trace metals: 8 nM Zn, 5 nM Co, 90 nM Mn, 3 nM Mo, 10 nM Se, 10 nM Ni, and 11.7 μm Fe ("Pro99" medium with 10x EDTA

and Fe, modified from Moore & Chisholm, 1999). *Emiliania huxleyi* (WH 1387) and the picoeukaryotes *Micromonas pusilla* (CCMP 489) and *Pelagomonas calceolata* (CCMP 1214), were grown on F/2 + Si media (Sigma-Aldrich, Inc.). Supplementary information on various carbon sources tested can be found in Appendix D.1. Reference temperature and light conditions were 23 ± 1.5 °C and ~ 90 ± 5 μE m^{-2} s^{-1} (1 E = 1 mole of photons) from cool-white fluorescent bulbs (14 hour light:10 hour dark cycle), except for *M. pusilla*, *P. calceolata*, and *E. huxleyi* incubations at ~ 45 ± 5 μE m^{-2} s^{-1}. Temperature ranges for the temperature variation experiment only were controlled with an aluminum temperature-gradient bar on a 14 hour light:10 hour dark cycle, at ~ 110 ± 10 μE $m^{-2}s^{-1}$ incident from below.

The 10-20 mL culture inoculation volumes used were incubated with ~ 500 mL media in gastight 1L Erlenmeyer flasks. These flasks were modified with glass threading to accommodate a dispersion tube for gas purging/sampling and a side syringe port for liquid withdrawal. Each flask was purged > 12 hours with purge gas (see Section 2.2) to remove residual NMHC before sterile, leaktight inoculation. Flasks were swirled before collection of 7 mL liquid samples with a sterile plastic syringe (Becton-Dickenson); this sampling occurred approximately daily, concurrent with gas samples. Fluorescence of liquid aliquots was measured on a Turner Designs 10-AU fluorometer, and pH measured with an Orion model 420A meter. Any pH measurements near 9 and above were used as an indicator of likely carbon limitation (Riebesell et al., 1993; Scarratt & Moore, 1996,1998), and were often reached in stationary phase cultures. Sub-aliquots of 1 mL volume were preserved with glutaraldehyde (final concentration 0.5%) in the dark for 10 minutes before storage in liquid nitrogen. When necessary, additional 20 mL aliquots were removed and filtered onto Whatman GF/F filters under low (< 5 mm Hg) vacuum and stored in liquid nitrogen for later pigment analysis. Pigments were extracted from filters using a 90% acetone method (Appendix C.3; Moore, 1995; Parsons et al., 1984) and measured spectrophotometrically using the equations of Jeffrey and Humphrey (1975). Throughout this paper we use "chlorophyll-a" to include divinyl chlorophyll-a, which is unique to *Prochlorococcus.* Sampling was done at approximately the same time each day to minimize the influence of diel variations in cell parameters.

Cell counts for growth rate calculations and production rate normalizations were obtained using a FACScan flow cytometer (Becton-Dickinson) modified for high sensitivity (Dusenberry and Frankel, 1994). Cells were identified by a combination of relative chlorophyll fluorescence and forward angle light scatter (FALS) signature. Mean chlorophyll fluorescence per cell and FALS are presented relative to 0.474 μm yellow-green fluorescent beads (Polysciences). Flow cytometric data were analyzed using 'Cyclops'. Gross photosynthetic rate, P (g C $cell^{-1}$ hr^{-1}), was calculated as in Moore (1997) from the measured growth rate as

$$P = \left(\frac{\mu K}{(1-R)(f)} \right)$$

with μ the growth rate in hr^{-1}, K the cellular carbon content in g C $cell^{-1}$, and R the fraction lost to respiration (assumed to be ~ 0.1 for cyanobacteria; Falkowski & Raven, 1997), and f the fraction of a day that is light (e.g. 14 light hours per every 24 hours). Cellular carbon content was calculated as 50% of the total cellular dry weight (Atlas, 1988). Biomass measurements (as total cellular dry weight) were made by harvesting axenic cultures on a Whatman GF/F filter, backed by a 0.2 μm pore diameter polycarbonate filter (Poretics, Inc.). Filters were then dried in a 37 °C oven for several days until the weight was constant, and corrected for a filtered media blank weight. Biomass estimates for bacterized cultures were performed using the equations of Verity et al. (1992).

Cell volumes for organisms cultured in this work were calculated using cylindrical shapes for the cyanobacteria, a spherical shape for *E. huxleyi*, and, prolate spheroids for the picoeukaryotes. Diameters were measured through 15 - 20 replicate microscopy field counts under phase contrast illumination (Zeiss Axiscope 2; Carl Zeiss, Inc.), and errors were propagated through the calculations. Organism sizes were estimated for species reported in the literature to produce isoprene, but for which no sizes were reported (e.g. Milne et al., 1995; McKay et al. 1996). Representative strain numbers from the Bigelow

Laboratory for Ocean Sciences' Center for Culture of Marine Phytoplankton (CCMP, http://ccmp.bigelow.org) were assumed for the relevant organisms if not given in the original sources. Reported cell length and width ranges were assumed to be one standard deviation error around an average. Cylindrical or spherical volumes were determined (depending on species) with the average dimensions, and the assumed error propagated through the calculations.

Heterotrophic populations lacking natural pigmentation were DNA-stained with SYBR Green I (Molecular Probes) for 15 minutes in the dark as per Noble & Fuhrman (1998) before microscopic counting. Tests for bacterial contamination in originally axenic cultures were performed with Marine Purity Test Broth (recipe from M. Saito and J. Waterbury at MIT/WHOI; Appendix C.4).

3.2.2 Hydrocarbon analysis. Gas samples were purged from the sealed culturing flasks with a 350 ppm CO_2/air mixure filtered through two SupelpureHC hydrocarbon filters (Supelco, Inc.) into evacuated 0.8 L electropolished stainless steel gas canisters (Electromatic, Inc., Goleta, CA). The analysis method is a modified version of that used by Donahue & Prinn (1993) and Graham (1998). Fifteen NMHC, including isoprene, previously identified with mass spectrometry (Hewlett-Packard 5972) were measured by capillary column gas chromatography (Hewlett-Packard 5890 Series II with a flame ionization detector (FID)). Samples were dried with a Nafion® dryer (Perma-Pure, Inc.), preconcentrated and refocused cryogenically with liquid argon, and separated on a PLOT Al_2O_3/Na_2SO_4 column (Chrompack, Inc.). Peak integration was done with Hewlett-Packard Chemstation 4.02A software. Hydrocarbon calibration is performed by comparison against gravimetrically-prepared in-house mixtures (Sprengnether, 1992; Donahue & Prinn, 1993) and a commercially produced standard mix (Scott Specialty Gases). Our results can be

compared to the National Center for Atmospheric Research (NCAR) calibration scale by dividing by the factors in Table 7, from the International Global Atmospheric Chemistry (IGAC) Non-Methane Hydrocarbon Intercomparison Experiment (NOMHICE) Task 2 (Apel et al., 1994), by our reported measurements. Relative analytical precisions were better than 10% for most compounds, and mole fraction detection limits were better than 25 parts per trillion in dry air (ppt) for a 580 cc sample. To quantify rates of production, integrated NMHC masses in the cultures for a given time step were corrected for those in blank incubations, as well as for < 100% purging efficiency, and carryover of remaining NMHC in the incubation flask to the next time step due to this efficiency (see Chapter 2, Sections 2.3, 2.5). Rates can then be normalized to biomass, biovolume, chlorophyll content, or cell count. Storage experiments indicate no significant sample composition or concentration changes in the gas canisters on the time scales of 10 days or less that were typical of the time between sampling and analysis. Halocarbons in the samples were analyzed by Dr. Benjamin R. Miller at Scripps Institute of Oceanography, LaJolla, CA, and calibrated against the AGAGE network standards (Miller et al., 1998; Prinn et al., 2000). One sample from a *Prochlorococcus* strain ss120 culture and one sample from a corresponding media blank were analyzed on each of two separate days (4 samples total), one during exponential phase and one in stationary phase.

Table 7. Mole fraction ratios of several NMHC in MIT standards to those in IGAC/NOMHICE standards

NMHC	Ratio	NMHC	Ratio
ethane	0.92	**1-butene**	0.92
ethene	0.93	**2-me-propene**	0.92
propene	0.82	**cyclopentane**	0.89
2-me-propane	0.93	**pentane**	0.69
butane	0.86	**isoprene**	0.81

3.2.3 Genomics. BLAST searching was carried out on the genomes of *Prochlorococcus* MED4 and MIT 9313 strains, as well as *Synechococcus* WH 8102. These are publicly available at the DOE-JGI Microbial Genomics website (http://spider.jgi-psf.org/JGI_microbial/html/). The amino acid sequences used for BLAST comparisons had Genbank Accession numbers as follows: HMG-CoA Reductase genes - *Haloferax volcanii* A42149, *Arabidopsis thaliania* A32107, *Sulfolobus solfataricus* O08424, *Pseudomonas mevalonii* P13702; DXS gene - *Synechococcus* PCC6301 CAB60078; MCT gene - *Batis maritima* BankIt217095 AF084829.

3.3 RESULTS

We cultured all phytoplankton strains through exponential growth phase, following most experiments until senescence. Samples were taken daily during approximately 2 week long incubations. *Prochlorococcus*, *Synechococcus*, *M. pusilla*, *P. calceolata*, and *E. huxleyi* all produced isoprene at levels higher than the media blanks, which were incubated under identical conditions as the cultures. The time course of cell counts over the course of a typical experiment has three growth phases: exponential increase, stationary phase, and death (Fig. 11A). Production rates in moles of isoprene per mL of culture per day (not shown) increased several orders of magnitude between the initial lag and exponential phases of culture growth, decreasing again during senescence. However when normalized to cell count, isoprene production rate is constant during the balanced exponential growth phase (Fig. 11B) at approximately $6x10^{-23}$ moles $cell^{-1}$ hr^{-1} or $1.4x10^{-21}$ moles $cell^{-1}$ day^{-1}. Constant daily averaged concentrations of cell components or metabolic rates are characteristic of this balanced growth (Eppley, 1981). This implies isoprene is indeed produced by the cells. The isoprene production rate begins to drop as stationary phase commences, decreasing further by two orders of magnitude as the population dies. Taking the average and standard deviation of all time points in exponential phase from all replicate incubations in this experiment gives a coefficient of variation of the isoprene production

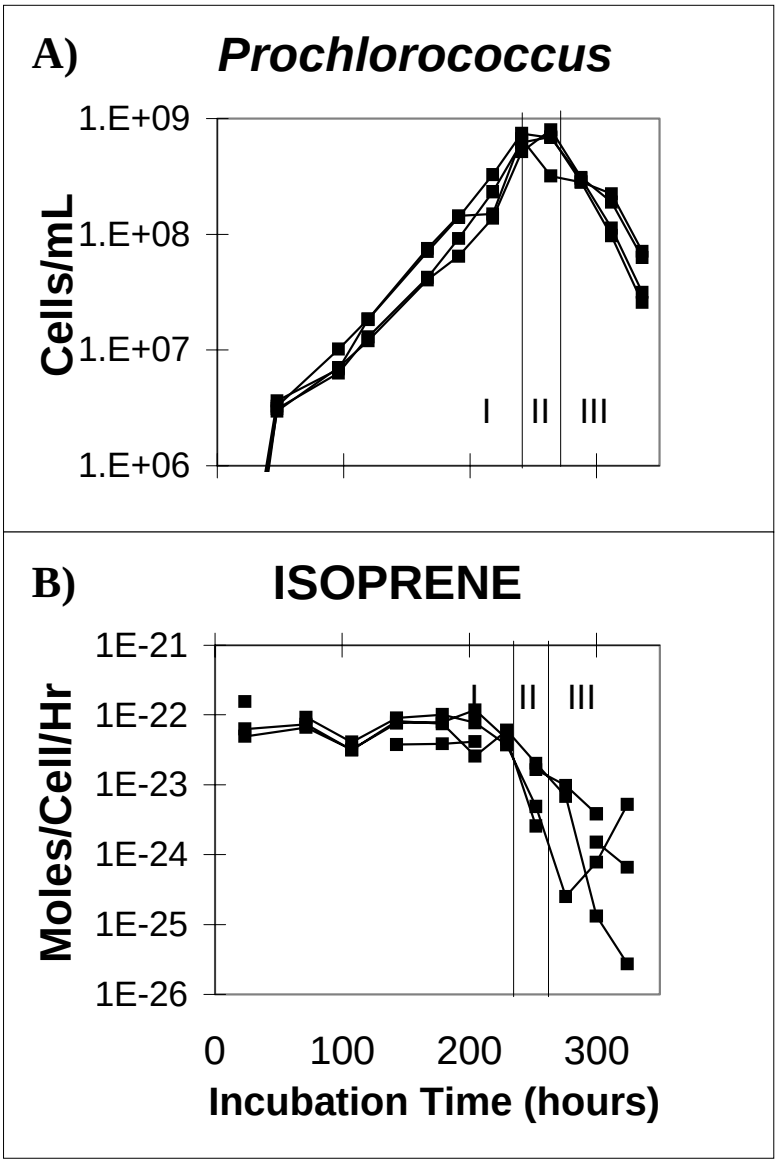

Figure 11: *Prochlorococcus* Produces Isoprene Isoprene production rate in moles cell^{-1} hr^{-1} as a function of time (B) over the *Prochlorococcus* (MIT axenic MED4 strain) growth cycle, in cells mL^{-1} (A). Results from four replicate cultures are plotted. Vertical bars distinguish between population phases exponential (I), stationary (II; equal cell growth and death), and death (or senescent; III) phases.

rate per cell of 65% (1 σ). Raw data for organisms other than *Prochlorococcus* can be found in Appendix D.2.

Isoprene production was found in both the axenic and bacterially contaminated cultures used in these experiments (see Appendix D.3). Rates measured in non-axenic cultures were not attributed to contaminating bacteria for the following reasons: 1) Bacterial inoculation of one *Prochlorococcus* culture in an experiment with four original axenic replicates (three remaining) had no discernible effect on isoprene production rate (axenic: $(6.4 \pm 2.4)x10^{-23}$ moles $cell^{-1}day^{-1}$; xenic: $(6.9 \pm 1.7)x10^{-23}$ moles $cell^{-1}day^{-1}$). 2) Additionally, isoprene production rates from two distinct experiments were compared, one with four replicates of axenic MIT MED4 *Prochlorococcus*, and one with four replicates of xenic MIT MED4 *Prochlorococcus*, and found to be statistically the same [$(0.9 \pm 0.2)x10^{-22}$ moles $cell^{-1}day^{-1}$ and $(1.2 \pm 0.3)x10^{-22}$ moles $cell^{-1}day^{-1}$, respectively].

Evidence was also found for production of methyl bromide, methyl chloride, and perhaps methyl iodide, by *Prochlorococcus* strain ss120 (Table 8). The methyl bromide production rate in exponential phase was on the order of $6x10^{-23}$ moles $cell^{-1}$ day^{-1}, or $0.01x10^{-6}$ moles $(g\ chlorophyll\text{-}a)^{-1}$ day^{-1}. It should be noted that only single gas samples were analyzed for the culture and blank at each of two time steps, one in exponential phase and one in stationary phase. Enhanced production rates for methyl bromide were found in stationary

Table 8. Methyl Halide Production Rates

	Per Cell *	**Per Cell ***	**Per Chlorophyll ***
	Exponential	Stationary	Exponential
CH_3Br	$6x10^{-23}$	$1x10^{-22}$	$7x10^{-8}$ **
CH_3Cl	$2x10^{-21}$	$6x10^{-22}$	$2x10^{-6}$ **

* Production rates in moles $cell^{-1}$ day^{-1} and moles $(g\ chlorophyll\text{-}a)^{-1}$ day^{-1} for *Prochlorococcus* strain SS120. Methyl iodide is not included in the table as it was not possible to calibrate it quantitatively. For comparison, Scarratt & Moore (1996, 1998) report rate ranges of <0.1 to $1x10^{-6}$ moles $(g\ chlorophyll\text{-}a)^{-1}$ day^{-1} for CH_3Cl, and of <0.1 to $1.4x10^{-7}$ moles $(g\ chlorophyll\text{-}a)^{-1}$ day^{-1} for CH_3Br ; Saemundsdottir & Matrai (1998) report 0.1 to $3x10^{-7}$ moles $(g\ chlorophyll\text{-}a)^{-1}$ day^{-1} for CH_3Br.

** Estimated from rates in moles $cell^{-1}$ day^{-1} and assumed typical chlorophyll-a content for ss120 of 0.9 fg $cell^{-1}$ at the experimental irradiance (Moore, 1995).

phase as compared to exponential phase (factor of 1.8); however, the opposite trend was found for methyl chloride (factor of 0.2).

Production rates of isoprene for the various phytoplankton cultured are shown in Table 9. Rates can be presented normalized to either cell number, cellular chlorophyll content, cell volume, or cell biomass. The biggest variation across species occurs when the rates are normalized to cell volume; the smallest variation occurs with a cellular chlorophyll content normalization. Figure 12 shows the distribution of isoprene production rates from this work, in moles cell^{-1} day^{-1}, as a function of organism size, in $(\mu m)^3$. A general trend of increasing isoprene production with organism size is clear, despite the limited data points. Note that the growth irradiance for the *M. pusilla*, *P. calceolata*, and *E. huxleyi* strain 373 cultures was ~ 45 μE m^{-2} s^{-1}, whereas the other cultures were grown at ~ 90 μE m^{-2} s^{-1}. A correction factor of 1.5 can be applied to the isoprene production rates measured at ~ 45 μE m^{-2} s^{-1} if we assume the irradiance dependence of isoprene production by *Prochlorococcus*, as discussed below, also applies to these three species. If the corrected relationship (dotted line) of isoprene to cell volume is extrapolated to approximately 400 $(\mu m)^3$, which is the average of our estimated volumes for cells tested by Milne et al. (1995), we estimate an isoprene production rate of approximately 3.3x10^{-18} moles cell $^{-1}$ day^{-1}. This figure corresponds well to the rates they report of (1 to 7) x10^{-18} moles cell^{-1} day^{-1}.

Given that isoprene production seems to be linked to cell metabolism, we did a series of experiments to examine the relationship between the growth light intensity and production rates. For these experiments, a *Prochlorococcus* MED4 stock culture was transferred to a range of light levels and grown for several generations until balanced growth was established. Thus the isoprene production rates reported are for long term steady state growth and photosynthesis rates at different light intensities, as opposed to the short term photosynthesis rates measured in similar experiments for higher plants (e.g. Monson & Fall, 1989; Loreto & Sharkey, 1990). *Prochlorococcus* growth rates increase rapidly with irradiance, then saturate at much lower PAR than other similar cyanobacteria, such as *Synechococcus* (Moore & Chisholm, 1999). Inhibition of growth and photosynthesis due to high light intensity for the MED4 strain occurred at approximately 150 μE m-^{2} s^{-1} and above

Table 9. Representative production rates of isoprene for a variety of phytoplankton

Culture	Cell Volume, $(\mu m)^3$	Cellular Dry Weight, fg $cell^{-1}$	Moles isoprene $cell^{-1}$ day^{-1} *	μmoles isoprene $(g\ chl\text{-}a)^{-1}$ day^{-1}*	10^{-20} moles isoprene $\mu m^{-3} day^{-1}$ *	nmoles isoprene $(g\ dry\ weight)^{-1}$ day^{-1} *	Reference
Prochlorococcus axenic MED4	0.13±0.08	155 ± 57	$(1.4\pm0.8)\times10^{-21}$	1.5 ± 0.9	1.1 ± 1.3	9 ± 8	This work
Prochlorococcus MIT 9401			$(1.7\pm1.3)\times10^{-21}$				This work
Prochlorococcus ss120			$(1.1\pm0.3)\times10^{-21}$				This work
Synechococcus sp. WH 8103	0.4 ± 0.3	320 ± 57	$(4.9\pm4.7)\times10^{-21}$	1.4	1.2 ± 1.9	15 ± 7	This work
Micromonas pusilla CCMP 489	7 ± 4	2340	$(2\pm1)\times10^{-20}$**	1.4 ± 0.8	0.3 ± 0.3	9	This work
Pelagomonas calceolata CCMP 1214	14 ± 9	4860	$(5.7\pm4.4)\times10^{-20}$**	1.6 ± 1.6	0.4 ± 0.6	12	This work
Emiliania huxleyi WH 1387			$(2\pm2)\times10^{-19}$				This work
Emiliania huxleyi CCMP 373	70 ± 28	25000	$(3.8\pm2.1)\times10^{-19}$**	1.0 ± 0.5	0.5 ± 0.5	19	This work
Skeletonema costatum CCMP 1332	385			1.8			Estimated † ; McKay et al., 1996††
Emiliania huxleyi MCH			2.3×10^{-18}				Milne et al., 1995‡

* Isoprene production rates, in moles day^{-1}, normalized to one of four cellular parameters: cell count ($cell^{-1}$), chlorophyll content ($(g\ chl\text{-}a)^{-1}$), cell volume(μm^{-3}), or cell biomass ($(g\ dry\ weight)^{-1}$). Averages and standard deviations (±1σ) are presented for all points in exponential phase growth from all replicate flasks of the same organism. Exceptions are for *M. pusilla*, *P. calceolata*, and *E. huxleyi* (strain WH 1387) cultures where only 1 flask was examined; in these cases we present the average and standard deviations (±1σ) values for all measured rates in exponential phase. Errors are not presented unless normalization parameters were determined in this work.

** Note that the growth irradiance for the *M. pusilla*, *P. calceolata*, and *E. huxleyi* 373 cultures was ~ 45 μE m^{-2} s^{-1}, whereas all other cultures were grown at ~ 90 ± 5 μE m^{-2} s^{-1}; we expect the difference to be about a factor of 2.

† Values from McKay et al. (1996) were estimated by calculating blank-corrected rates from their concentration plots. No error estimate was calculated due to the following uncharacterizable assumptions used: 1) Incubation liquid volume changed from an initial 3 L + 350 mL inoculum - (22 mL $sample^{-1}$)(1 sample day^{-1})(time interval in days from rate estimation), 2) Constant cellular chlorophyll content over the three month incubation for *S. troichoidea* and *S. costatum*.

††, ‡ Average growth irradiance for McKay et al. (1996) was 85 μE m^{-2} s^{-1}, but was not reported for Milne et al. (1995).

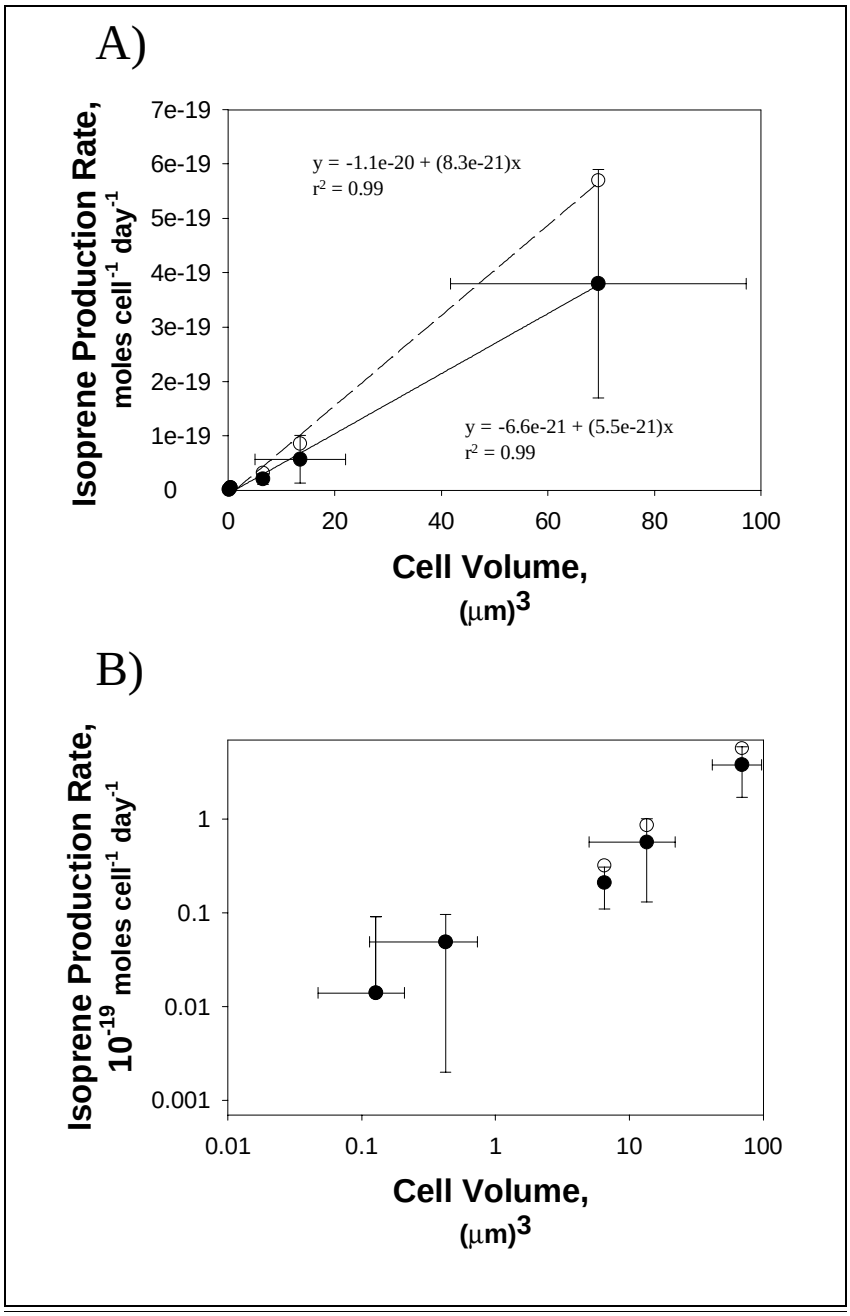

Figure 12: Isoprene Production Rate for Several Organisms A) Isoprene rates are determined from compiling all experiments, n, done with each organism, and are explained in Table 9. The organisms included, in order of increasing size are *Prochlorococcus* (n=8), *Synechococcus* (n=2), *Micromonas pusilla* (n=1), *Pelagomonas calceolata* (n=1), and *Emiliania huxleyi* (n=2). On this scale *Prochlorococcus* and *Synechococcus* appear as one point near 1 $(\mu m)^3$. Error bars in cell volume for these organisms are smaller than the symbols. Both original data (filled circles) and data corrected from growth at ~ 45 to ~ 90 $\mu E\ m^{-2}\ s^{-1}$ (open circles) are plotted for the 3 largest organisms (see text and Chapter 5). Linear fits to the data are plotted and discussed further in this chapter and Chapter 5. B) As for panel A, but with both cell volume and isoprene production rate on a log scale.

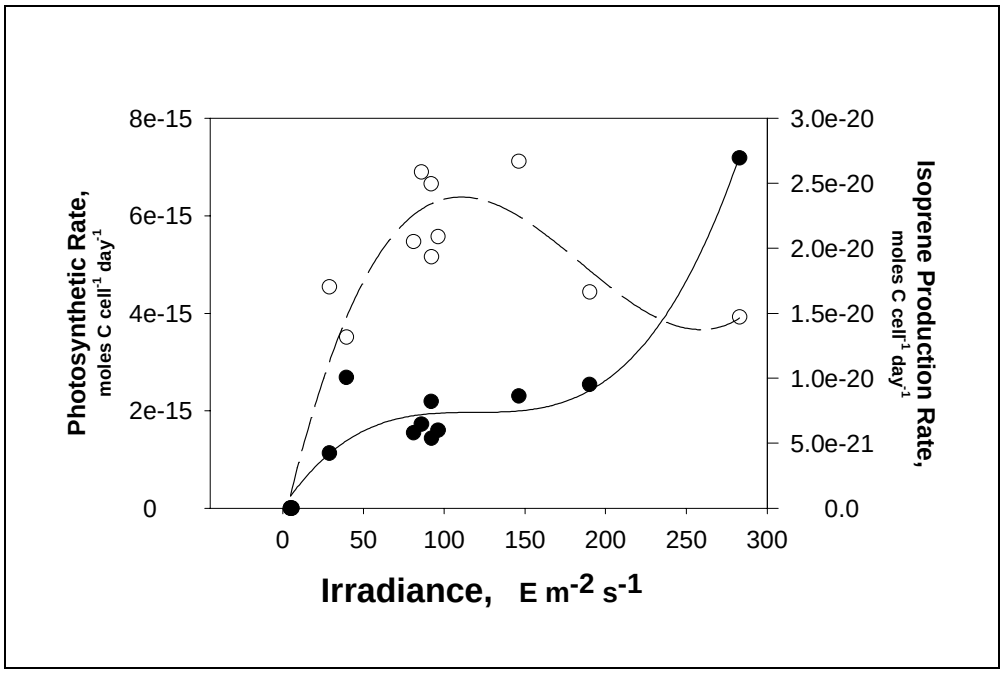

Figure 13. Effect of Growth Irradiance on Isoprene Production. Isoprene production rate (moles C cell^{-1} day^{-1}) is shown in filled circles, and photosynthesis rate (moles C cell^{-1} day^{-1}) is shown in open circles, calculated as in the text, for Prochlorococcus MED4 cultures. Photosynthesis rates at 4.8 and 5.6 E m^{-2} s^{-1} are zero. Note the isoprene production rate values of zero at those irradiances (open circles are located under the filled circles) at were not determined experimentally, but were assumed to be zero due to an observed growth rate of zero for the cultures. As we have never observed any isoprene production without cell growth, this is a reasonable assumption.

(Figure 13). The data appear to follow the expected shape for photoinhibited phytoplanktonic photosynthesis (Platt et al., 1980): a linear increase to a maximum, then a sharp initial decrease at higher irradiances which levels off. The isoprene production rate also increases with irradiance below 100 E m^{-2} s^{-1}, and continues to increase up to 283 E m^{-2} s^{-1}, the maximal irradiance tested.

The dependency of isoprene production on photosynthesis was further examined by subjecting cultures to extended darkness. Replicate flasks inoculated with equal volumes of the same stock culture were allowed to grow to mid-exponential phase. At this point one flask was placed in the dark. After 23 hours there was virtually no difference (3%) in cell counts between the two flasks (see Figure 14A), but chlorophyll fluorescence per cell measured by the flow cytometer had increased (see Figure 14B), indicating the

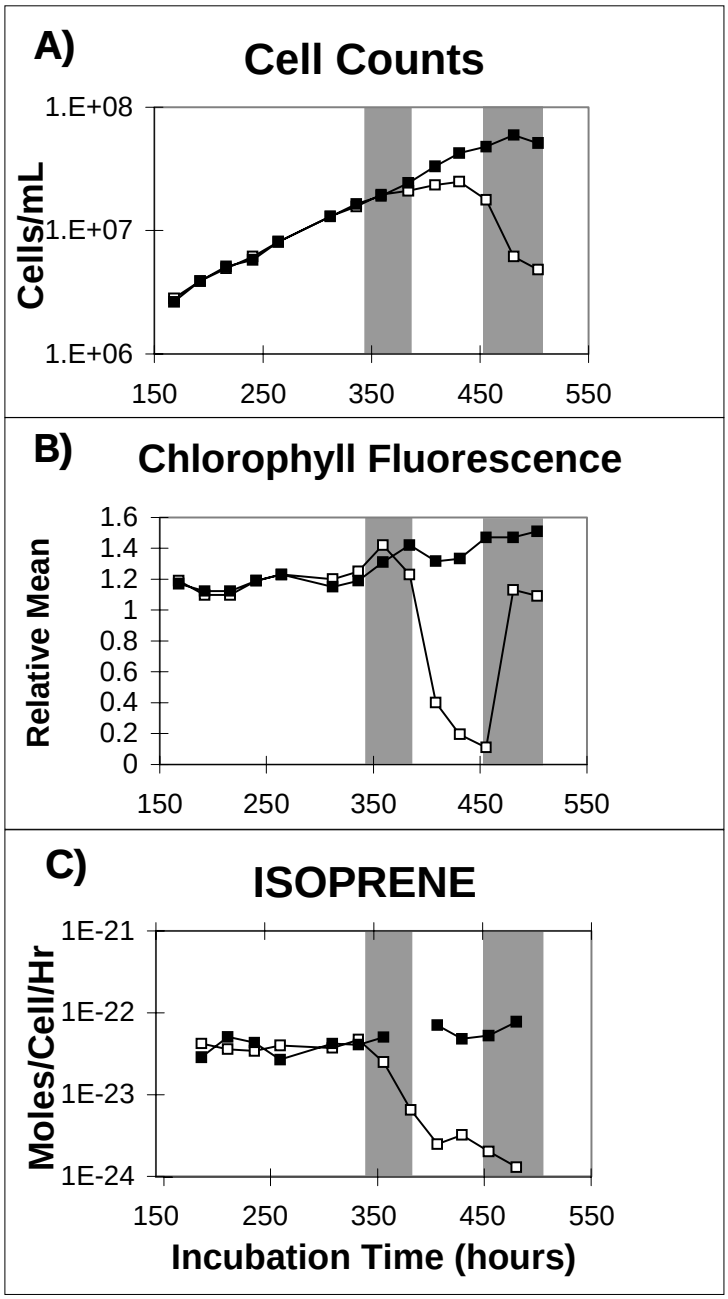

Figure 14: Effect of Extended Darkness Periods on Isoprene Production A) Cells mL^{-1} of Prochlorococcus strain SS120. Filled squares represent the reference culture, open squares the darkened culture. Cells were grown on a 14:10 hour light:dark cycle, on top of which the darkened culture was exposed to complete darkness for the time periods outlined by the gray bars. B) Mean chlorophyll fluorescence per cell for the two incubation cell populations. C) Corresponding isoprene production.

Prochlorococcus cells were showing signs of low-light stress. Also, isoprene production had dropped slightly (Figure 14C). After 48 hours, cell growth rates had slowed from 0.25 day^{-1} to 0.08 day^{-1}, and isoprene production had decreased to about 16% ($6.5x10^{-24}$ moles $cell^{-1}$ hr^{-1} or $1.6x10^{-22}$ moles $cell^{-1}$ day^{-1}) of the average mid-exponential value [$(3.9\pm0.5)x10^{-23}$ moles $cell^{-1}$ hr^{-1} or $[(9.4\pm0.1)x10^{-22}$ moles $cell^{-1}$ day^{-1}]. The culture was then exposed to light again at the same level which it had experienced previous to darkness. A drop in chlorophyll fluorescence per cell greater than about 68% occurred, with the cell growth rate remaining very low at ~ 0.08 day^{-1}. Isoprene production dropped further, but began to stabilize at a rate about 10% of the average mid-exponential rate. Three days later the culture was again darkened, and both cell counts and isoprene production decreased significantly.

The temperature sensitivity of isoprene production was also examined. Aliquots from a single MED4 stock culture were acclimated to a variety of temperatures over the entire range for *Prochlorococcus* growth (about 13 to 28 °C, Moore et al., 1995). The resulting photosynthesis and isoprene production rates are shown in Figure 15. A broad maximum in photosynthesis is observed, quite similar to Moore et al. (1995), with a sharper maximum in isoprene near 296 K (23 °C). Both datasets appear to generally follow the expected patterns of enzyme temperature response, with increasing activity from low to mid-range temperatures, and then decreasing activity at high temperatures (Kuzma et al., 1995; Singsaas et al., 1997; Fall & Wildermuth, 1998). Further information on the relationship between isoprene production rate and growth rate can be found in Appendix D.4.

Isoprene production rates from these marine phytoplankton are compared with those from several terrestrial plants in Table 10. These numbers have been compiled from all experiments performed with each organism, and the average growth irradiances for these expeirments are also noted. The rates normalized to biomass are much smaller for the marine organisms than the land plants, with those for the eukaryote larger by an order of magnitude than for the cyanobacteria. The ratio of isoprene production rate to photosynthesis rate is also presented in Table 10 and expressed as a percentage. This

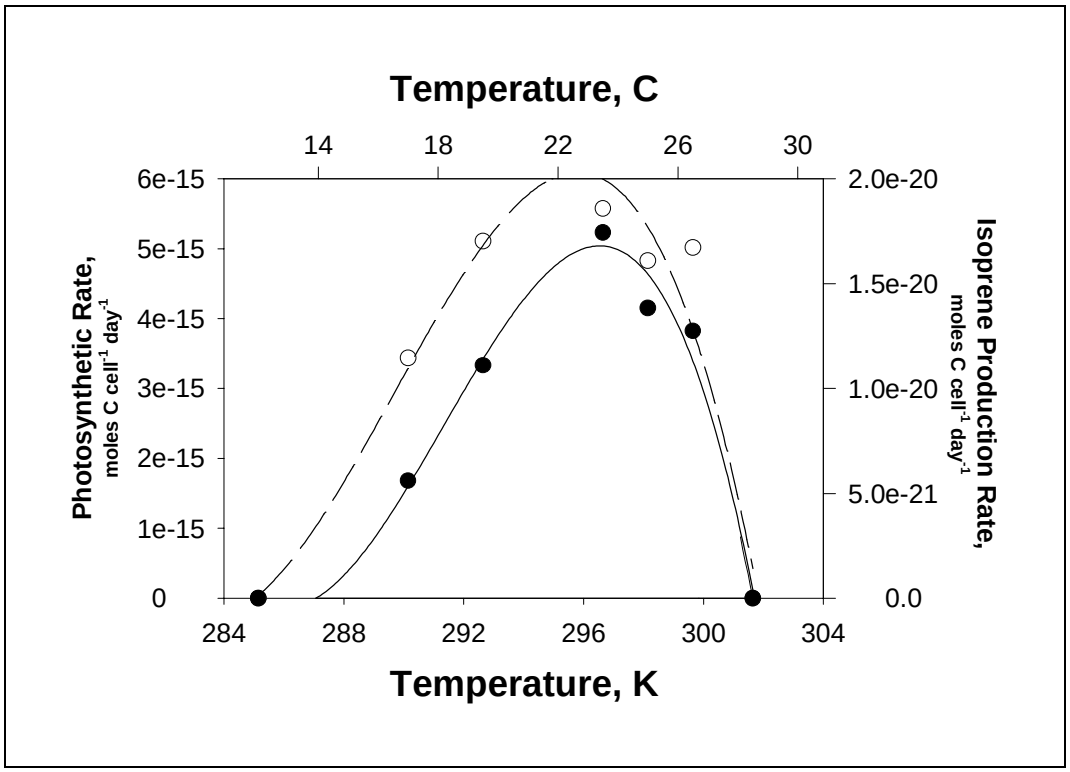

Figure 15. Temperature sensitivity of isoprene production. Isoprene production rate (moles C cell^{-1} day^{-1}) is shown in filled circles, and photosynthesis rate (moles C cell^{-1} day^{-1}) is shown in open circles, calculated as in the text, for Prochlorococcus MED4 cultures. Photosynthesis rate points at 12 and 28.5 ˚C are both zero, and are hidden under the isoprene production rate points. As in Figure 3, isoprene production rates of zero were assumed for cultures at 12 and 28.5 ˚C.

represents the amount of carbon fixed during photosynthesis that is lost to isoprene; this value is extremely small for the phytoplankton, and is on the order of 10^{-4} %.

Table 10: Marine and Terrestrial Plant Isoprene Production Rates

	Moles (g dry weight)$^{-1}$ day^{-1}	**Growth Irradiance***	**% of Carbon Fixation ****
Prochlorococcus	9 x10^{-9}	~ 90 μE m^{-2} s^{-1}	~ 10^{-4}
Synechococcus	1.5x10^{-8}	~ 75 μE m^{-2} s^{-1}	~ 10^{-4}
Emiliania huxleyi	1.9x10^{-8}	~ 45 μE m^{-2} s^{-1}	~ 10^{-4}
Pinaceae (spruce and fir)	(0.4-6)x10^{-6} †	~1000 μE m^{-2} s^{-1}	0.5-2††
Quercus (oaks)	(4-50)x10^{-6} †	~1000 μE m^{-2} s^{-1}	0.5-2††

* Approximate growth irradiance of the organisms for which isoprene production was measured. For the trees this irradiance is in the light-saturated regime. For *Prochlorococcus* and *Synechococcus*, these irradiances are just under the irradiances corresponding to optimum growth rate (~ 150 μE m^{-2} s^{-1} for *Prochlorococcus* MED4; ~ 200 μE m^{-2} s^{-1} for *Synechococcus* WH8103; Moore, 1997). If we adjust the *Prochlorococcus* rate to the optimum growth irradiance, the rate would change by approximately a factor of 1.2, assuming the cellular biomass does not change.

** Approximate % of carbon fixation lost to isoprene was calculated from isoprene and photosynthesis rates as explained in the text.

† *Pinaceae* and *Quercus* production rate ranges are taken from Kesselmeier and Staudt (1999) for standard emissions conditions (30 ºC, and 1000 mmol m^{-2} s^{-1}).

†† Percentage ranges are typical for a variety of tree species, from Tingey et al. (1979).

3.4 DISCUSSION

We report convincing and explicit evidence for isoprene production from several species of marine phytoplankton and cyanobacteria. This phenomenon has been hinted at from *in situ* correlations of isoprene and bulk chlorophyll concentrations in the water column, and seen in other studies of phytoplankton cultures, but our results help to clarify the process. We see strong links between isoprene production and healthy growth of 5 different phytoplankton species. This is not entirely unexpected, as it has been shown that isoprene biosynthesis in higher plants occurs in the chloroplasts (Sanadze et al., 1990; Lichtenthaler, 1999), which is also where photosynthesis occurs, and cyanobacteria are thought to be the

ancestors of chloroplast compartments (Madigan et al., 2000). Thus all photosynthetic organisms might be expected to produce isoprene. The only cell species grown in this work that were reported to be examined by other workers were *Emiliania huxleyi* (strain MCH) and a species of *Synechococcus* (strain DC2, which is the same as WH 7803), cultured by Milne et al. (1995). These authors reported a production from *Emiliania huxleyi* that corresponds well to our values, considering we see factor 4 or more differences for production by the same organisms over various light and temperature ranges. Although these authors note *Synechococcus* did produce isoprene, no production rate values were determined or reported.

Biosynthesis of chemicals with isoprenoid structure, such as sterols, plastiquinone, and phytol, can occur through one of two routes in higher plants. Cytosolic isoprenoids, such as sterols, are formed through the acetate/mevalonate (MVA) pathway, while plastidic isoprenoids, including isoprene, are synthesized by the 1-deoxy-D-xylulose-5-phosphate (DOXP) pathway (Lichtenthaler, 1999). Several cyanobacteria, red algae, and green algae were shown to use the DOXP pathway (Lichtenthaler, 1999; Miller et al., 1999). The only enzyme from this pathway whose genetic sequence is characterized as yet is 1-deoxy-D-xyulose-5-phosphate synthase (DXS). BLAST searches of the *Prochlorococcus* MED4 & MIT 9313 and *Synechococcus* WH 8102 strain genomes using the *dxs* gene from *Synechococcus* PCC 6301 revealed open reading frames (ORFs) in all 3 strains with high amino acid sequence homology (68% for all; all have an Evalue, or probability that the homology occurred by chance, of 0.0). The putative thiamine diphosphate binding site motif within the *dxs* sequence (Lichtenthaler, 1999) is highly conserved in all 3 strains. Additionally, neither the *Prochlorococcus* or *Synechococcus* genomes contains open reading frames with significant homology to any of four genes (*hmgA*) encoding hydroxy-methylglutaryl-CoA (HMG-CoA) reductase from bacteria, archaea, and a plant. HMG-CoA reductase is a key enzyme in the MVA pathway (Dewick, 1999), and so this implies

Prochlorococcus and *Synechococcus* produce isoprene through the DOXP pathway. It should be noted that the genome of only one strain cultured in this work is available (*Prochlorococcus* MED4). The other two strains for which we have the genome sequence were not examined in the laboratory for isoprene production. However, *Synechococcus* WH 8102 is closely related to WH 8103, which was used in this study, as they are both members of the same motile clade of *Synechococcus* genetically defined by *rpoCl* (Toledo et al., 1999) and ITS (Rocap et al., 2001).

The three methyl halides potentially produced by *Prochlorococcus* have all been previously shown to be produced by other phytoplankton at rates similar to ours (Mtolera et al., 1996; Scarratt & Moore, 1996, 1998; Saemundsdottir & Matrai, 1998). An enhanced stationary phase production rate, as we report for methyl bromide, is often seen for various halocarbons, and has been attributed to a possible autolytic source that requires intact cells (Scarratt & Moore, 1996, 1998), or to a function in relieving oxidative stress that occurs in stationary phase (Pedersen et al. 1996). The biosynthesis of methyl chloride by a fungus, red algae, and ice plant was shown to occur enzymatically from 2 reagents: chloride ions and S-adenosyl methionine (Wuosmaa and Hager, 1990), a derivative of the essential amino acid methionine. The necessary enzymes can also transform bromide and iodide ions, at efficiencies even greater than for chloride ions, although chloride ions are most common in seawater. A BLAST search of the *Prochlorococcus* and *Synechococcus* genome sequences did not find any open reading frames with significant amino acid homology to a methyl chloride transferase (MCT) gene in *Batis maritima*, a salt march succulent (Ni & Hager, 1998). This could indicate there is no MCT gene in *Prochlorococcus*, or that its form is quite different from the only published gene sequence. During field measurements in the north Atlantic Ocean, Smythe-Wright et al. (1999) found correlations between divinyl-chlorophyll-a, a specific pigment marker for the Prochlorophytes, including *Prochlorococcus*, and dissolved methyl iodide concentrations at various depths in the water

column. There was a supersaturation of over 1000% for methyl iodide during the bulk of the measurements. However, Baker et al. (1999) found no correlation between divinyl chlorophyll-a and methyl bromide concentrations in the surface waters of a northeast Atlantic cruise track. This combination of evidence for a potential *Prochlorococcus* production of methyl halides is intriguing as the global source-sink balance of these chemicals is still not understood (Butler, 2000).

Light and temperature are the primary control mechanisms for isoprene production and emission in higher plants. Over a variety of light levels isoprene production responds similarly to leaf photosynthetic CO_2 assimilation or photosynthetic electron transport (Monson and Fall, 1989, Loreto and Sharkey, 1990, Niinemets et al., 1999), although isoprene production does not completely saturate at high light intensity (Monson et al., 1992; Keller and Lerdau, 1997). The increase of isoprene production rate with irradiance in *Prochlorococcus*' light-limited region (< 150 $\mu E\ m^{-2}\ s^{-1}$) is similar to what has been seen for higher plants. Increases continued through light saturation and into the inhibition regime (> 150 $\mu E\ m^{-2}\ s^{-1}$). The maximum isoprene production rate observed here is over 4.5 times that near light saturation. This results in a much higher percent of photosynthetically fixed carbon being lost in the light-inhibited (~7.8×10^{-4} % at 283 $\mu E\ m^{-2}\ s^{-1}$) as compared to light-limited regimes [$(1.2 \pm 0.1) \times 10^{-4}$ %]. Factor of two higher percentages have been observed at high irradiances for several tropical trees (Lerdau & Throop, 1999). However, it should be noted that the isolated datum at 283 $\mu E\ m^{-2}\ s^{-1}$ contributes significantly to these deductions.

Terrestrial higher plant isoprene production by healthy leaves has been shown to cease within minutes of applying darkness (Harley et al. 1999; Loreto & Sharkey, 1990). In our experiment, isoprene production showed a 37% reduction at 24 hours past darkness application, and approximately an 84% reduction after 48 hours. This may be due to a lack of newly fixed carbon (Monson and Fall, 1989; Loreto and Sharkey, 1990; Loreto and

Sharkey, 1993), although it has been shown that isoprene production does not immediately drop, as does photosynthesis, when CO_2 is removed, and it can continue at a minimal level using carbon reserves (Lerdau, 1997; Monson and Fall, 1989; Loreto & Sharkey, 1990). This may explain the non-zero production after several days of darkened incubation. It is also possible that low levels of isoprene emission could be produced by non-enzymatic hydrolysis of cellular DMAPP (Fall 1999), although this seems to be most efficient at very low pH (~ 1; Deneris et al., 1985).

Lewis et al. (2001, 1999) reported diurnal concentration profiles for several NMHC, including isoprene, in boundary layer air reaching both Mace Head, Ireland and Cape Grim, Tasmania. Air parcels determined to be of oceanic origin had NMHC maxima at local solar noon and minima (usually near detection limits) during the night. The most abundant oceanic alkenes are known to have photochemical sources in the water column which likely explain their diurnality (Lee & Baker, 1992; Ratte et al., 1993; Ratte et al., 1998; Riemer et al., 2000). Terrestrial isoprene production also exhibits a daytime maxima in concentration, usually in middle to late afternoon (Lewis et al., 2001; Fehsenfeld et al., 1992). This work demonstrates that phytoplanktonic isoprene production is also a function of light intensity. It is logical that the maximum PAR flux at the surface near solar noon penetrates deepest into the water column, potentially increasing biological isoprene production substantially. Laboratory cultures have been shown to re-acclimate to irradiance changes of ~50 uE m^{-2} s^{-1} after about 1 day (Cailliau et al., 1996). Dusenberry et al. (2001) also demonstrate photoacclimation kinetics for field populations of *Prochlorococcus* of 0.9 - 2 day^{-1}, so the cells can clearly adjust to variations in irradiance on such time scales. Whether isoprene production can be induced in phytoplankton that rapidly, and if the gas can be mixed to the surface and transferred to the atmosphere soon after, is unknown.

Temperature profiles from both leaf cuvette experiments (Monson & Fall, 1989; Sharkey & Loreto, 1993), and a willow leaf isoprene synthase *in vitro* (Monson et al., 1992), show an

exponential increase of isoprene emission with temperature to a maximum around 40 - 45 °C, then a rapid decline. Thus isoprene production by vegetation appears linked to photosynthetic processes, but likely not directly as isoprene continues to be actively synthesized at high temperatures (~ 30 °C) when photosynthetic rates begin to cease (Monson et al., 1992). As for higher plants, isoprene production from *Prochlorococcus* also increases with temperature to an maximum, then decreases at higher temperatures. However, this maximum occurs at a temperature (~ 23 °C) at which the photosynthetic rate is also maximal.

Because of its distinct relationship with temperature in terrestrial plants, isoprene production has been hypothesized to function as a thermal protectant. Singsaas et al. (1997) showed that the temperature at which thylakoid membranes in a kudzu vine were irreversibly heat-damaged was increased by 3-10 °C when immersed in an isoprene-containing environment. However, attempts by other researchers to repeat these results were unsuccessful (Logan & Monson, 1999). Hanson et al. (1999) hypothesize that higher plant isoprene emission would have evolved as land was colonized by originally aquatic plants. The potential isoprene production would have been an advantage as they were adjusting to a lower heat capacity environment. Following this argument, it would be expected that marine photosynthetic organisms would have a significantly reduced need for the hypothesized thermoprotective function. Our results are consistent with this idea, since the amount of carbon fixed by the cultured phytoplankton lost to isoprene is several orders of magnitude smaller than for land plants, and phytoplanktonic isoprene production has a temperature optimum coincident with the maximum in photosynthesis.

Other compelling theories for isoprene's role in leaf metabolism are as a sink for excess energy or reducing power (Fall, 1991), or as an overflow metabolite (Wagner et al., 1999). Our high isoprene production rates in the *Prochlorococcus* photoinhibited regime might support the former theory. Photoinhibition in phytoplankton occurs when the photosystem

II repair cycle is damaged such that proteins necessary for energy transfer are degraded faster than they can be replaced. If the electron capture capacity of the cell exceeds the rate of energy transfer, or photosynthetic electron transport, the result is a light-dependent drop in the quantum yield of photosynthesis (Campbell et al., 1998). In this case the excess energy could then be shunted to isoprene. While our measurements do not eliminate any of these possibilities for phytoplankton, such small amounts of isoprene production (10^{-4}% of the photosynthetic carbon fixation rate, as opposed to 0.5-2% for terrestrial higher plants (Tingey et al., 1979; Monson & Fall, 1989)) seem likely to be a carbon 'leak' as opposed to a functional release.

Assuming that similar physiological patterns of isoprene production occur *in situ* as for the laboratory incubations, we can make a rough estimate of the maximum sea-to-air flux of isoprene for the oligotrophic oceans. In oceanic regions with extremely low nutrient levels, the microbiology is controlled by the microbial loop (Azam, 1983), where potentially fast phytoplankton growth rates derived from bacterial nutrient recycling are rapidly controlled by grazing (Waterbury & Valois, 1993; Liu et al., 1997; Mann & Chisholm, 2000) or phage lysis (Suttle & Chan, 1994). In this scenario, weak seasonal scale variations in cell abundance exist. *Prochlorococcus, Synechococcus,* and picoeukaryote cell abundances have been shown to vary by factors of 2, 3-4, and 3, respectively, in the North Pacific, and by factors of 3,5, and 2, respectively, in the Sargasso Sea over such time scales (Olson et al., 1990; Campbell et al., 1997). We assume a seasonally averaged water column characteristics as measured in the JGOFS Equatorial Pacific cruises (Binder et al., 1996; Bidigare & Ondrusek, 1996; http:// www1.whoi.edu/jgofs.html). This provides direct flow cytometric counts of *Prochlorococcus*, *Synechococcus*, and picoeukaryotes (representing a significant fraction of the total chlorophyll), as well as bulk chlorophyll concentrations in the water column, in both spring and fall at 0 °N, 140 °W. Using the representative isoprene production rates measured in this work for each group of organisms (in units of

either moles cell^{-1} day^{-1} or moles (g chlorophyll-a)$^{-1}$ day^{-1}), we can calculate a depth-integrated seasonal average of isoprene production in the mixed layer (Table 11; further explanations and calculations can be found in Chapter 5). This assumes a one dimensional (e.g. no horizontal mixing) profile, and that all isoprene produced in the mixed layer is vented to the atmosphere (hence we designate our estimates as maximum). These estimates of maximum local isoprene fluxes are quite similar to recent estimates of actual fluxes from other open ocean sites calculated from *in situ* measured seawater and atmospheric boundary layer concentrations (Bonsang et al., 1992; Milne et al., 1995; Broadgate et al., 1997; Baker et al., 2000), despite different biogeographical characteristics of the various regions. Optimally, depth profiles of cell counts of representative phytoplankton groups in a given region would be measured concurrently with NMHC concentrations to provide these estimates. Then maximum isoprene fluxes could be calculated by incorporating laboratory production rates and compared directly to the measured fluxes to give a first order estimate of the isoprene cycling rates in the ocean mixed layer.

Table 11. Calculated sea-to-air isoprene fluxes.

	Location	**10^7 Molecules (cm)$^{-2}$ s^{-1}**	**Tg C yr^{-1}**
This work *	Eq. Pacific	8.6 (3.6)	1 (0.4)
Baker et al., 2000 **	North Sea	3.5	0.4
Broadgate et al., 1997 **	North Sea, Southern Ocean	1.7	0.19
Milne et al., 1995 **	Florida Straits	3.4	0.38
Bonsang et al., 1992 **	Eq. Pacific, N. Atlantic, and Mediterranean	11	1.2

* Fluxes from this work determined as in the text. Entry in parenthesis was calculated from isoprene production rates in moles (g chlorophyll-a)$^{-1}$ day^{-1} and water column chlorophyll content.

** Fluxes from the literature are either reported directly or extrapolated to the globe using an open ocean area of 3.62×10^{14} m^2 (Broadgate et al., 1997).

† Baker et al. (2000) values were taken as the average of all offshore measurements.

3.5 CONCLUSIONS

Isoprene production was detected and quantified from several phytoplankton species in laboratory cultures. Cell-normalized production rates varied with cellular growth phase; constant, maximum rates were achieved in balanced exponential phase, while decreasing rates were found during the senescent phase. Larger cells produced more isoprene on a per cell basis than smaller cells. The light sensitivity of isoprene production rates per cell were similar in pattern to those previously reported in the literature for higher plants, however the temperature sensitivity of isoprene production rates per cell maximized at the same temperature that growth rate maximized. Results suggest that if the production rates measured here are extrapolated under certain conditions to the open ocean, the resulting maximum sea-to-air fluxes of isoprene are the same order of magnitude as previously observed fluxes determined from air and water concentrations.

CHAPTER FOUR

EVIDENCE FOR MINIMAL ROLES OF PHYTOPLANKTON AND HETEROTROPHIC MICROBES IN OCEANIC NON-METHANE HYDROCARBON CYCLING

Light (C_2-C_6) non-methane hydrocarbons (NMHC) are present in the upper ~ 200 m of the open (unpolluted) oceans at concentrations reaching > 100 pmol L^{-1}. Previous work has shown that oceanic sources include phytoplankton and photochemical processes. However, only a few phytoplankton have been studied, and no assessment has been performed of the effects of other pelagic microorganisms on NMHC cycling. We report here no clear production or consumption of any NMHC, except isoprene, by five phytoplankton species tested in controlled laboratory experiments. The presence of heterotrophic bacteria in phytoplankton cultures had no effect on isoprene production rates per phytoplankton cell, although a temporary isoprene production was seen in bacteria-only cultures grown in enriched organic media. Nanoflagellate grazing by *Cafeteria roenbergensis* on *Prochlorococcus* had no detectable effect on the cycling of any NMHC. The only effect of these organisms was to control total isoprene produced in the flask through phytoplankton cell counts. Besides controlling phytoplankton counts, infection by phage decreased the isoprene production rate per cell during latent period of infection as compared to healthy cells. Any effect the several organisms studied may have on NMHC cycling, other than for isoprene, likely involves other processes (such as photchemistry) as well as biology.

4.1 INTRODUCTION

Evidence for an oceanic source of reactive non-methane hydrocarbons (NMHC) was first presented by Swinnerton and Linnenbon (1967) and subsequently confirmed by many others (e.g. Bonsang, 1992; Donahue & Prinn, 1990, 1993). Seawater concentrations can reach >100 pmol L^{-1}, and are largest for the smallest molecular weight C_2-C_3 compounds (Bonsang et al., 1992; Plass-Dulmer et al., 1995; Broadgate et al., 1997). Emission into the atmosphere is considered to be the major loss process (Reimer et al., 2000), and anti-correlations of surface water NMHC concentration with transfer velocity have been found (Ratte et al., 1995; Plass-Dulmer et al., 1995; Pszenny et al., 1999). However there are no reported examinations of potential biological or chemical losses in the water column. Total NMHC flux estimates (summed over a range of individual NMHCs) calculated from *in situ* measured ocean and air concentrations and bulk flux formulae range from 2 to 50 Tg yr^{-1} (Bonsang et al., 1988; Milne et al, 1995; Plass-Dulmer et al., 1995). Fluxes of this magnitude may be significant for atmospheric boundary layer photochemistry in certain regions (Donahue & Prinn, 1990, 1993; Carlslaw et al., 1998). Many NMHC have a distinct seasonal cycle in surface water concentration with amplitudes of approximately 2 orders of magnitude, and with summer maxima and winter minima (Broadgate et al., 1997). Significant variability on much shorter time scales is also observed, potentially obscuring relationships of NMHC to environmental parameters (Plass-Dulmer et al.,1995; Ratte et al., 1995)

While isoprene production has been shown to have distinct relationships with phytoplankton abundance and bulk chlorophyll concentration (Bonsang et al., 1992; Moore et al., 1994; Milne et al., 1995; McKay et al., 1996; Broadgate et al., 1997; Baker et al., 2000; this work), production of other alkenes appears to be additionally or exclusively linked to

photochemistry. Culture experiments have demonstrated that phytoplankton-derived dissolved organic carbon (DOC) (Wilson, 1970; Ratte et al., 1993), possibly polyunsaturated fatty acids (PUFA) (Lee & Baker, 1992), can be transformed photochemically into NMHC (Ratte et al., 1998; Reimer et al., 2000). Release of potential NMHC precursors may occur during both normal phytoplankton metabolism and when the cells are lysed (Schobert & Elstner, 1980; Lee & Wakeham, 1989). While it is rare to observe *in situ* correlations of non-isoprene alkenes with bulk chlorophyll concentrations (Ratte et al., 1995; Broadgate et al, 1997), Ratte et al. (1995) detected a weak correlation between ethene and "photochemically-reactive DOC" (defined as the DOC oxidized during UV incubation) for limited samples in the Atlantic.

The sources of alkane species have been more nebulous. Links to a photochemical origin have been found, such as a weak correlation with photochemically-reactive DOC (Ratte et al., 1995). However, UV and short-wavelength visible laboratory incubations had no discernable effect on alkanes (Ratte et al., 1998; Reimer et al., 2000). Additionally, ethane and propane production has been observed in some phytoplankton cultures (Schobert & Elstner, 1980; McKay et al., 1996), although reported *in situ* correlations with bulk chlorophyll concentrations are sparse.

It is possible that other pelagic microorganisms, such as heterotrophic bacteria, protists, or phage, can affect NMHC cycling in the water column. This could be through a direct production or consumption, or through interactions with the phytoplankton and/or their exudates. For example, grazing on (or phage lysis of) phytoplankton which produce dimethylsulfonium propionate (DMSP) results in enriched water column DMSP concentrations, which are then transformed by DMSP lyase-containing organisms into dimethylsulfide (DMS) (Dacey and Wakeham, 1986; Wolfe & Steinke, 1996; Hill et al., 1998; Malin et al., 1998). Perhaps grazing on, or phage lysis of, phytoplankton is a source of biologically-derived precursors of NMHC. Additionally, neglecting these

microorganisms gives an incomplete picture of the surface oceans, particularly in oligotrophic regions where the microbial loop is dominant (Azam et al., 1983). Here bacterial biomass can often dominate the < 20 μm size fraction (Li et al., 1992; Cavender-Bares, 2001), and grazing controls phytoplankton distributions (Mann & Chisholm, 2000; Waterbury and Valois, 1993; Suttle and Chan, 1994). Also, grazing, in combination with phage lysis, controls bacteria populations in these regions (Fuhrman et al., 1999).

4.2 METHODS

Our study involved incubations, microorganism characterization, NMHC analysis, and microbial genomics, all of which are discussed below.

4.2.1 Experimental Design

Phytoplankton stock culture aliquots of 10-20 mL were incubated with ~ 500 mL media. When necessary, ~50 mL aliquots of protists were added in mid-exponential phase. For phage experiments, 1 mL and 100 μL phage stock aliquots (at ~ 10^7 phage mL^{-1}) were each combined with 19 mL of phytoplankton inoculum (~ $5x10^8$ cells mL^{-1}) and allowed to mix in a 25 mm diameter test tube for 20 minutes before flask inoculation (500 mL media). This allows for sufficient diffusive mixing for phage adhesion onto cells despite the low multiplicity of infection (MOI; defined as the ratio of phage counts to cell counts at inoculation) of 0.001 and 0.0001. Experiments were performed in 1 L Erlenmeyer flasks at 23 ± 1.5 °C; the gas and liquid sampling, sample preservation, and pigment analysis protocols are described in detail in Chapter 3.3.

4.2.2 Culturing, flow cytometry, and microscopy

4.2.2.1 Phytoplankton: *Prochlorococcus* (strains MIT 9401, SS120, axenic and xenic MED4 (CCMP 1378)), *Synechococcus* (axenic WH 8103), *Emiliania huxleyi* (WH 1387), *Micromonas pusilla* (CCMP 489) and *Pelagomonas calceolata* (CCMP 1214) were cultured

as described in Chapter 3.3. Relevant flow cytometric techniques are also described in that section.

4.2.2.2 Heterotrophic Bacteria: Bacteria were isolated from Charles River water (Cambridge, MA) by filtration with 1.2 μm pore diameter Poretics filters. Laboratory bacterial stock cultures of *H. halodurans* (previously *Pelagomonas halodurans* - Lim, pers. comm.) were also cultured. All bacteria were grown in the dark at 24.5 ± 2.8 ºC on a seawater-based medium enriched with DIFCO-AC yeast extract (final concentration 0.005% wt./vol.). Bacteria counts were performed as in Chapter 3.3. Cell biomass for *H. halodurans* was taken from Caron et al. (1991), as the stock used here was derived from ones used in that work.

4.2.2.3 Nanoflagellate Protist: *Cafeteria roenbergensis* (Strain SR6), originally isolated from coastal Rhode Island, USA seawater (Lim et al., 2001), was maintained on either *H. halodurans* in yeast media or *Prochlorococcus* cultures in Pro99 media. The protist was acclimated to prey cultures of *Prochlorococcus* for at least one week before experimentation. Grazer cell counts were obtained using a DNA staining protocol (see Appendix C.2). In short, culture samples of 1 mL were mixed with 10 μL of 10 mg mL^{-1} DAPI and 50 μL 10% formalin for 15 minutes in the dark before filtration onto a 0.8 μm pore diameter black top filter and 0.45 μm pore diameter regular bottom filter (Poretics) using < 5 mm Hg vacuum. Microscope counting was performed with a UV filter. Culture samples were diluted, if necessary, to ensure accurate counting. Grazing rates were determined from

$$g = \left[\frac{\ln(N_2) - \ln(N_1)}{t_2 - t_1}\right] - \left[\frac{\ln(M_2) - \ln(M_1)}{t_2 - t_1}\right] \qquad (1)$$

where g is the specific grazing rate (day^{-1}), and N and M are the phytoplankton concentrations (cells mL^{-1}) in the reference and grazed incubations, respectively, at times t_1

and t_2. The first and second terms in this equation are the specific growth rates of the phytoplankton in the reference and grazed cultures (day^{-1}), respectively.

4.2.2.4 *Prochlorococcus* Phage: Concentrated phage stocks specific for *Prochlorococcus* MED4 were obtained from M. Sullivan (MIT/WHOI), and kept in the dark at 4 °C until use (Sullivan, 2001). Phage titers were determined by a "Most Probable Number" (MPN) analysis method (Waterbury & Valois, 1993). Cell stock aliquots of 30-60 μL were incubated in 150-120 μL Pro99 media (total 180 μL) in 96-well plates. Ten replicate control wells of media and cells were established, as well as 10 replicate wells each of a variety of phage treatments. Treated wells contained the media and cell mixture described above, plus phage samples from the cultures at various serial 10-fold dilutions (to 75 μL). Plates were incubated in continuous low light (30 μE m^{-2} s^{-1}), and 19 °C, and were monitored daily for cell growth and clearing (phage lysis), and MPN statistics were calculated as per Gerhardt (1981).

4.2.3 Hydrocarbon analysis

Analytical techniques are identical to those in Chapter 3. In situations where no direct link between individual NMHC and the cultured cells could be found, production rates are normalized to culture liquid volume instead of cell parameters.

4.2.4 Genomics

BLAST searching was carried out on the genomes of *Prochlorococcus* MED4 and MIT 9313 strains, and *Synechococcus* WH 8102. These are publicly available at the DOE-JGI Microbial Genomics website (http://spider.jgi-psf.org/JGI_microbial/ html/). The amino acid sequences used for BLAST comparisons had Genbank Accession numbers as follows: ACC synthase genes - *Malus x domestica* 6980404, *Penicillium citrinium* BAA92149; ACC oxidase genes - *Petunia x hybrida* Q08506; ACC deaminase genes - *Penicillium citrinium*

BAA92150; Ethylene-forming-enzyme - *Pseudomonas syringae* AAB32415; Alkane monooxygenases - *Pseudomonas putida* gene cluster AJ245436, *Pseudomonas chlororaphis* CAB59525, *Pseudomonas erythropolis* CAB40951; Alkene monooxygenases - *Nocardia corallina* D37875, *Xanthobacter sp*. AJ012090; Putative isoprene monooxygenases - *Rhodococcus sp. AD4* alpha subunit CAB55825, beta subunit CAB55829, gamma subunit CAB55826.

4.3 RESULTS AND DISCUSSION

4.3.1 Phytoplankton

Samples for NMHC analyses were drawn from cultures daily over a one to two week period spanning the exponential growth phase. Occasionally samples were drawn over longer time periods until the cultures senesced. No clear production or consumption patterns of any NMHC ,except isoprene (see Chapter 3.3), were observed for any of the species studied, including *Prochlorococcus, Synechococcus, Emiliania huxleyi, Micromonas pusilla,* and *Pelagomonas calceolata.* A total of ~ 40 individual treatments distributed across 14 experiments were monitored for NMHC. All phytoplankton cultures grew normally through exponential and stationary phases as shown in Figure 16A.

There is much variation in the NMHC signal, represented here by ethane and ethene (Figure 16B, 16D). Production rates (moles mL^{-1} hr^{-1}) are often significantly negative, signifying that the NMHC production is higher in the media blank than the cultures, and sometimes centered around zero. For example, at hour 96 ethene production rates for the four replicates are centered around zero. This means that two of the cultures had ethene production rates greater than those in the media blanks, and that two of the cultures had ethene production rates less than those in the media blanks. While measurements of

production rates for individual cultures or blanks are far above the detection limits of the analytical system (see Chapter 2.1.2), the net production rates due to the cells (calculated by subtracting the blank production rates from those of the cultures, along with other corrections (see Chapter 2.5)) are positive on some days during the experiment and negative on others. In comparison, isoprene production rates measured concurrently increase during exponential phase, and decrease during senescence, paralleling the patterns of cell abundance (see Chapter 3.3). When isoprene production is normalized to cell abundance (Figure 16C), there is a clear, constant production in exponential phase that decreases when the cells reach stationary phase. The media blank values, for which we correct in the production rate calculation, were almost always zero for isoprene, or at least one order of magnitude lower than the media blank values for the other NMHC. This is because isoprene was not detected as a contaminant leached from the incubation system as were ethane, ethene, propane, and others (see Chapter 2). Production rate patterns observed for ethane and hexane, the two alkanes monitored in these experiments, were similar to each other within each of the 14 experiments. Production rate patterns observed for ethene, propene, and 2-methyl-propene (isobutene), the alkenes monitored, were also similar to each other within each of the experiments. Thus throughout this work we represent the responses of all other alkanes and alkenes by those of ethane and ethene, respectively.

This lack of NMHC production, other than isoprene, is interesting because many terrestrial photosynthetic plants, yeasts, molds, and bacteria do produce directly at least one NMHC, ethene (reviewed in Kesselmeier & Staudt, 1999; Fukuda et al., 1993; Fujii et al., 1987). Links between growth of other phytoplankton species and NMHC other than isoprene have also been reported at levels above corresponding media blanks (ethene and propene by *Thalassiosira rotula* (Ratte et al. (1998)); ethene, propene, and hexane by *Skeletonema*

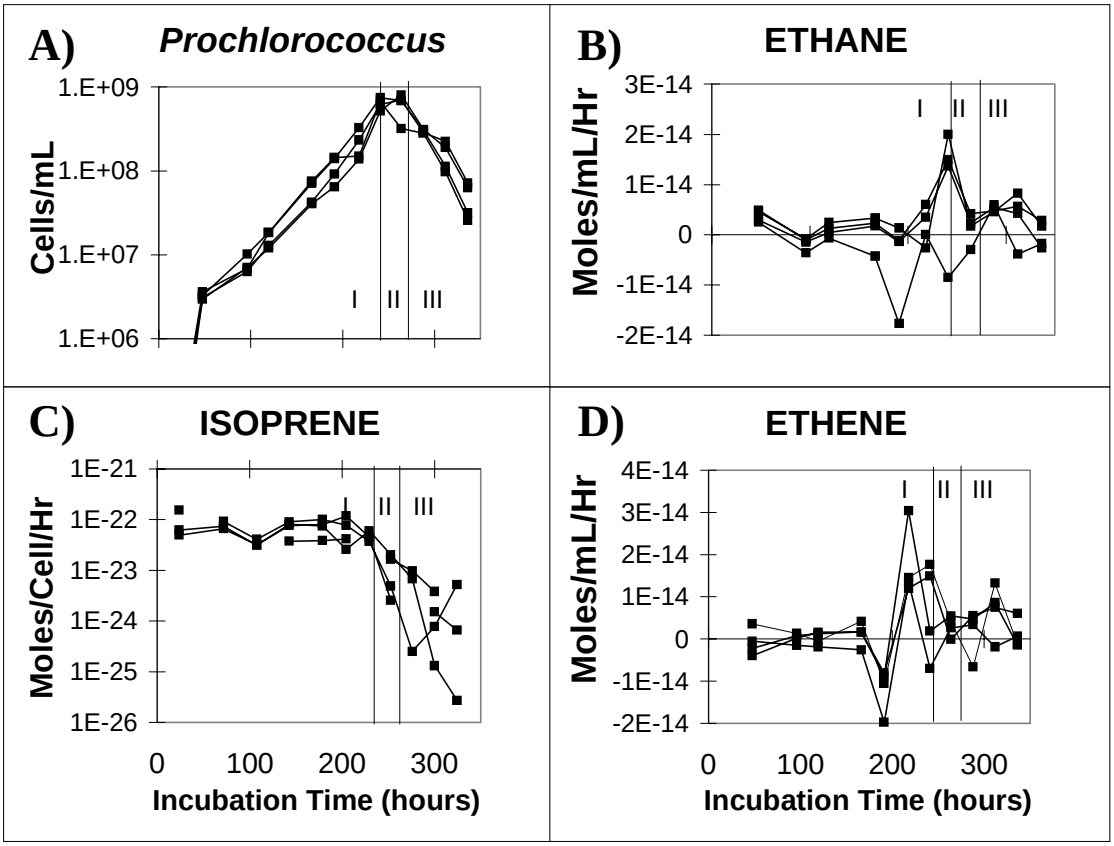

Figure 16: *Prochlorocccus* Do Not Produce or Consume Ethane or Ethene. NMHC production rates in moles $cell^{-1}$ hr^{-1} or moles mL^{-1} hr^{-1} as a function of time (B-D) over the *Prochlorococcus* (MIT axenic MED4 strain) growth cycle, in cells mL^{-1} (A). Results from four replicate cultures are plotted. Vertical bars distinguish between population phases exponential (I), stationary (II; equal cell growth and death), and death (III) phases. Note that panel C is on a log scale, while panels B, D are not. Ethane and ethene are not normalized to cell counts because the volume-normalized rates range from positive to negative, with no clear link to cell abundance. In contrast, isoprene production rates normalized to volume followed a similar pattern to cell counts (as in panel A): increasing during exponential phase, and decreasing during senescence, with a faster decrease during senescence than cell counts.

costatum, and ethene, propane, and propene by *Scripsiella troichoidea* (McKay et al., 1996); C_2, propane, propene, and butane by *Chaetoceros galvestonensis* (Wilson et al. (1970))). McKay et al. (1996) also reported ethane, ethene, propane, and propene production in dying *Skeletonema costatum* cultures. Schobert & Elstner (1980) reported ethane and ethene production by dying *Phaeodactylum tricornutum* cultures, but it is unclear if their NMHC measurements are corrected for blank incubations. The only cell species grown in this work

that were reported to be examined by other workers were *Emiliania huxleyi* (strain MCH) and a species of *Synechococcus* (strain DC2, which is the same as WH 7803), cultured by Milne et al. (1995). These authors reported isoprene production only; it is unknown if any other NMHC were monitored.

It is possible we did not detect any production because of the particular cell species we have chosen, or perhaps other unknown environmental parameters can affect NMHC. Alternatively, it is possible that a signal is obscured in our experiments due to the non-zero media blank levels of NMHC (see Chapter 2.2). However, our chromatographic detection limits (0.6, 0.5, and 0.1 picomoles for ethane, ethene, and isoprene, respectively; see Chapter 2.1.2) are near to or better than those of other researchers who have investigated phytoplanktonic NMHC production (< 7 pmol L^{-1} for 1 L liquid samples - < 7 picomoles (Ratte et al., 1998); 10 ppt for 100 to 400 cc of gas - 0.04 to 0.2 picomoles (McKay et al., 1996); 100 ppt to 1 ppb for 300 mL of gas - 0.2 to 2 picomoles (Milne et al., 1995)). Additionally, the clean, repeatable patterns detected for isoprene give us significant confidence in our culturing methodology and analysis techniques.

We also examined the *Prochlorococcus* and *Synechococcus* genomes for evidence of NMHC production and consumption. Ethene biosynthesis in microorganisms can occur through one of two known intermediates: 2-keto-4-methylthiobutyric acid (KMBA) or 2-oxoglutarate (Fukuda et al., 1993). While the former intermediate was found in virtually all ethene-producing bacteria, no sequences are publicly available for genes in that production pathway. We compared the *Prochlorococcus* and *Synechococcus* genomes with representative genes from the 2-oxoglutarate pathway in *Pseudomonas syringae*, and found no putative homologs. Ethene biosynthesis in higher plants occurs by reaction of 1-Aminocyclopropane 1-carboxylate (ACC), which is derived from methionine, with ACC oxidase (reviewed in Fall, 1999). We compared the three genomes (2 *Prochlorococcus*, 1 *Synechococcus*) with representative ACC synthase, ACC oxidase, and ACC deaminase

genes, and found no regions in the genomes with E-values less than 0.5. An E-value is a measure of the probability that the similarity between the known gene and the target genome region arose by chance; generally E-values less than $1x10^{-6}$ are considered to be acceptable probabilities. We also searched for alkane, alkene, and isoprene monooxygenases, which would assist cells in metabolizing these NMHC. No homologs to any of the 8 genes tested were found in the *Prochlorococcus* or *Synechococcus* genomes. We thus conclude that if ethene biosynthesis by these organisms occurs, which we did not detect, it is through either the KMBA pathway or a pathway involving novel genes. Additionally, the lack of homologs to the representative monooxygenases implies that these strains of *Prochlorococcus* and *Synechococcus* do not metabolize these NMHC; or if they can use these chemicals as carbon sources, it must be through a novel pathway.

4.3.2 Heterotrophic Bacteria

The bacterial species *H. halodurans* and a natural river water bacterial assemblage were both cultured in enriched yeast media broth to test for NMHC production. Bacteria grew rapidly in each of the experiments, with cell density increasing by about one order of magnitude after 1.5 days (Figure 17A). Production rates of ethene, propene, and 2-methyl-propene (all represented by ethene; Figure 17D), and ethane and hexane (both represented by ethane; Figure 17B), were centered around zero and did not display a clear relationship to bacterial abundance. The only potential exception is the relatively large negative ethane rate at hour 36, which may indicate a biological consumption of this alkane. It is interesting that both *H. halodurans* and the natural assemblage display this behavior over the same interval, implying some sort of experimental artifact. It is possible that this strong negative rate is due to an abnormality in the sampling purging process for that day, but detailed examination of the raw data could not confirm or deny this. Isoprene was produced at a rate of $\sim 4x10^{-22}$

moles cell^{-1} day^{-1} in mid growth, which then decreased by 2 orders of magnitude as the cells continued to grow (Figure 16B). This maximal rate is on the same order of magnitude as isoprene production from phytoplankton incubations (see Chapter 3.3).

Several species of bacteria isolated from soil environments, including *Bacillus subtilis*, have also been shown to produce isoprene (Wagner et al., 1999; Kuzma et al., 1995). This production is also maximal in the mid growth phase, and occurs with a temperature maximum ~ 40 °C, similar to higher plants. Interestingly, the bacterial production rates (~ 2x10^{-7} moles (g dry weight)$^{-1}$ day^{-1}) represent a tiny fraction of glucose metabolism (Wagner et al., 1999), and fall between those for marine phytoplankton (order of 10^{-9} to 10^{-8} moles (g dry weight)$^{-1}$ day^{-1}) and plant leaves (order of 10^{-7} to 10^{-5} moles (g dry weight)$^{-1}$ day^{-1}). However, the above soil bacteria were grown in the organically-enriched LB medium, just as our cultures of marine bacteria were grown in a different organically-enriched medium, and thus may represent maximum production rates that might not be reached *in situ*.

There is the possibility that our culture flasks were not clean of NMHC at the start of the bacteria experiments. Thus the decreasing isoprene production rate with time (Figure 17B) could be interpreted as simply the venting of an original isoprene contaminant occurring in the culture flasks, but not the media blank flasks, over several sampling periods. This occasionally does occur in either the culture or blank flasks, but typically the experiments are long enough (~ 1.5 to 2 weeks) to allow the first day or so of data to be removed. We anticipated this might be an issue here, so we intentionally purged the flasks at a higher purge rate, and ~ 25% longer than usual (see Chapter 2.3). We infer from our results that any bacterial isoprene production in seawater by these strains appears to be insignificant compared to phytoplanktonic production. However, the potential for bacterial NMHC consumption in seawater still needs to be investigated further. Bacteria can use a variety of organic carbon sources; some have been reported to metabolize isoprene (e.g. *Rhodococcus* Hylckama Vlieg et al., 2000; *Arthro*- and *Xanthobacter* - Hou et al., 1981; *Nocardia* - van

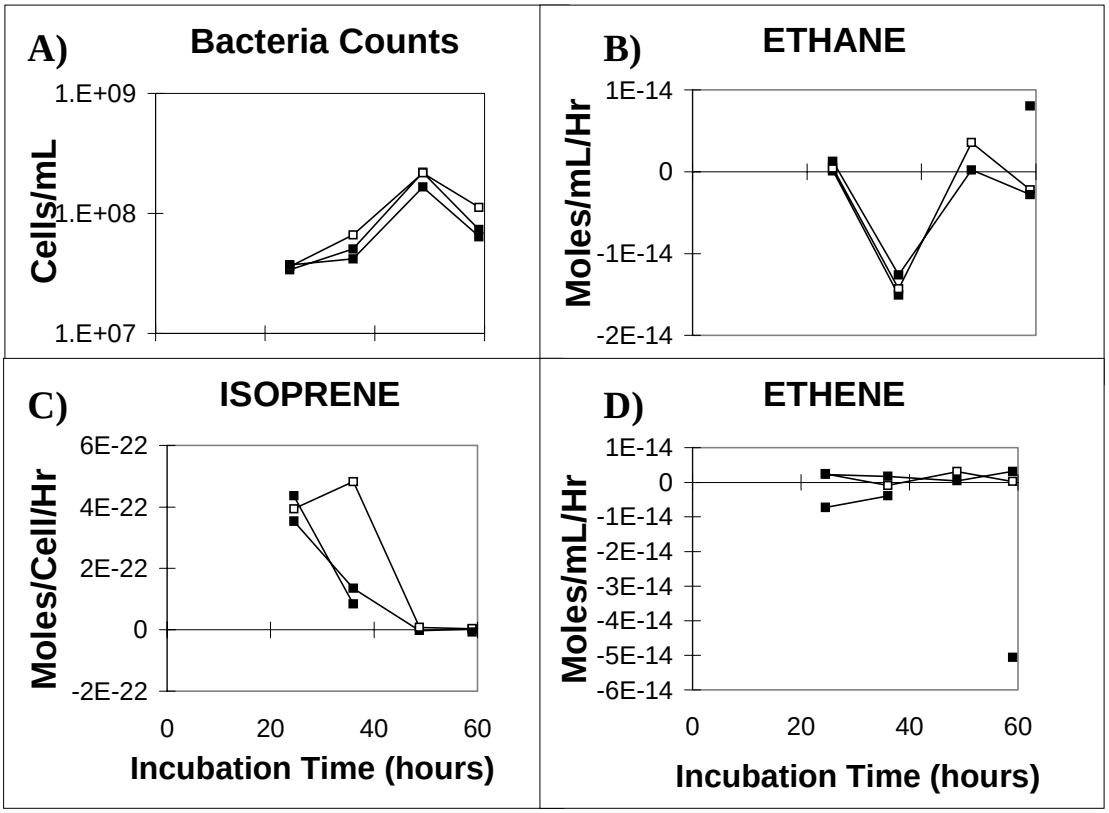

Figure 17: Bacterial Cultures. NMHC production rates as a function of time (B-D) in two cultures of bacteria throughout a growth curve, in cells mL^{-1} (A). Filled squares represent *H. halomonas*, and open squares represent the natural assemblage.

Ginkel et al., 1987; forest soils - Cleveland and Yavitt, 1998) and a variety of other low molecular weight NMHC (Hamamura & Arp, 2000; Saeki & Furuhashi, 1994; Patel et al., - 1983). Evidence for or against NMHC consumption is inconclusive in our experiments. The potential for marine bacteria to utilize these compounds is interesting as it has been difficult to consistently relate the alkanes, in particular, to common phytoplanktonic, chemical, or physical parameters. Perhaps a bacterial involvement in alkane cycling would account for this confusion.

4.3.3 Nanoflagellate Protists

Nanoplanktonic protists are thought to be the primary consumers of picoplankton (Weisse, 1993; Caron et al., 1991), so a typical nanoflagellate, *Cafeteria roenbergensis* (Lim et al., 2001), was chosen to graze on *Prochlorococcus.* *C. roenbergensis* rapidly reduced the phytoplankton counts. Figure 18A displays the cell counts in four *Prochlorococcus* cultures, originally all replicates, growing at 0.7 day^{-1}. At the point marked by the arrow, the protists were introduced into two of the four replicates (open squares). *Prochlorococcus* population growth slows after 39 hours, and the cells are almost completely removed after 2.6 days. *C. roenbergensis* density approximately doubles, with a specific grazing rate of 1.7 day^{-1}. NMHC production rates are represented by ethane, ethene, and isoprene and are shown in Figure 18B-18D. The patterns are quite variable from day to day for ethane and ethene, and are centered around zero, implying there is no difference between the cultures and the blanks. Cell-normalized isoprene production rate in the reference culture ($(5.4 \pm 0.4)\times10^{-23}$ moles $cell^{-1}$ hr^{-1}) remains constant during the exponential phase (Figure 18C). It decreases at and beyond stationary phase (filled squares). Isoprene in the grazed cultures is also constant, at statistically the same rate ($(4.8 \pm 0.2)\times10^{-23}$ moles $cell^{-1}$ hr^{-1}), during the period of time encompassing the exponential phase in the reference culture. In other words, during hours 94-143 when the cell counts in the grazed culture are rapidly decreasing, isoprene production *per cell* remains equivalent to that of the reference culture. This implies that while many of the cells are being ingested by the nanoflagellate, and the population as a whole is beginning to decline, individual cells are still growing normally and producing isoprene at typical rates. Additionally, a single control culture of just *C. roenbergensis* was examined, with no *Prochlorococcus.* *C. roenbergensis* cell counts remained fairly constant in that control culture over the course of the experiment (open

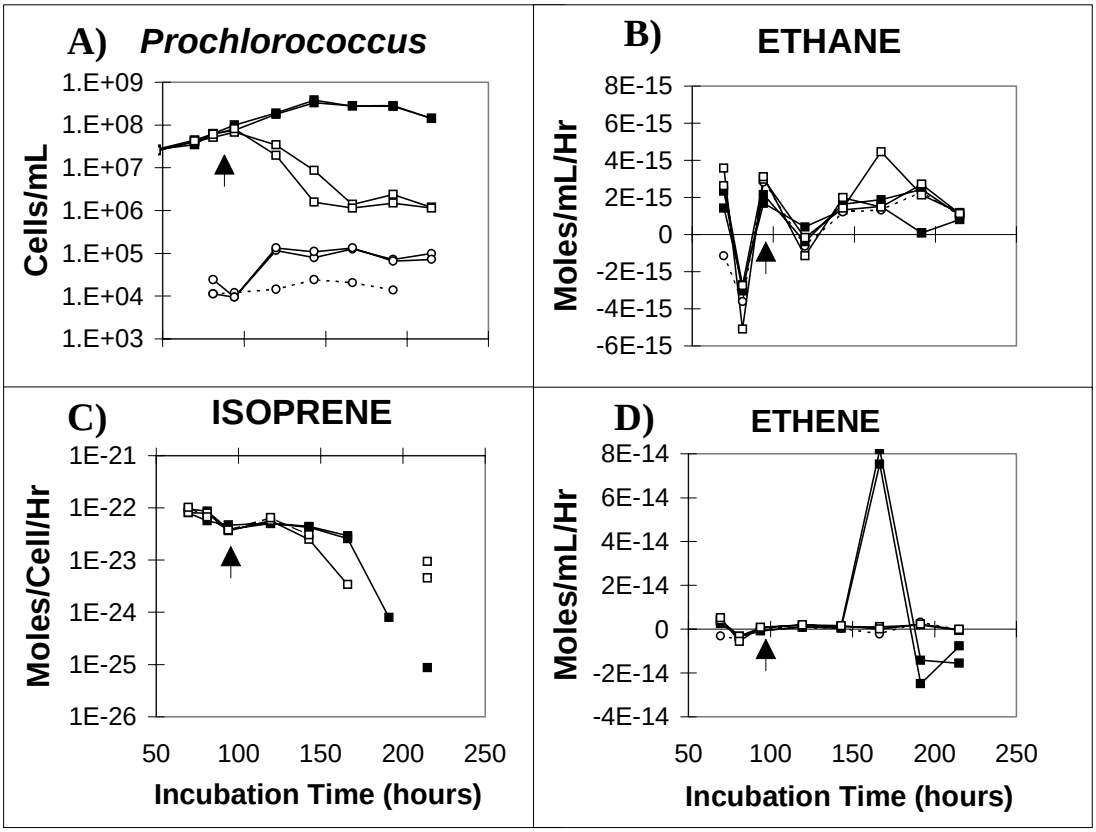

Figure 18: Effects of Grazing on *Prochlorococcus*. NMHC production rates as a function of time (B-D) over the growth cycle, in cells mL^{-1} (A). Filled squares represent *Prochlorococcus*, open squares represent *Prochlorococcus* in the grazed incubation, open circles represent *C. roenbergensis* in the *Prochlorococcus* cultures, and open circles with dashed lines represent a *C. roenbergensis* control with no *Prochlorococcus*. Arrows indicate the point of protist introduction. Note that the two 'missing' isoprene rates at hour 192 were slightly negative (meaning the production rates were slightly less than those in the blanks) and were not able to be plotted on the log scale. Also, isoprene production rates in the *C. roenbergensis* control with no *Prochlorococcus* (not plotted here) were always at least one order of magnitude less than that in any *Prochlorococcus* culture (moles mL^{-1} hr^{-1}) when it appeared (approximately half of the sampling points), and showed no links to *C. roenbergensis* abundance.

circles, dashed lines). Isoprene production in the control culture was only detected on several days throughout the experiment, and always at rates at least one order of magnitude lower than for the grazed or reference *Prochlorococcus* cultures. This combination of evidence implies there is no direct production or consumption of isoprene by this protist. No other NMHC observed in this work appeared to be affected by protist grazing.

4.3.4 Phage infection

Since protists tend to ingest food whole (Strom et al., 1993), the potential for grazing to produce precursors for NMHC is small, although both sloppy feeding and DOC egestion from protist food vacuoles are possible (Strom et al., 1997). We used a marine phage to lyse the *Prochlorococcus* cells to ensure this was not the reason that no NMHC appeared to be produced or consumed by grazing. Phage infect the cells and replicate, eventually bursting their hosts and creating cell fragment debris, which can be available for or further chemical conversion in the water column bacteria (Gobler 1997; Suttle & Chan, 1994). Physical lysis techniques were also possible, but would have required external modification to cultures in the middle of the experiment. We use a 50 nm long Podovirus specific for *Prochlorococcus* MED4 that was recently isolated and characterized (Sullivan et al., 2001). Four *Prochlorococcus* cultures were established from a single stock (two as reference cultures and two as phage-infected cultures). The only difference between the reference and phage-infected cultures was that the latter had an aliquot of phage stock culture added. One of these phage-infected cultures was inoculated with 10 times as much volume as the other (e.g. 100 μL and 1 mL phage stock). The reference cultures grew exponentially, while both of the phage-infected cultures grew for a short time (until hour 47), then retained a fairly constant cell density for ~ 2 days (Figure 19A). At this point these cultures are likely composed of both infected and healthy cells. A reduction in *Prochlorococcus* counts occurs near hour 125. NMHC production rates are shown in Figure 19B-19D. Ethane and ethene are again not clearly linked to the cells or phage. Isoprene production rate per cell in the reference culture (closed squares) is fairly constant during exponential phase, but decreases consistently during the same time period in the phage-infected culture (Figure 19C). One exception occurs in the phage incubation inoculated with 1 mL of phage stock, when the

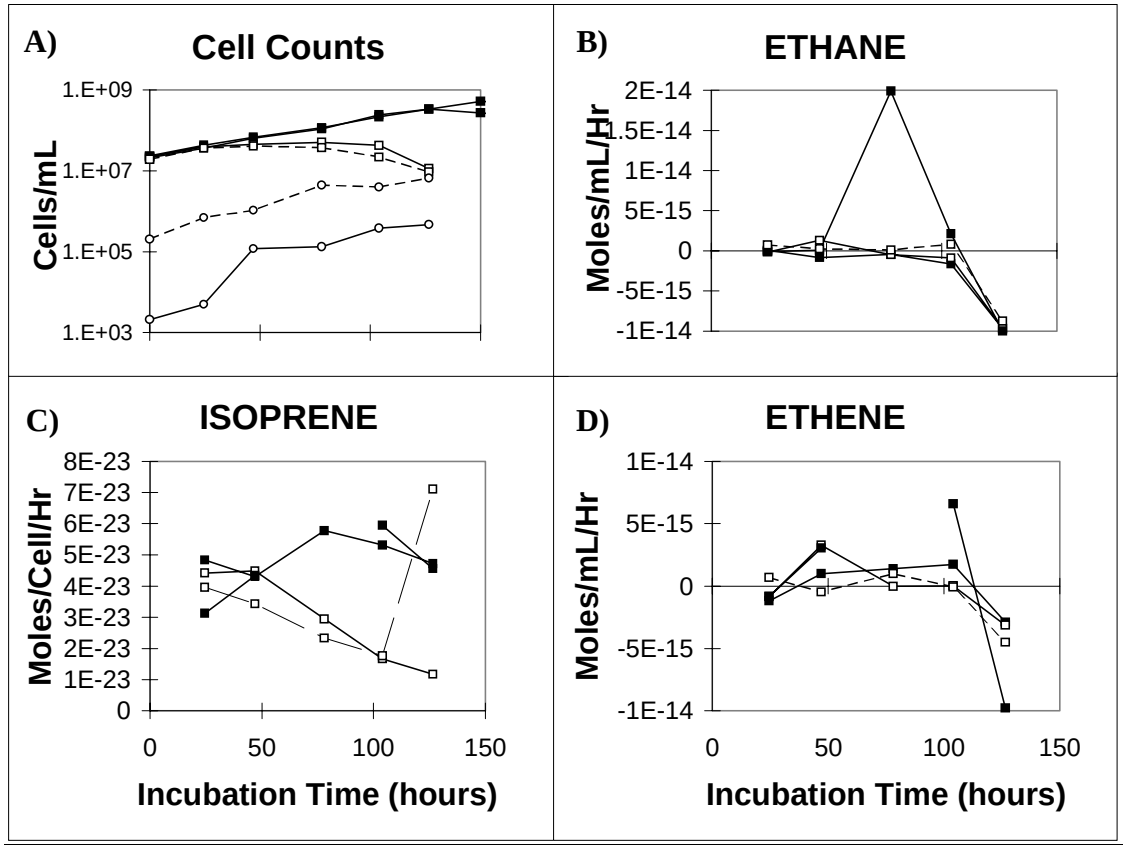

Figure 19: Phage Infection of *Prochlorococcus*. NMHC production rates as a function of time (B-D) over the growth cycle, in cells mL^{-1} (A). Filled squares represent cultures of *Prochlorococcus* grown alone, open squares represent phage-infected *Prochlorococcus* cultures, and open circles represent the number of phage. The dashed lines identify the phage incubation inoculated with 1 mL of stock culture as explained in the text.

isoprene production increased sharply at hour 125 (dashed line; Figure 19C). We have no clear explanation for this phenomenon. However, flow cytometric analysis of samples taken after hour 125 showed that a sub-population of the *Prochlorococcus* in that flask had begun to regrow. This potentially phage-resistant sub-population may be responsible for the isoprene increase, although the increase cell count occurred *after* the increase in isoprene production rate.

Phage both stressed and lysed the *Prochlorococcus* cells, decreasing isoprene production rate per cell during the infection. As phage-infected cells have been shown to continue

photosynthesis until a late stage of infection (Brussard et al., 1999; Benson & Martin, 1981), it is not surprising that isoprene continues to be produced, albeit at decreasing rates. Decreasing isoprene production implies that the biosynthetic pathway is somehow disturbed during the latent period between infection and lysis of the photosynthetic cell. This may be due to a redistribution of cellular resources from the isoprene pathway to one more immediately necessary for cellular repair and fighting the infection. There was, however, no detectable change due to phage on the production of any other NMHC. Further information on changes in other cellular parameters due to phage infection can be found in Appendix D.6

4.3.5 Summary

The lack of NMHC response to grazing and phage infection could be an effect of choosing only one representative nanoflagellate and phage species that happen to not be involved in NMHC cycling. Alternatively, our instrument sensitivity to non-isoprene NMHC might be too low to detect these processes if they are weak. We believe the process is more complex, as other researchers have suggested, potentially involving other environmental parameters such as UVB light. Preliminary experimental data on this topic is presented in Appendix D.7. Lee & Baker (1992) and Ratte et al. (1993) proposed that NMHC are produced photochemically from phytoplankton-derived precursors. If those precursors were PUFA-like material, such as membranes or other lipids, we might have expected to observe an increase in NMHC with physical lysis of cells. However, it is the compounds in the cytoplasm that are released with best efficiency as opposed to those embedded in cell structures, such as membranes (Gobler et al., 1997; Reinfelder & Fisher, 1991). As the cells were stressed by phage infection, we might have also expected a direct production and emission of ethene, which is released in higher plants during physical wounding or other stresses (Yang & Pratt, 1978). This was not the case.

Ratte et al. (1995) observed significant positive correlations between phytoplankton density (and bulk chlorophyll concentration) and NMHC concentrations in regions with low phytoplankton density, and negative correlations between phytoplankton density and NMHC concentrations in regions with high phytoplankton density. These results led us to suspect that organisms other than phytoplankton might be somehow involved in NMHC cycling, as heterotrophic organisms such as bacteria, protists, and phage particles, can become very abundant when phytoplankton abundance is low, such as at the end of a bloom (Ducklow et al., 1993; Sieracki et al., 1993; Bratbak et al., 1993) or during the late summer/fall when phytoplankton have utilized all available nutrients (Campbell et al., 1997). From our experiments it appears that any contributions heterotrophic organisms have on oceanic NMHC are more complex than simple production or consumption relationships. Biological incubations would need to be done in concert with careful photochemistry, and perhaps isotopic labeling, to elucidate these potential processes.

4.4 CONCLUSIONS

We detected no systematic production or consumption of any NMHC, except isoprene, from five different phytoplankton species and two bacterial assemblages in laboratory cultures. A natural assemblage of bacteria and a cultured species, *H. halomonas*, were shown to produce isoprene in organically-enriched cultures at rates similar to those by phytoplankton (see Chapter 3.3). Protist grazing affected no NMHC except isoprene; total isoprene production in the incubations was decreased simply through controlling phytoplankton abundances. Phage infection also affected no NMHC except isoprene. This occurred through both the control of phytoplankton abundances, and some intracellular change during the latent period of infection which decreased the isoprene production rate per cell.

CHAPTER FIVE

DETERMINATION OF REGIONAL ISOPRENE FLUX

One motivation for this work was the potential impact of oceanic NMHC on atmospheric photooxidant chemistry. To investigate that impact, we first need to know the magnitude of the individual NMHC fluxes from the oceans. Then one could take those fluxes and use known rate constants in a chemistry model to determine atmospheric impacts. With the acquisition of our data set on cellular isoprene production rates, we can now estimate an isoprene flux from the oceans.

We used reported depth profiles of phytoplankton abundance, N, from the literature. These could be measured as either bulk chlorophyll content ((μg chlorophyll-a) mL^{-1}) or as cell counts (cells mL^{-1}) for individual phytoplankton groups or species. These abundances were multiplied by our isoprene production rates, I, in units of either moles $(\mu g \text{ chlorophyll-a})^{-1}$ day^{-1} or moles $cell^{-1}$ day^{-1}. The resulting production rates were integrated over the reported 'water-column' depth. This produces an integrated isoprene production for the water column. If we assume all of this integrated production is lost to the atmosphere (e.g. there are no other loss processes), and the system is in steady state, then we have a maximum estimate of the ocean-air isoprene flux, F (moles $(cm)^{-2}$ day^{-1}), defined as follows:

$$F = \sum_{SD=1,D} \sum_{ORG=1,S} \left[N \times I \times (z'' - z') \right]$$

where SD is an index of water sampling depth ranging from 1 to D, ORG is an index of phytoplankton group or species (e.g. *Prochlorococcus*, cyanobacteria, ultraplankton) ranging from 1 to S, and z' and z'' are depths in centimeters of the top and bottom of each sampled slab of water. Midpoints between sampling depths are calculated to define water slabs with 'known' thickness (e.g. depths of top and bottom of each slab).

5.1 PREFERRED UNITS FOR THE CALCULATION

Phytoplankton abundance in the field can be determined directly, by counts of individual cell species, or by chlorophyll-a (treated as an approximate proxy). The first method is much preferred, but the bulk chlorophyll measurement is quicker and easier than identifying and counting individual species. The benefits of a bulk chlorophyll concentration include the assurance that all phytoplankton species are encompassed in the measurement, and that many field measurements are publicly available for this parameter. These include global maps of a proxy for chlorophyll-a (which, as noted above, is itself a proxy for cell abundance) which are created from SeaWiFS satellite data (http://seawifs.gsfc.nasa.gov/SEAWIFS.html). However, cellular chlorophyll content is a plastic parameter that is very dependent upon species, growth stage, and environmental conditions, and thus does not necessarily accurately represent the phytoplankton abundance. Additionally, the satellites can only sense down to about one optical depth, and thus may not represent the entirety of the phytoplankton-populated portion of the water column.

Our laboratory data of isoprene production rates vary with organism size and chlorophyll content. Figure 20A shows isoprene production rates for the five phytoplankton species cultured, in moles cell^{-1} day^{-1}, increasing with cell volume, in $(\mu m)^3$. A linear regression results in a slope of 5.5×10^{-21} moles cell^{-1} day^{-1} $(\mu m)^{-3}$. However, the three larger species were grown at ~ 45 $\mu E\ m^{-2}\ s^{-1}$, while the two smaller species were grown at ~ 90 $\mu E\ m^{-2}\ s^{-1}$. We estimate a correction factor due to this difference by assuming the magnitude of the isoprene production rate dependence on irradiance is the same for these organisms as it is for *Prochlorococcus* (see Chapter 3.3). This correction is approximately a factor of 1.5, and the corrected slope is 8.3×10^{-21} moles cell^{-1} day^{-1} $(\mu m)^{-3}$. This lies just within the error bars of replicate cultures. Figure 20B is similar, but shows isoprene production rate in moles (g chlorophyll-a)$^{-1}$ day^{-1}. The original isoprene production rates in 'per gram chlorophyll' unites appear to decrease with increasing cell volume, although all values significantly overlap with the error bars. A correction factor of 1.7 is then applied to the 'per gram

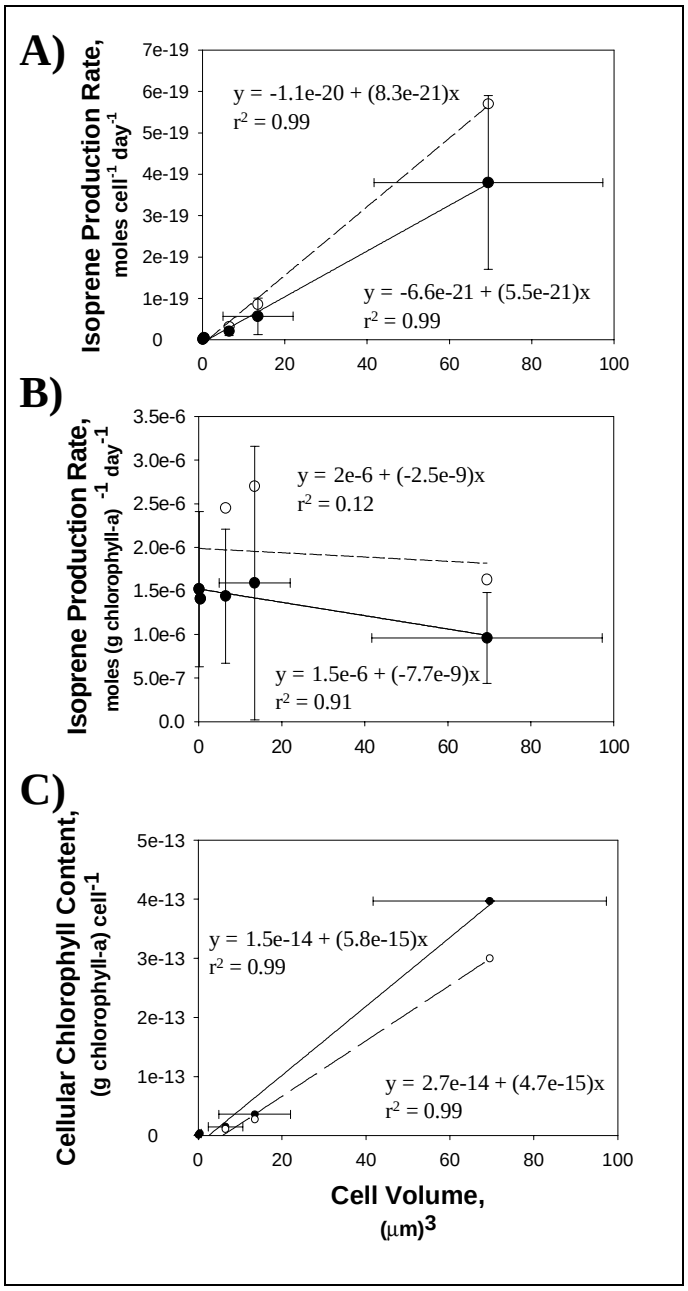

Fig 20: Isoprene Production Rate for Several Organisms A) Isoprene production rate in moles cell^{-1} day^{-1} versus cell volume in $(\mu m)^3$. Isoprene rates were compiled from all experiments (n) done with each organism (from Table 1). The species in order of increasing size are *Prochlorococcus* (n=8), *Synechococcus* (n=2), *Micromonas pusilla* (n=1), *Pelagomonas calceolata* (n=1), and *Emiliania huxleyi* (n=2). *Prochlorococcus* and *Synechococcus* appear as one point near 1 $(\mu m)^3$; cell volume error bars for these two species are smaller than the symbols. Both original data (filled circles) and data corrected from growth at 45 to 90 μE m^{-2} s^{-1} (open circles) are plotted for the 3 largest species. Note that panel A is reprinted from Chapter 3, Figure 12A. B) As in panel A, except isoprene production rate is in moles (g chlorophyll-a)$^{-1}$ day^{-1}. C) Cellular chlorophyll content ((g chlorophyll-a) cell^{-1}) versus cell volume. Chlorophyll content error bars are included for *Prochlorococcus* and *Emiliania huxleyi*, and are smaller than the symbols.

chlorophyll' production rates from cells grown at 45 μE m^{-2} s^{-1}. This factor of 1.7 is calculated from the ratio of the correction factor for isoprene production rate per cell from 45 to 90 μE m^{-2} s^{-1} (~ 1.5, as in Figure 20A), and changes in cellular chlorophyll content due an increase in light level between 45 and 90 μE m^{-2} s^{-1} (~ 0.9 for this cell strain; Moore et al., 1995). The corrected rates are roughly constant with cell volume; the corresponding corrected slope is approximately -2.5×10^{-9} moles (g chlorophyll-a)$^{-1}$ day^{-1} (μm)$^{-3}$. The slope for 'per gram chlorophyll' isoprene production rate units is much closer to zero than the slope for 'per cell' units. This is because cellular chlorophyll content increases with cell volume (slope ~ 5.8×10^{-15} (g chlorophyll-a)$^{-1}$ cell^{-1} (μm)$^{-3}$, corrected slope ~ 4.7×10^{-15} (g chlorophyll-a)$^{-1}$ cell^{-1} (μm)$^{-3}$) as does the isoprene production rate (Figure 20C). Cellular chlorophyll content of the 3 largest species is corrected from growth at 45 to 90 μE m^{-2} s^{-1} by multiplying by a factor (0.75). This is calculated as the average of the factor changes in cellular chlorophyll content due to this increase in light level for *Prochlorococcus* and *Synechococcus* from Moore et al. (1995), as we have no such information for the other species. Isoprene production rate per cellular chlorophyll content is thus a more robust parameter over the cell size range we tested (e.g. it does not depend heavily upon cell species). In conclusion, we recommend the use of isoprene production rates in moles (μg chlorophyll-a)$^{-1}$ day^{-1} for modeling calculations. In situations where detailed species information is available, 'per cell' units would still be useful for comparative purposes, or for determining isoprene production from a subset of the species present in a given location.

As mentioned earlier, cellular chlorophyll content for any given species is quite variable with irradiance (and thus opacity and depth in the water column), as well as other parameters; isoprene production has similar dependencies. The combined effect of these two parameters is plotted in Figure 21 for *Prochlorococcus*. As irradiance increases, isoprene production rate per cell increases (see Chapter 3.3), and cellular chlorophyll content decreases (Moore et al., 1995). We thus expect to see isoprene production rate per cellular chlorophyll content decreasing with increasing cellular chlorophyll content. We do see this pattern in the data (Figure 21B), with a factor of 3 change over the indicated cellular chlorophyll content range for *Prochlorococcus* resulting from growth at irradiances up to

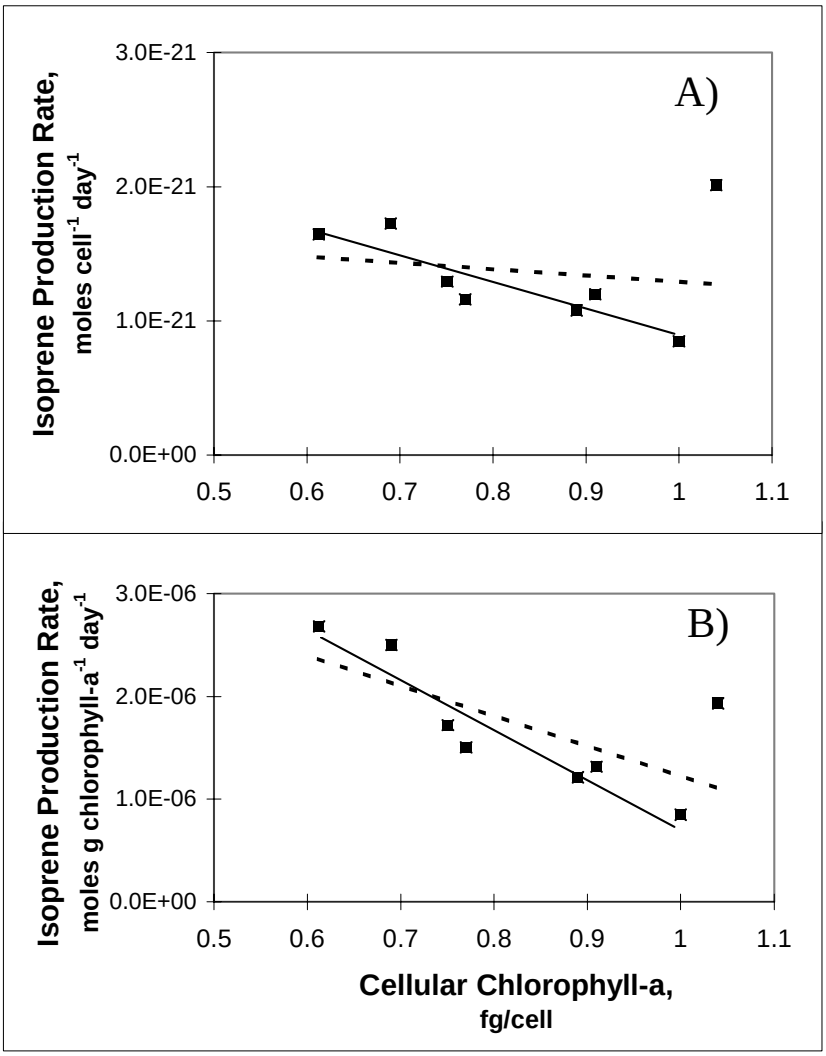

Figure 21: Isoprene Production versus Chlorophyll Content A) Isoprene production in units of moles cell^{-1} day^{-1} versus cellular chlorophyll content, in (fg chlorophyll-a) cell^{-1} for *Prochlorococcus* cultures grown in a range of non-inhibiting irradiances. Data plotted are from a subset of the experiments used to produce Figure 13 in Chapter 3. Linear regressions to the data are shown with (dotted line) and without (solid line) a suspect datum at 1.04 (fg chlorophyll-a) cell^{-1}. B) As in panel A, but for isoprene production in units of moles (g chlorophyll-a)$^{-1}$ day^{-1}

light-saturating conditions. Variations of a factor of 3 can be larger than the calculated errors from replicate incubations, and should therefore be taken into account in the development of detailed predictive models. However, these variations with light (and those detected for temperature) were not included in the analysis in this chapter for three reasons:

1) to illustrate the simplest possible case, 2) effects of these environmental parameters are only known for *Prochlorococcus* at present, and 3) it was difficult to obtain datasets with light and temperature measurements *and* detailed species information. Instead, we simply scale-up the overall production rates compiled from all available experiments that are presented in Table 9 (Chapter 3).

5.2 NORTH ATLANTIC SPRING BLOOM CONDITIONS

Baker et al. (2000) estimated fluxes of a variety of trace gases, including dimethylsulfide, methyl iodide, and selected NMHC, in the eastern Atlantic Ocean during May 1997 using bulk flux calculations. While they did not perform extensive organism identifications and counts, they did report the major phytoplankton taxa represented, as well as bulk chlorophyll concentrations, down to 80 meters depth in the water. They report an average flux of about 3.4×10^7 molecules cm^{-2} s^{-1} for isoprene during this cruise.

Scaling-up our laboratory production rates with their bulk chlorophyll measurements as described above results in an estimated maximum flux of (3.4 to 5.6) $\times 10^7$ molecules cm^{-2} s^{-1} (Table 12), depending on how much of the water column is taken into account. These two estimates compare favorably, but it is important to note that our phytoplankton assemblage was biased to typical species abundant in remote oligotrophic waters. These types of cells (diameter < 5 μm) are significantly smaller than those found in North Atlantic blooms, where prymnesiophytes (~ 5 μm) and diatoms from 5 - 10 μm, or larger, can dominate (Harrison et al., 1992; Sieracki et al., 1992). Baker et al. (2000) reported primarily diatoms (e.g. *Rhizosolenia, Thalassiosira*) at the beginning of the bloom, and dinoflagellates (e.g. *Scripsiella, Gyrodinium*) near the end, as the typical species observed. Sizes of the typical cells in these blooms vary widely from those used in our experiments. One species of *Thalassiosira* that dominated the early stages of the bloom was approximately 40 μm in diameter, and reported cell sizes ranged to low values of 4 μm diameters. As we have demonstrated here, isoprene production rates can be a significant function of cell size. Thus we may be under- or overestimating the maximum isoprene flux

during the North Atlantic spring bloom conditions if our assumption of nearly constant isoprene production rates per cellular chlorophyll content do not hold for cells larger than those tested in this work (> 5 μm diameter).

5.3 EQUATORIAL PACIFIC AND ATLANTIC CONDITIONS

In the oligotrophic equatorial regions the biology is fairly well characterized as to species identification and abundances (http://www.bbsr.edu/users/ctd/; http://hahana.soest.hawaii.edu/hot/hot_jgofs.html). The organisms we cultured were representative of these regions, and thus we have most confidence in our estimates for the equatorial Pacific and Sargasso Sea. The only flux measurements in the Pacific with which we have to compare our estimates (Table 12) are from Bonsang et al. (1992). Our maximum 'per cell' estimates

Table 12: Estimated Maximum Isoprene Flux

	Using **Moles cell^{-1} day^{-1}** (whole column)	Using **Moles cell^{-1} day^{-1}** (mixed layer)	Using **Moles (g chlorophyll-a)$^{-1}$ day^{-1}** (wholecolumn)	Using **Moles (g chlorophyll -a)$^{-1}$ day^{-1}** (mixed layer)	**Chlorophyll or Cell Concentration Reference**	**Sampling Period**
North Atlantic bloom	---	---	5.6	3.4	Baker et al. (2000)	May 1997
Equatorial Pacific	9.2	8.6	4.1	3.6	Binder et al. (1995); Bidigare & Ondrusek (1996)	March and October, 1992
Sargasso Sea	3.5	1.1	5.9	1.0	Li et al. (1992)	September 1988
Atlantic N	7.7	7.7	5.2	5.2		
Transect: mid	7.9	3.0	3.4	1.4	Veldhuis et al. (1993)	August 1989
S	2.6	0.5	7.0	3.8		

Maximum isoprene flux in 10^7 molecules $(cm)^{-2}$ s^{-1} from either the whole water column or mixed layer (depths as defined in original references) for two different isoprene production rate normalizations: moles $cell^{-1}$ day^{-1} and moles (g chlorophyll-a)$^{-1}$ day^{-1}.

of (8.6-9.2)x10^7 molecules $(cm)^{-2}$ s^{-1} are quite close to Bonsang et al.'s (1992) isoprene flux estimates of approximately 11x10^7 molecules $(cm)^{-2}$ s^{-1} (summarized in Broadgate et al., 1997). Despite the low cellular chlorophyll content of the small species populating these regions, high cell abundances and the existence of cells at depths down to 150 meters result in isoprene flux estimates on the same order of magnitude as for the spring bloom.

We see approximately a factor of 2 difference between the estimates calculated from 'per cell' and 'per gram chlorophyll' isoprene production rates. These data demonstrate that knowing a significant portion of the species assemblage present in a given geographical region is not necessarily enough information; in these situations dependencies upon solar irradiance and other parameters become important.

5.4 ATLANTIC TRANSECT

Veldhuis et al. (1993) determined abundances of three organism groups (prochlorophytes, cyanobacteria, and ultraplankton) on an Atlantic transect from spring bloom conditions (60 °N, 20 °W) to oligotrophic mid-Atlantic waters (33 °N, 20 °W) during the summer of 1989. For the northern part of the transect, which occurred during part of a spring bloom dominated by small prymnesiophytes (*Emiliania huxleyi*), our estimates by 'per cell' and 'per gram chlorophyll' isoprene production rate units are quite similar. This is likely due to an accurate assessment by Velduis et al. (1993) of the organism identifications and abundances in the water column during that time because of the dominate bloom.

In the middle (47 °N, 20 °W) and southern regions of the transect they observed a switch to cyanobacteria-dominated then prochlorophyte-dominated regions. For these two regions we generally see factor of two differences between our estimates based on 'per cell' or 'per gram chlorophyll' units, as in the equatorial Pacific and Sargasso Sea.

5.5 SUMMARY

The most striking thing to note about these estimates is that despite the variety of oceanic regions studied by various workers, the estimates of isoprene fluxes are all of the same order of magnitude. For the 'per cell' estimates, this is presumably because the smaller cells produce less isoprene per cell, but are generally more abundant than larger cells. This is particularly important in the Equatorial Pacific, where cells exist at depths down to 150 meters or below, as compared to the North Atlantic where cells typically exist to depths less than 100 meters. For the 'per gram chlorophyll' estimates, the laboratory isoprene production rates per cellular chlorophyll content were fairly constant over the different species, and depth integrated bulk chlorophyll concentrations in the two locations were fairly similar. However, we are neglecting many sources of variation in this simple analysis. We do not have a basis in the laboratory data to understand isoprene production from cells larger than 5 μm, which are typical in the North Atlantic spring bloom. Thus, we could potentially be misrepresenting the maximum isoprene fluxes in that region. Additionally, we have used production rates measured or estimated at irradiances of 90 μE m^{-2} s^{-1} as representative of the North Atlantic, equatorial Pacific, and equatorial Atlantic at various points over the year, at all depths in the water column. A more realistic light level in North Atlantic waters could be much lower, so a more accurate production rate for that region's calculations would also be lower, if we assume the variation of isoprene production with light for *Prochlorococcus* is generally representative of the response for other species. The result would be a lower estimated flux in the North Atlantic than presented here. Similarly, as the data for *Prochlorococcus* shows a maximum in isoprene production rate at a temperature more representative of the oligotrophic ocean regions than the North Atlantic (~ 23 °C), including temperature variation of the isoprene production rate is likely to elevate the maximum isoprene flux estimate in the oligotrophic regions further as compared to the North Atlantic. The overall effect of including these environmental parameter dependencies would likely be to bring the geographical differences in the estimated fluxes (~ (3 to 8)x10^7 molecules $(cm)^{-2}$ s^{-1} for oligotrophic waters and ~ (0.5 to 9)x10^7 molecules $(cm)^{-2}$ s^{-1} in the North Atlantic; Table 12) more in line with the geographical differences in previously

reported fluxes (~ 11×10^7 molecules $(cm)^{-2}\, s^{-1}$ for oligotrophic waters and ~ (1 to 4)$\times 10^7$ molecules $(cm)^{-2}\, s^{-1}$ in the North Atlantic; Table 11).

To get a more accurate estimate of how geographical differences can affect maximum isoprene fluxes, a simple model could be developed based on our laboratory data. Three of the important parameters that isoprene production depends upon are cell abundance, cell size, and irradiance. We recommend an equation of the following form for isoprene production, I, which could then be summed over the various organisms present:

$$I = (a + bV + cL) \times N$$

with V representing cell volume, L a measure of irradiance experienced by the cell, N the cell abundance, and a, b, and c empirical coefficients derived from fits to the data. Figure 22 shows a planar fit to all data from this work, from which we obtained the following estimates for the coefficients:

a: ~ -5.5×10^{-21},

b: ~ 5.5×10^{-21} [moles $cell^{-1}\, day^{-1}$] / $(\mu m)^3$, and

c: ~ 5.5×10^{-23} [moles $cell^{-1}\, day^{-1}$] / ($\mu E\, m^{-2}\, s^{-1}$).

Values for b and c are similar to results from linear regressions of the data from Figure 12 (5.5×10^{-21}), and from a linear fit to the non-inhibiting irradiances (< 146 mE $m^{-2}\, s^{-1}$) in Figure 13 (1×10^{-23}), respectively.

This predictive isoprene production equation is a linear combination of the dependencies upon cell size and irradiance, which appears reasonable for the limited data available. Many more culturing experiments similar to those performed in this work would be necessary to

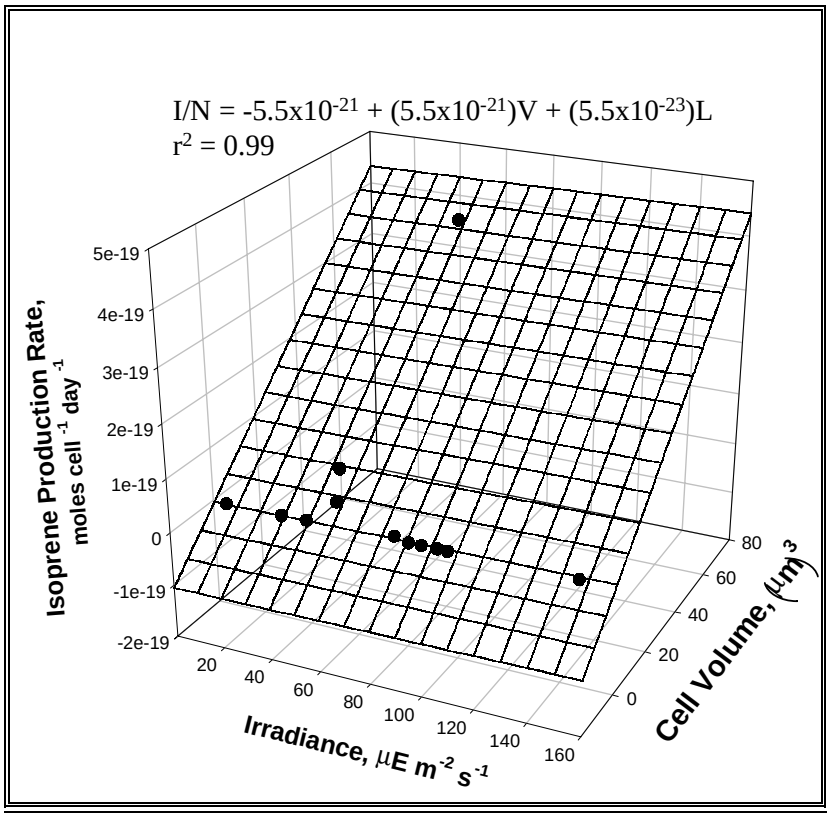

Figure 22: Isoprene Production Rates as a Function of Organism Size and Irradiance A planar fit to the data is presented in graphical and mathematical format. A cross-section through this figure at a constant cell volume results in the relationship of isoprene production with irradiance for a given organism (e.g. For ~ 0.13 $(\mu m)^3$, the cross-section is identical to Figure 13). Note that only *Prochlorococcus* was cultured at a variety of irradiances, and thus we assume the pattern of isoprene production with light for all other phytoplankton to be similar to the pattern for this species. A cross-section through the figure at a constant irradiance results in the relationship of isoprene production with cell volume (e.g. For ~ 45 $\mu E\ m^{-2}\ s^{-1}$, the cross-section is identical to Figure 12). Note that the slope of the plane depends heavily upon the point at 69.5 $(\mu m)^3$ representing *Emiliania huxleyi* for which we have two replicate experiments with good precision ($\pm 1\sigma$ = 54%; see Appendix I, Figure I3).

verify the choice of this equation form, or equivalently to ensure that all the data lie on or close to the inclined plane in Figure 22 or some other definable 3D surface (for similar work see Guenther et al. (1991)). These additional experiments might include an examination of isoprene production rates as a function of growth irradiance for several different phytoplankton species, for example. More complicated terms would be necessary in the production equation if the light dependency at inhibiting irradiances or the temperature dependency were to be included. This type of model could be incorporated into a simple 1-

dimensional vertical diffusion and flux model of the surface oceans to predict isoprene concentrations at the water surface. Then it would be straightforward to determine the resulting flux from these concentrations at the given location using a bulk flux model.

CHAPTER SIX

CONCLUSIONS

6.1 SUMMARY AND IMPLICATIONS

We set out in this thesis to elucidate the effects of marine microbiological cycling on NMHC in the oceans. This builds upon the body of literature on oceanic sources of other trace gases in the marine atmosphere, such as DMS and halocarbons (e.g. methyl halides). To achieve this we created a laboratory-based culturing system with which we could test the effects of environmental parameters, bacteria, protists, and phage on trace gas production by phytoplankton. Air-tight vessels were designed from Pyrex Erlenmeyer flasks that would be non-toxic to cells, yet minimally permeable to the trace levels of the relevant hydrocarbon compounds which are potentially prevalent in the laboratory air. Replicate cultures grown in these flasks and analyzed on the GC-FID had good precision, more than sufficient to elucidate the effects of various parameters on isoprene production.

With this system we were able to determine definitively that isoprene production is a biological process. All five photosynthetic organisms tested produced isoprene, including several cyanobacteria and eukaryotic phytoplankton. Production rates were approximately constant during healthy growth when normalized to cell number, but at different values for each organism. An allometric relationship was observed where species with larger cell volumes had larger production rates per cell. Additionally, isoprene production as a function of light and temperature generally had the same relationships as growth rate. The exception was at high irradiances where growth was photoinhibited but isoprene production rates continued to increase.

These patterns imply that isoprene is related to phytoplanktonic photosynthesis, but two cultures of heterotrophic bacteria were also shown to produce isoprene during part of their growth cycle in organically enriched media. However, the presence of bacteria in seawater did not affect phytoplanktonic isoprene production rates. Isoprene production by the

bacteria cultured in this work may thus only be induced when an excess of organics are available. The single protist tested, *Cafeteria roenbergensis*, affected isoprene production by *Prochlorococcus* cultures only through controlling the phytoplankton counts, but phage-infected cells had lower isoprene production rates than healthy cells on a per cell basis. These results indicate that it is reasonable to create ocean emission models that are directly dependent upon photosynthetic cell type and count, or indirectly dependent upon bulk chlorophyll concentration. However, physiological conditions, such as cellular responses to light and temperature, affected isoprene production by *Prochlorococcus* by factors on the order of 5. These physiological effects would also need to be taken into account to accurately capture the natural variability in phytoplanktonic isoprene sources.

What does it tell us that marine phytoplankton, as well as terrestrial plants, have been shown to produce isoprene? The major difference between these two photosynthetic sources is in the magnitude of the production rate. This may indicate a different functionality for the gas in phytoplankton as compared to higher plants, or perhaps it is simply an environmental issue. Isoprene could be released as a convenient way to remove excess reducing power from the leaf cells as Fall (1991) proposed. Leaves, particularly sun exposed ones, can experience irradiances up to several thousand $\mu E\ m^{-2}\ s^{-1}$, with the potential for large amounts of absorbed energy that cannot be used for photosynthesis. In contrast, water column irradiances can only rarely reach 1000 $\mu E\ m^{-2}\ s^{-1}$ just under the water surface. Unless mixed upwards to very shallow depths for extended periods of time, submerged cells generally experience irradiances in their light-limited or light-saturated growth regimes; thus *in situ* isoprene production might be expected to be quite low. When cells were exposed to photoinhibiting irradiances in our laboratory cultures, isoprene production increased significantly, supporting this hypothesis. Perhaps further work with phytoplanktonic or bacterial isoprene production processes will help elucidate the biological function of this gas in both these and other organisms.

This study additionally confirmed, with more careful attention to biological monitoring than past studies, that marine NMHC other than isoprene have more complex sources than a

simple microbial production or consumption. These conclusions apply to both alkanes (e.g. ethane), and alkenes (e.g. ethene). This is most likely a real effect, and not a matter of background NMHC contamination in our incubation system.

6.2 FUTURE DIRECTIONS

Many questions remain to be answered; thus there are a variety of directions in which to continue this work. A fundamental limitation in these experiments were the non-zero concentrations of non-isoprene NMHC in the media blanks. These background signals were likely due to the purge gas and plastic incubation flask materials. Improvements made in this background signal may clarify the existence of any (albeit weak) biological cycling of these NMHC, particularly ethane and ethene.

The importance of replicates in biological experiments should be emphasized. The light and temperature responses of *Prochlorococcus* growth rates and isoprene production reported here generally follow expected trends, but fundamentally represent only single measurements at each point. While further experimentation was not possible for this thesis because of the effort involved, duplicates, at least, would be required before reliable empirical models of these relationships can be developed. Other cell species should also be tested and the results combined into a more robust model for use in any sort of predictive capacity.

The potential bacterial influence on NMHC cycling is interesting; while there are hints of isoprene production by marine heterotrophic bacteria, further work would be needed to see if similar relationships with temperature or growth rate occur as for phytoplankton or for terrestrial bacteria (Kuzma et al., 1995; Wagner et al., 1999). Additionally, no consistent bacterial consumption of any NHMC was detected here, but more detailed experiments are necessary to determine this absolutely. Isotopic tracers would be one potential method to explicitly determine any bacterial utilization or production of NMHC in an incubation spiked with high initial NMHC levels.

The preliminary indications of methyl halide production by *Prochlorococcus* reported here are also intriguing as there are still missing sources of these chemicals on a global scale needed to balance their budgets. Full incubation experiments would be the next step in exploring this potential source.

6.3 POSSIBILITIES

The original goal motivating this work was to be able to calculate the sea-to-air flux of NMHC from water column cycling processes accurately enough to determine any effects on tropospheric chemistry. While we are still far from that point, significant improvements to our understanding of water column NMHC cycling have been made, including the dependence of isoprene production on light, temperature, organism species, and organism size, and the effects of a few representative heterotrophic organisms. One of the more interesting next steps would be to combine these laboratory results with *in situ* measurements to see if we can create a mass balance for isoprene in a fairly well characterized system, such as the BATS station in the Sargasso Sea. By combining the empirically measured laboratory production rates with cell counts, bulk chlorophyll concentration, or growth rates of representative species in the water column, one could calculate isoprene production and potential ocean-air flux as we did here in Chapter 5. This could be compared to an isoprene flux measured simultaneously using bulk flux calculations, such as those done by Liss & Merlivat (1986). If designed properly, this method could help to identify other potential sources or sinks of isoprene, and to validate empirical models of oceanic isoprene emission.

GLOSSARY

axenic	Free from other living organisms
cell lysis	Rupture of a cell, resulting in loss of cell contents
eutrophic	Nutrient rich
eutrophication	Exhaustion of the oxygen pool in water due to organic carbon decomposition
exudance	Cellular release of chemicals; Can occur throughout healthy life cycle, as well as during senescence
oligotrophic	Nutrient poor
pelagic	Of or pertaining to the open ocean; Applied especially to animals that live at the surface of the ocean, away from the coast
senescence	The state of growing old, dying

COMMON ACRONYMS

DOC/M	Dissolved Organic Carbon/Matter
FID	Flame Ionization Detector
GC	Gas Chromatograph
LMW	Low Molecular Weight
NMHC	Non-Methane HydroCarbon
PAR	Photosynthetically Active Radiation
PUFA	Poly-Unsaturated Fatty Acids
UHP	Ultra High Purity
RT	Retention Time

BIBLIOGRAPHY

Abeles, F.B. (1973) *Ethylene in Plant Biology*, Academic Press, New York.

Andersen, R. A., R. R. Bidigare, M. Keller, and L. Mikel (1996) A comparison of HPLC pigment signatures and electron microscopic observations for oligotrophic waters of the North Atlantic and Pacific Oceans, *Deep Sea Res.* **43**(2-3), 517-537.

Andersen, R. A., G. W. Saunders, M. P. Paskind, and J. P. Sexton (1993) Ultrastructure and 18S rRNA gene sequence for Pelagomonas calceolata gen. et sp. nov. And the description of a new algal class, the Pelagophyceae classis nov., *J. Phycol*. **29**, 701-715.

Apel, E.C., J.G. Calvert, and F.C. Fehsenfeld (1994) The Nonmethane Hydrocarbon Intercomparison Experiment (NOMHICE): Tasks 1 and 2, *J. Geophys. Res*. **99**, 16651-16664.

Atkinson, R. (1989) Kinetics and mechanisms of the gas-phase reactions of the hydroxyl radical with organic compounds, *J. Phys. Chem. Ref. Data* **1**, 268.

Atkinson, R., and W. Carter (1984) Kinetics and mechanisms of the gas phase reactions of ozone with organic compounds under atmospheric conditions, *Chem. Rev*., **83**, 437-470.

Atlas, R. M. (1988) *Microbiology*, Macmillan Pub. Co., New York.

Ayers, G. P., R. W. Gillett, H. Granek, C. de Serves, R. A. Cox (1997) Formaldehyde production in clean marine air, *Geophys. Res. Lett*. **24**(4) 401-404.

Azam, F, T. Fenchel, J.G. Field, L.A. Meyer-Reil, F. Thingstad (1983) The ecological role of water-column microbes in the sea, *Mar. Ecol. Prog. Ser*. **10**, 257-263.

Baker, J.M., C.E. Reeves, P.D. Nightengale, S.A. Penkett, S.W. Gibb, and A.D. Hatton (1999) Biological Producation of methyl bromide in the coastal waters of the North Sea and open ocean of the northeast Atlantic, *Marine Chem*. **64**, 267-285.

Baker, A. R., S.M. Turner, W. J. Broadgate, A. Thompson, G. B. McFiggans, O. Vesperii, P. D. Nightengale, P. S. Liss, and T. D. Jickells (2000) Distribution and sea-air fluxes of biogenic trace gases in the eastern Atlantic Ocean., *Glob. Biogeochem. Cyc*. **14**(3), 871-886.

Benson, R. & E. Martin (1981) Effects of photosynthetic inhibitors and light-dark regimes on the replication of cyanophages SM-2, *Arch. Microbiol*. **129**, 165-167.

Bidigare, R.R., and M.E. Ondrusek (1996) Spatial and temporal variability of phytoplankton pigment distributions in the central equatorial Pacific Ocean, *Deep-Sea Res. II* **43**, 809-833.

Binder, B. J., S. W. Chisholm, R. J. Olson, S. L. Frankel, and A. Z. Worden (1996) Dynamics of picophytoplankton, ultraphytoplankton, and bacteria in the central equatorial Pacific. *Deep-Sea Res.* **43**(4-6), 907-931.

Bonsang, B., M. Kanakidou, G. Lambert, and P. Monfray (1988) The Marine Source of C_2-C_6 Aliphatic Hydrocarbons, *J. Atmos. Chem.* **6,** 3-20.

Bonsang, B., C. Polle, and G. Lambert (1992) Evidence for Marine Production of Isoprene, *Geophys. Res. Lett.* **19**, 1129-1132.

Brand, L.E., R.R. Guillard, and L.S. Murphy (1981) A method for the rapid and precise determination of acclimated phytoplankton reproduction rates, *J. Plankton Res.* **3**: 193-201.

Bratbak, G., J. K. Egge, and M. Heldal (1993) Viral mortality of the marine alga Emiliania hyxleyi (Haptphyceae) and termination of algal blooms, *Mar. Ecol. Prog. Ser.* **93,** 39-48.

Brimblecombe, P., and D. Shooter (1986) Photooxidation of dimethylsulfide in aqueous solution, *Mar. Chem.* **19**, 343-353.

Broadgate, W.J., P.S. Liss, and S.A. Penkett (1997) Seasonal emissions of isoprene and other reactive hydrocarbon gases from the ocean, *Geophys. Res. Lett.* **24**(21), 2675-2678

Brussard, C.P.D., R. Thyrhaug, D. Marine, and G. Bratbak (1999) Flow cytometric analysis of viral infection in two marine phytoplankton species, *Micromonas pusilla* (Prasinophyceae) and *Phaeocystis pouchetii* (Prymnesiophyceae), *J. Phycol.* **35**, 941-948.

Bullister, J.L. and R.F Weiss (1988) Determination of CCl3F and CCl2F2 in seawater and air, *Deep Sea Res.* **35**(5), 839-853.

Buma, A.G.J., H.J. Zemmelink. K. Sjollema, and W.W.C. Gieskes (1996) UVB radiation modifies protein and photosynthetic pigment content, volume, and ultrastructure of marine diatoms, *Mar. Ecol. Prog. Ser.* **142**, 47-54.

Butler, J. (2000) Better budgets for methyl halides? *Nature,* **403**(20) 260-261.

Cailliau, C., H. Claustre, F. Vidussi, D. Marie, and D. Vaulot (1996) Carbon biomass, and gross growth rates as estimated from 14C pigment labelling, during photoacclimatino in *Prochlorococcus* CCMP 1378, *Mar. Ecol. Prog. Ser.* **145**, 209-221.

Campbell, D., M.J. Eriksson, G. Oquist, P. Gustafsson, and A.K. Clarke (1998) The cyanobacterium *Synechococcus* resists UV-B by exchanging photosystem II reaction-center D1 proteins, *Proc. Natl. Acad. Sci. USA* **95**, 364-369.

Campbell, L., H. Liu, H.A. Nolla, and D. Vaulot (1997) Annual variability of phytoplankton and bacteria in the subtropical North Pacific Ocean at Station ALOHA during the 1991-1994 ENSO event, *Deep-Sea Res.* **44**(2), 167-192.

Campbell, L., H.A. Nolla, and D. Vaulot. 1994. The importance of *Prochlorococcus* to community structure in the central North Pacific Ocean. *Limnol. Oceanogr.* **39**(4): 955-961.

Caron, D.A., E.L. Lim, G. Miceli, J.B. Waterbury, and F.W. Valois (1991) Grazing and utilization of chroococcoid cyanobacteria and heterotrophic bacteria by protozoa in laboratory cultures and a coastal plankton community, *Mar. Ecol. Prog. Ser.* **76**, 205-217.

Carlsaw, N., D.J. Creasey, D. E. Heard, A. C. Lewis, J. B. Mcquiad, M. J. Pilling, P. S. Monks, B, J, Bandy, and S. A. Penkett (1999) Modeling OH, HO2, and RO2 radicals in the marine boundary layer 1. Model construction and comparison with field measurements., *J. Geophys. Res.* **104**(D23), 30241-30255.

Cavender-Bares, K.K, D.M. Karl, and S.W. Chisholm (2001) Nutrient gradients in the western North Atlantic Ocean: Relationships to microbial community structure, and comparison to patterns in the Pacific Ocean, *Deep-Sea Res.*, in press.

Chisholm., S. W. (1992) Phytoplankton Size, *in Primary Productivity and Biogeochemical Cycles in the Sea*, (P.G. Falkowski and A. D. Woodhead, eds.), Plenum Press, New York.

Chisholm, S. W., S. L. Frankel, R. Goericke, R. J. Olson, B. Palenik., J. B. Waterbury, and N. A. Welschmeyer (1992) *Prochlorococcus marinus* nov. Gen. Nov. Sp.: an oxyphototrophic marine prokaryote containing divinyl chlorophyll a and b. *Arch. Microbiol.* **157**, 297-300.

Chisholm, S. W., R. J. Olson, E. R. Zettler, R. Goericke, J. B. Waterbury, and N. A. Welschmeyer (1988) A novel free-living prochlorophyte abundant in the oceanic euphotic zone, *Nature* **334**(28), 340-343.

Cleveland, C.C., and J. B. Yavitt (1998) Microbial consumption of atmospheric isoprene in a temperate forest soil., *App. Environ. Microbiol.* **64**(1) 172-177.

Cortes, M. Y., J. Bollmann, H. R. Thierstein (2001) Coccolithophore ecology at the HOT station ALOHA, Hawaii, *Deep-Sea Res. II* **48**, 1957-1981.

Cuhel R. L. and Waterbury J. B. (1984) Biochemical composition and short term nutrient incorporation patterns in a unicellular marine cyanobacterium, Synechococcus (WH7803). *Limnol. and Oceanogr.* **29**, 370-374.

Dacey, J. W. H, and S. G. Wakeham (1986) Oceanic Dimethylsulfide: Production during zooplankton grazing on phytoplankton. *Science* **233**, 1314-1316.

Deneris, E. S., R. A Stein, and J. F. Mead (1985) Acid-catalyzed formation of isoprene from a mevalonate-derived product using a rat liver cytosolic fraction, *J. Biol. Chem.* **260**(3), 1382-1385.

Dewick, P. (1999) The biosynthesis of C5-C25 terpenoids, *Nat. Prod. Rep.* **16**, 97-130.

Donahue, N. (1991) Nonmethane hydrocarbon chemistry in the remote marine atmosphere, Ph.D. Thesis, *MIT Center for Global Change Science Report* **8**.

Donahue, N & R. G. Prinn (1990) Nonmethane Hydrocarbon Chemistry in the Remote Marine Boundary Layer, *J. Geophys. Res.* **95**(D11), 18387-18411.

Donahue, N & R. G. Prinn (1993) *In situ* Nonmethane Hydrocarbon Measurements on SAGA 3, *J. Geophys. Res.* **98**(D9), 16915-16932.

Ducklow, H.W., D.L. Kirchman, H.L. Quinby., C.A. Carlson, and H.G. Dam (1993) Stocks and dynamics of bacterioplankton carbon during the spring bloom in the eastern North Atlantic Ocean, *Deep-Sea Res. II* **40**(1/2), 245-263.

Durand, M. D., R. J. Olson, and S. W. Chisholm (2001) Phytoplankton population dynamics at the Bermuda Atlantic Time Series station in the Sargasso Sea., *Deep-Sea Res. II* **48**, 1983-2003.

Dusenberry, J. A. and S. L. Frankel (1994) Increasing the sensitivity of a FACScan flow cytometer to study oceanic picoplankton., *Limnol. Oceanogr.* **39** (1), 206-209.

Dusenberry, J. A., R. J. Olson, and S. W. Chisholm (2001), Photoacclimation kinetics of single-cell fluorescence in laboratory and field populations of *Prochlorococcus, Deep Sea Res.* **48**(6), 1443-1458.

Elliot, S., and F. S. Rowland (1995) Methyl halides hydrolysis rates in natural waters. *J. Atmos. Chem.* **20**, 229-237.

Eppley, R. W. (1981) Relations between nutrient assimilation and growth in phytoplankton with a brief review of estimates of growth rates in the ocean, *in Physiological Bases of Phytoplankton Ecology* (ed. T. Platt), Canadian Department of Fisheries and Oceans, Ottawa, pp. 251-263.

Evans, M. J., et al. (2000) Evaluation of a Lagrangian box model using field measurements from EASE (Eastern Atlantic Summer Experiment) 1996, *Atm. Environ.* **34**, 3843-3863.

Falkowski, P. G. and J. A. Raven (1997) *Aquatic Photosynthesis*, Blackwell Science, Malden, Mass.

Fall, R. (1991) Isoprene emission from plants: summary and discussion, in *Trace Gas Emissions by Plants*, T. Sharkey ed. 209-216.

Fall, R. (1999) Biogenic Emissions of Volatile Organic Compounds from Higher Plants, in *Reactive Hydrocarbons in the Atmosphere*, Academic Press.

Fall, R. And M. C. Wildermuth (1998) Isoprene synthase: From biochemical mechanism to emission algorithm. *J. Geophys. Res.* **103** (D19), 25599-25609.

Fehsenfeld, F., J. Calvert, R. Fall, P. Goldan, A.B. Guenther, C.N. Hewitt, B. Lamb, S. Liu, M. Trainer, H. Westberg, and P. Zimmerman (1992) Emissions of volatile organic compounds from vegetation and the implications for atmospheric chemistry, *Glob. Biogeochem. Cyc.* **6**(4), 389-430.

Finlayson-Pitts, B and J. Pitts (2000) *Chemistry of the Upper and Lower Atmosphere*, Academic Press, San Diego.

Fuentes, J.D., B.P. Hayden, M. Garstang, M. Lerdau, D. Firzgarrald, D.D. Baldocchi, R. Monson, B. Lamb, C. Geron (2001) New Directions: VOCs and biosphere-atmosphere feedbacks, *Atm. Environ*. **35**, 189-191.

Fuhrman, J. (1999) Marine viruses and their biogeochemial and ecological effects, *Nature* **399**, 541-548.

Fujii, T., T. Ogawa, and H. Fukuda (1987) Isobutene production by Rhodotorula minuta, *Appl. Microbiol. Biotechnol*. **25**, 430-433.

Fukuda, H., T. Ogawa, ane S. Tanase (1993) Ethylene Production by Microorganisms, in *Advances in Microbial Physiology* **35,** (A. H. Rose, ed.), Academic Press, London.

Gerhardt, P., ed. (1981) *Manual of Methods for General Bacteriology*, Amer. Soc. Microbiol., Wash., D.C.

Gobler, C. J., D. A. Hutchins, N. S. Fisher, E. M. Cosper, and S. A. Sanudo-Wilhelmy (1997) Release and bioavailability of C, N, P, Se, and Fe following viral lysis of a marine chrysophyte, *Limnol. Oceanogr*. **42**(7), 1492-1504.

Goericke, R., and N. A. Welschmeyer (1993) The marine prochlorophyte *Prochlorococcus* contributes significantly to phytoplankton biomass and primary production in the Sargasso Sea, *Deep Sea Res.* **40**, 2283-2294.

Gong, Q. and K. Demerjian (1995) Hydrocarbon losses on a regenerated Nafion Dryer, *J. Air Waste Manage. Assoc.* **45**, 490-493.

Goodwin, K., J. K. Schaefer, and R. S. Oremland (1998) Bacterial oxidation of dibromomethane and methyl bromide in natural waters and enrichment cultures, *Appl. Environ. Microbiol.* **64**(12), 4629-4636.

Graham, J. (1998) Seasonal Measurements of Nonmethane Hydrocarbons in a Sub-tropical Evergreen Forest in Southern China, PhD Thesis, *MIT Center for Global Change Science Report* **59**, Cambridge, Mass.

Granier, C. G. Petron, J-F Muller, and G. Brasseur (2000) The Impact of Natural and Anthropogenic Hydrocarbons on the Tropospheric Budget of Carbon Monoxide, *Atm. Envir.* **34**, 5255-5270.

Greenberg, J. P., and P. R. Zimmerman (1984) Nonmethane hydrocarbons in remote tropical, continental, and marine atmospheres, *J. Geophys. Res.* **89**, 4767-4778.

Guenther, A., C. N. Hewitt, D. Erickson, R. Fall, C. Geron, T. Graedel, P. Harley, L. Klinger, M. Lerdau, W. McKay, T. Pierce, B. Scholes, R. Steinbrecher, R. Tallamraju, J. Taylor and P. Zimmerman, A global model of natural volatile organic compound emissions, *J. Geophys. Res.* **100**, 8873-8892, 1995.

Guenther, A.B., R. K. Monson, and R. Fall (1991) Isoprene and Monoterpene Emission Rate Variability: Observations with eucalyptus and emission rate algorithm development, *J. Geophys. Res.* **96**, 107999-10808.

Guenther, A.B., P.R. Zimmerman, P.C. Harley, R.K. Monson, and R. Fall (1993) Isoprene and Monoterpene Emission Rate Variability: Model Evaluations and Sensitivity Analyses, *J. Geophys. Res.* **98** (D7), 12609-12617.

Gschwend, P. M., and J.K. MacFarlane, and K. A. Newman (1985) Volatile halogenated organic compounds released to seawater from temperate marine macroalgae, *Science* **227**, 1033-1035.

Hagstrom, A., F. Azam, A. Andersson, J. Wikner, and F. Rassoulzadegan (1988) microbial loop in an oligotrophic pelagic ecosystem: possible roles of cyanobacteria and nanoflagellates in the organic fluxes, *Mar. Ecol. Prog. Ser.* **49**, 171-178.

Haidar, A.T., and H. R. Thierstein (2001) Coccolithophore dynamics off Bermuda (N. Atlantic), *Deep-Sea Res. II* **48**, 1925-1956.

Hamamura, N, and D.J. Arp (2000) Isolation and characterization of alkane-utilizing *Nocardioides sp.* Strain CF8, *FEMS Microbiol. Lett.* **186**(1) 21-26.

Hansen, B., P.K. Bjornsen, and P. J. Hansen (1994) The size ratio between planktonic predators and their prey, *Limnol. Ocean.* **39**, 395-403.

Hanson, D. T., S. Swanson, L.E. Graham, and T. D. Sharkey (1999) Evolutionary significance of isoprene emission from mosses, *Amer. J. Bot.* **86**(5), 634-639.

Harley, P., G. Deem, S. Flint, and M. Caldwell (1996) Effects of growth under elevated UV-B on photosynthesis and isoprene emission in *Quercus gambelii* and *Mucuna pruriens*, *Glob. Change Biol***. 2**, 149-154.

Harley, P., R. Monson, and M. Lerdau (1999) Ecological and evolutionary aspects of isoprene emission from plants, *Oecologia* **118**, 109-123.

Harrison, W.G., E.J.H. Head, E.P.W. Horne, B. Irwin, W.K.W. Li, A.R. Longhurst, M.A. Paranjape, and T. Platt (1992) The western North Atlantic Bloom Experiment, *Deep-Sea Res. II* **40**(1/2) 279-305.

Helmig, D. (1997) Ozone removal techniques in the sampling of atmospheric volatile organic trace gases. *Atmos. Env.* **31**(21), 3635-3651.

Hill, R.W., B.A.White, M.T. Cotrell, J.W.H. Dacey (1998) Virus-mediated total release of dimethylsulfoniopropionate from marine phytoplankton: a potential climate process, *Aquat. Microb. Ecol.* **14**, 1-6.

Holligan, P. M., E. Fernandez, and 13 others (1993) A biogeochemical study of the coccolithophore, *Emiliania huxleyi*, in the North Atlantic, *Glob. Biogeochem. Cyc.*, **7(4)**, 879-900.

Hou, C.T., R. N. Patel, N. Laskin, N. Barnabe, and I. Barist (1981) Epoxidation and hydroxylation of C4- and C5- branched-chain alkenes and alkanes by methanotrophs., *Ind. Microbiol.* **23**, 477-482.

Jeffrey, S.W. , and G.F. Humphrey (1975) New spectrophotometric equations for determining chlorophylls a, b, c1, and c2 in higher plants, algae, and natural phytoplankton, *Biochem. Physiol. Pflanzen* **167**, 191-194.

Keene, W.C., D.J. Jacob, and S.M. Fan (1996) Reactive chlorine: A potential sink for dimethylsulfide and hydrocarbons in the marine boundary layer, *Atm. Env.* **30 (6)**, i -iii.

Keller, M.D. W.K. Bellows and R.R.L. Guillard. 1989. Dimethyl sulfide production in marine phytoplankton, in *Biogenic sulfur in the environment* (E.S. Saltzman and W.J. Cooper, eds.) A.C.S. Symposium Series. No. 393 pp.167-182.

Keller, M., and W. Korjeff-Bellows (1996) Physiological aspects of the production of dimethylsulfoniopropionate (DMSP) by marine phytoplankton, in *Biological and Environmental Chemistry of DMSP and Related Sulfonium Compounds*, Kiene, R. P, ed. Plenum Press, New York, 131-142.

Keller, M. and M. Lerdau (1997) Isoprene emission from tropical forest canopy leaves., *Glob. Biogeochem. Cycles* **13** (1), 19-29.

Kesselmeier, J. and M. Staudt (1999) Biogenic Volatile Organic Compounds (VOC): An Overview on Emission, Physiology, and Ecology, *J. Atmos. Chem.* **33**, 23-88.

Kiene, R. P., and T. S. Bates (1990) Biological removal of dimethyl sulphide from seawater. *Nature* **345**, 702-705.

Kiene, R.P., P.T. Visscher, M.D. Keller, and G.O. Kirst, editors (1996) *Biological and Environmental Chemistry of DMSP and Related Sulfonium Compounds*, Plenum Press, New York.

Kimmerer, T. W., and T. T. Kozlowski (1982) Ethylene, ethane, acetaldehyde, and ethanol production by plants under stress, *Plant Physiol.* **69**, 840-847.

King, D. B., and E. S. Saltzman (1997) Removal of methyl bromide in coastal seawater: chemical and biological rates, *J. Geophys. Res.* **102**(D8), 18715-18721.

Kirchmer, C. J. (1988) Estimation of Detection Limits for Environmental Analytical Procedures, in *Detection in Analytical Chemistry* (L.A. Currie, ed.), ACS Symposium series: 361, American Chemical Society.

Kleiman, G. (1999) Measurement and Deduction of Emissions of Short-lived Atmospheric Organo-chlorine Compounds, Ph.D. Thesis, *MIT Center for Global Change Science Report* **64**, Cambridge, Mass.

Koppman, R. F.J. Johnen, A, Khedim, J. Rudolph, A. Wedel, and B. Wiards (1995) The influence of ozone on light nonmethane hydrocarbons during cryogenic preconcentration, *J. Geophys. Res.* **100**, 11383-11391.

Kuzma, J., M. Nemecek-Marshall, W. Pollock, R. Fall (1995) Bacteria produce the volatile hydrocarbon isoprene, *Current Microbiology* **30**, 97-103.

Lee, R.F. and J. Baker (1992) Ethylene and ethane production in an estuarine river: formation from the decomposition of polyunsaturated fatty acids, *Mar. Chem.* **38**, 25-36.

Lee, C. and S.G. Wakeham (1989) Chapter 49: Organic Matter in Seawater: Biogeochemical Processes, in *Chemical Oceanography* **9**, Academic Press, Ltd., 2-51.

Lerdau, M., A. Guenther, and R. Monson (1997) Plant Production and Emission of Volatile Organic Compounds, *BioScience* **47**(6), 373-383.

Lerdau, M., and H. Throop (1999) Isoprene emission and photosynthesis in a tropical forest canopy: Implications for model development, *Ecol. App.* **9** (4), 1109-1117.

Lewis, A. C., J.B. L. J. Carpenter, and M.J. Pilling (2001) Nonmethane hydrocarbons in Southern Ocean boundary layer air, *J. Geophys. Res.* **106**(D5), 4987-4994.

Lewis, A. C., J.B. McQuaid, N. Carslaw, and M.J. Pilling (1999) Diurnal cycles of short-lived tropospheric alkenes at a north Atlantic coastal site, *Atmos. Env*. **33**, 2417-2422.

Li, W.K.W., P.M. Dickie, B.D. Irwin, and A.M. Wood (1992) Biomass of bacteria, cyanobacteria, prochlorophytes, and photosynthetic eukaryotes in the Sargasso Sea, *Deep-Sea Res.* **39** (3/4), 501-519.

Lichthenthaler, H. K. (1999) The 1-Deoxy-D-Xylulose-5-Phosphate Pathway of Isoprenoid Biosynthesis in Plants, *Ann. Rev. Plant Physiol. Plant. Mol. Biol*. **50**, 47-65.

Lim, E. L., M.R. Dennett & D.A. Caron (2001) Identification of heterotrophic nanoflagellates by restriction fragment length polymorphism analysis of small subunit ribosomal DNA. *J. of Euk. Microbiol.*, **48**(3): 247-257.

Liss, P. S., and L. Merlivat (1986) Air-Sea Gas Exchange Rates: Introduction and Synthesis, in *The Role of Air-Sea Exchange in Geochemical Cycling*, (P. Buat-Menard, ed.), D. Reidel Publishing Company, 113-127.

Liu, H., H. A. Nolla, and L. Campbell (1997) Prochlorococcus growth rate and contribution to primary production in the equatorial and subtropical North Pacific Ocean. *Aquat. Microb. Ecol.* **12**, 39-47.

Logan, B. A. and R. K. Monson (1999) Thermotolerance of leaf discs from four isoprene-emitting species is not enhanced by exposure to exogenous isoprene, *Plant. Physiol*. **120**, 821-825.

Loreto, F., and T. D. Sharkey (1990) A gas-exchange study of photosynthesis and isoprene emission in Quercus rubra L., *Planta* **182**, 523-531.

Loreto, F., and T. D. Sharkey (1993) On the relationship between isoprene emission and the photosynthetic metabolites under different environmental conditions, *Planta* **189**, 420-424.

MacKay, D. and W.Y.Shiu (1981) Critical review of Henry's Law constants for chemicals of environmental interest, *J. Phys. Chem. Ref. Data*, **10**, 1175-1199.

Madigan, M. T., J. M. Martinko, J. Parker (2000) *Brock Biology of Microorganisms 9th Edition*, Prentice-Hall, Upper Saddle River, NJ.

Malin, G., W.H. Wilson, G. Bratbak, P. S. Liss, and N. H. Mann (1998) Elevated production of dimethylsulfide resulting from viral infection of cultures of *Phaeocystic pouchettii*, *Limnol. and Oceanogr*. **43**(6), 1389-1393.

Manley S.L. and M.N. Dastoor (1987) Methyl halide (CH3X) production from the giant kelp, *Macrocystis* and estimates of global CH3X production by kelp. *Limnol Oceanogr*. **23**: 709-715.

Mann, E., and S.W.Chisholm (2000) Iron limits the cell division rate of Prochlorococcus in the Eastern Pacific Ocean, *Limnol. Ocean*. **45**(5), 1067-1076.

McClenny, W. A., J. D. Pleil, M. W. Holdren, and R. N. Smith (1984) Automated Cryogenic Preconcentration and Gas Chromatographic Determination of Volatile Organic Compounds in Air, *Anal. Chem.* **56**, 2947-2951.

McKay, W. A., M. F. Turner, B.M.R. Jones, C. M. Halliwell (1996) Emissions of hydrocarbons from marine phytoplankton - Some results from controlled laboratory experiments, *Atmos. Env.* **30,** 2583-2593.

Miller, B., T. Heuser, and W. Zimmer (1999) A *Synechococcus leopoliensis* SAUG 1402-1 operon harboring the 1-deoxyxylulose 5-phosphate synthase gene and two additional open reading frames is functionally involved in the dimethylallyl diphosphate synthesis, *FEBS Letters* **460**, 485-490.

Miller, B. R., J. Huang, R. F. Weiss, R. G. Prinn, and P. J. Fraser (1998) Atmospheric trend and lifetime of chlorodifluoromethane (HCFC-22) and the global tropospheric OH concentration, *J. Geophys. Res.* **103**, 13,237-13,248.

Milne, P. J. , D. D. Reimer, R. G. Zika, L. E. Brand (1995) Measurement of vertical distribution of isoprene in surface sea water, its chemical fate, and its emission from several phytoplankton monocultures, *Marine Chem.* **48**, 237-244.

Monson, R.K., C.H. Jaeger, W.W. Adams, E.M. Driggers, G.M. Silver, and R. Fall (1992) Relationships among isoprene emission rate, photosynthesis and isoprene synthase activity as influenced by temperature. *Plant Physiol.* **98**, 1175-1180.

Monson, R.K. and R. Fall (1989) Isoprene Emission from Aspen Leaves, *Plant Physiol*. **90**, 267-274.

Monson, R.K., C. H. Jaeger, W. W. Adams III, E. M. Driggers, G. M. Silver, and R. Fall (1992) Relationships among Isoprene Emission Rate, Photosynthesis, and Isoprene Synthase Activity as Influenced by Temperature, *Plant Physiol*. **98**, 1175-1180.

Moore, L. R. (1997) Physiological ecology of *Prochlorococcus*: A comparison of isolates from diverse oceanographic regimes, PhD Thesis, MIT Department of Civil and Environmental Engineering, Cambridge, Mass.

Moore, L. and S. W. Chisholm (1999) Photophysiology of the marine cyanobacterium *Prochlorococcus*: Ecotypic differences among cultured isolates, Limnol. Oceanogr. **44**(3), 628-638.

Moore, L.W.J., R. Goericke, and S.W. Chisholm (1995) Comparative physiology of *Synechococcus* and *Prochlorococcus*: influence of light and temperature on growth, pigments, fluorescence and absorptive properties, *Mar. Ecol. Prog. Ser.* **116**, 259-275.

Moore, R.M., D.E. Oram, and S.A. Penkett (1994) Production of isoprene by marine phytoplankton cultures, *Geophys. Res. Lett*. **21(23)**, 2507-2510.

Moore, R.M., M. Webb, R. Tokarczyk, and R. Wever (1996) Bromoperoxidase and iodoperoxidase enzymes and production of halogenated methanes in marine diatom cultures, *J. Geophys. Res.* **101**, 20899-20908.

Moore, R. M. and O. C. Zafiriou (1994) Photochemical production of methyl iodide in seawater, *J. Geophys. Res.* **99**(D8), 16415-16420.

Mtolera, M. S. P., J. Collen, M. Pedersen, A. Ejkdall, K. Abrahamsson, and A. K. Semesi (1996) Stress-induced production of volatile halogenated organic compounds in Eucheuma denticulatum (Rhodophyta) caused by elevated pH and high light intensities, *Eur. J. Phycol.* **31**, 89-95.

Ni, K., and L. P. Hager (1998) DNA cloning of Batis maritima methyl chloride transferase and purification of the enzyme, *Proc. Natl. Acad. Sci. USA* **95**, 1286-12871.

Niinemets, U., J. D. Tenhunen, P.C. Harley, and R. Steinbrecher (1999) A model of isoprene emission based on energetic requirements for isoprene synthesis and leaf photosynthetic properties for *Liquidambar* and *Quercus*, *Plant, Cell, and Envir.* **22**, 1319-1335.

Noble, R. T., and J. A. Fuhrman (1998) Use of SYBR Green I for rapid epifluorescence counts of marine viruses and bacteria, *Aquat. Microb. Ecol*. **14**, 113-118.

Olson, R. J., S. W. Chisholm, E. R. Zettler, M. A. Altabet, and J. A. Dusenberry (1990) Spatial and temporal distributions of prochlorophyte picoplankton in the North Atlantic Ocean. *Deep-Sea Res.* **37**(6), 1033-1051.

Pandis, S. N., L. M. Russell, and J. H. Seinfeld (1994) The relationship between DMS flux and CCN concentration in remote marine regions. *J. Geophys. Res.* **99**, 16945-16957.

Parsons, T. R., Y. Maita, and C. M Lalli (1984*) A manual of chemical and biological methods for seawater analysis.* Pergamon Press, Oxford.

Partensky, F., W.R. Hess, and D. Vaulot (1999) *Prochlorococcus*, a Marine Photosynthetic Prokaryote of Global Significance, *Microb. Mol. Biol. Rev*. **63**(1),106-127.

Pate, B., R. K. M. Jayanty, M. R. Peterson, and G. F. Evans (1992) Temporal Stability of Polar Organic Compounds in Stainless Steel Canisters, *J. Air Waste Man. Assoc*., 460-462.

Patel, R.N., C.T. Hou, A.I. Laskin, A. Felix, and P. Derelanko (1983) Oxidation of alkanes by organisms grown on C2-C4 alkanes, *J. Appl. Biochem*. **5**, 107-120.

Pedersen, M., J. Collen, K. Abrahamsson, and A. Ekdahl (1996) Production of halocarbons from seaweeds: an oxidative stress reaction?, *Sci. Mar*. **60** (Supp.1), 257-263.

Peiser, G. D., and S. F. Yang (1979) Ethylene and ethane production from sulfur dioxide-injured plants, *Plant Physiol*. **63**, 142-145.

Plass, C., R. Koppman, and J. Rudolph (1992) Light Hydrocarbons in the Surface Water of the Mid-Atlantic, *J. Atmos. Chem.* **15**, 234-251.

Plass-Dulmer, C., R. Koppman, M. Ratte, and J. Rudolph (1995) Light nonmethane hydrocarbons in seawater, *Glob. Biogeochem. Cyc*. **9**, 79-100.

Platt, T., C. L. Gallegos, and W. G. Harrison (1980) Photoinhibition of phytosynthesis in natural assemblages of marine phytoplankton, *J. Mar. Res.* **38**, 687-701.

Pliel, J., K. Oliver, and W. McClenny (1987) Enhanced performance of Nafion dryers in removing water from air samples prior to gas chromatographic analysis, *J. Air Poll. Cont. Assoc.* **37**, 244-248.

Poisson, N., M. Kanakidou, and P. J. Crutzen (2000) Impact of non-methane hydrocarbons on tropospheric chemistry and the oxidizing power of the global tropophere: 3-Dimensional modelling results, *J. Atm. Chem*. **36**, 157-230.

R.G. Prinn, R. F. Weiss, P. J. Fraser, P. G. Simmonds, D. M. Cunnold, F. N. Alyea, S. O'Doherty, P.Salameh, B. R. Miller, J. Huang, R. H., J. Wang, D. E. Hartley, C. Harth, L. P. Steele, G. Sturrock, P. M. Midgley, and A. McCulloch (2000) A history of chemically and radiatively important gases in air deduced from ALE/GAGE/AGAGE, *J. Geophys. Res.* **105**, 17,751-17,792.

Pszenny, A.A.P., R.G. Prinn, G.L. Kleiman, X. Shi, and T.S. Bates, Nonmethane hydrocarbons in surface waters, their sea-air fluxes and impact on OH in the marine boundary layer during ACE–1, *J. Geophys. Res.* **104**, 21,785-21,801, 1999.

Ratte, M., O Bujok, A. Spitzy, J. Rudolph (1998) Photochemical alkene formation in seawater from dissolved organic carbon : Results from laboratory experiments, *J. Geophys. Res*. **103** (D5), 5707-5717.

Ratte, M., C. Plass-Dulmer, R. Koppman, and J. Rudolph (1993) Production mechanism of C_2-C_4 hydrocarbons in seawater: Field measurements and experiments, *Glob. Biogeochem. Cyc.* **7**, 369-378.

Ratte, M., C. Plass-Dulmer, R. Koppman, and J. Rudolph (1995) Horizontal and vertical profiles of light hydrocarbons in seawater related to biological, chemical, and physical parameters, *Tellus* **47B**, 607-623.

Reimer, D. D., P. J. Milne, R. G. Zika, and W. H. Pos (2000) Photoproduction of nonmethane hydrocarbons (NMHC) in seawater, *Mar. Chem.* **71**, 177-198.

Reinfelder, J. R. and N. S. Fisher (1991) The assimilation of elements ingested by marine copepods. *Science* **251**, 794-796.

Riebesell, U., Wolf-Gladrow, D.A., and V. Smetacek (1993) Carbon dioxide limitation of marine phytoplankton growth rates, *Nature* **361**, 249-251.

Rocap, G, D.L. Distel, J.B. Waterbury, and S.W. Chisholm (2001) Resolution of *Prochlorococcus* and *Synechococcus* ecotypes using 16S-23S rDNA Internal Transcribed Spacer (ITS) Sequences, submitted to *Appl. Environ. Microbiol.*

Rontani, J. F. (1991) Identification by GC/MS of acidic compounds produced during the photosensitized oxidation of normal and isoprenoid alkanes in seawater, *Int. J. Environ. Anal. Chem*. **45**, 1-9.

Rudolph, J. & D.H. Ehhalt (1981) Measurements of C2 - C5 hydrocarbons over the North Atlantic, *J. Geophys. Res*. **86**, 11,959-11,964.

Rudolph, J. & Johnen, F.J. (1990) Measurements of Light Atmospheric Hydrocarbons Over the Atlantic in Regions of Low Biological Activity, *J. Geophys. Res.* **95** (D12), 20583-20591.

Saeki, H., and K. Furuhashi (1994) Cloning and characterization of a Nocardia corallina B-276 gene cluster encoding alkene monoxygenase, *J. Ferment. Bioeng*. **78**, 339-406.

Saemondsdottir, S., and P. A. Matrai (1998) Biological production of methyl bromide by cultures of marine phytoplankton, *Limnol. and Oceanogr*. **43**(1), 81-87.

Saini, H. S., J. M. Attieh, and A. D. Hanson (1995) Biosynthesis of halomethanes and methanethiol by higher plants via a novel methyltransferase reaction, *Plant Cell & Environ.* **18**, 1027-1033.

Sanadze, G. A. (1990) The principle scheme of photosynthetic carbon conversion in cells of isoprene releasing plants, in *Current Research in Photosynthesis IV* (ed. M. Baltscheffsky), pp 231-237. Kluwer Academic Publishers, Dodrecht.

Sander, R. (1996) http://www.science.yorku.ca/cac/people/sander/res/henry.html

Scarratt, M. G and R. M. Moore (1996) Production of methyl chloride and methyl bromide in laboratory cultures of marine phytoplankton, *Marine Chem.* **54**, 263-272.

Scarratt, M. G and R. M. Moore (1998) Production of methyl chloride and methyl bromide in laboratory cultures of marine phytoplankton II, *Marine Chem.* **59**, 311-320.

Schobert, B., and E. Elstner (1980), Producation of Hexanal and Ethane by Phaeodactylum tricornutum and Its Correlation to Fatty Acid Oxidation and Bleaching of Photosynthetic Pigments, *Plant Physiol.* **6**, 215-219.

Schmidbauer, N and Oehmn, M. (1988) *Fresemius Z. Anal. Chem.* **332**.

Seinfeld, J. H., and S. N. Pandis (1998) *Atmospheric Chemistry and Physics: From Air pollution to climate change*, John Wiley & Sons, Inc., New York.

Sharkey, T. D. & F. Loreto (1993) Water stress, temperature, and light effects on the capacity for isoprene emission and photosynthesis of kudzu leaves, *Oecologia* **95**, 328-333.

Sieracki, M.E., P.G. Verity, and D. K. Stoecker (1992) Plankton community response to sequential silicate and nitrate depletion during the 1989 North Atlantic spring bloom, *Deep-Sea Res. II* **40**(1/2), 213-225.

Simon, N., R. G. Barlow, D. Marie, F. Partensky, D, Vaulot (1994) Characterization of oceanic photosynthetic picoeukaryotes by flow cytometry, *J. Phycol.* **30**(6), 922-935.

Singh, H.B., and L. J. Salas (1982) Measurement of selected light hydrocarbons over the Pacific Ocean: Latitudinal and Seasonal variations, *Geophys. Res. Lett,* **9,** 842-845.

Singh, H.B., and P. R. Zimmerman (1992) Atmospheric distribution and sources of nonmethane hydrocarbons, in *Gaseous Pollutants: Characterization and Cycling*, J. O. Nriagu, ed., John Wiley & Sons, New York, 177-235.

Singsass, E. L., M. Lerdau, K. Winter, and T. D. Sharkey (1997) Isoprene increases thermotolerance of isoprene-emitting species, *Plant Physiol.* **115**, 1413-1420.

Smythe-Wright, D., R. Davidson, and S. Boswell (2000) Low Molecular weight halocarbon production in the Atlantic Ocean, presented at SOLAS Feb. 2000.

Soloman, S., R. R.. Garcia, and A. R. Ravishankara (1994) On the role of iodine in ozone depletion, *J. Geophys. Res*. **99**, 20491-20499.

Sprengnether, M. (1992) An Active Titration Method for the Local Measurement of Tropospheric Hydroxyl Radical, Ph.D. Thesis, *MIT Center for Global Change Science Report* **16**, Cambridge, Mass.

Stefels, J., and E. H. M Van Boekel (1993) Production of DMS and dissolved DMSP in axenic cultures of the marine phytoplankton species *Phaeocystis sp, Mar. Ecol. Prog. Ser*. **97**, 11-18.

Stein, J.R. (1973) *Handbook of Phycological Methods,* Cambridge University Press, Cambridge.

Strom, S. L., R. Benner, S. Ziegler, and M. J. Dagg. (1997) Planktonic grazers are a potentially important source of marine dissolved organic carbon. *Limnol. Oceanogr*. **42**: 1364-1374.

Strom, S. L. and E. J. Buskey. (1993) Feeding, growth, and behavior of the thecate heterotrophic dinoflagellate *Oblea rotunda, Limnol. Oceanogr*. **38**: 965-977.

Sullivan, M. (2001) *Prochlorococcus* cyanophage: Isolation, preliminary characterization and natural abundances, M.S. Thesis, MIT, Cambridge, Mass.

Suttle, C. A. and A. M. Chan (1994) Dynamics and distribution of cyanophages and their effects on marine *Synechococcus spp., Appl. Environ. Microbiol*. **60**(9), 3167-3174.

Swinnerton, J.W. and V. J. Linnenbom (1967*) J. Gas Chromatog*. **5**, 570.

Swinnerton, J.W. and R.A. Lamontagne (1974) Oceanic distribution of low molecular weight hydrocarbons, baseline measurements, *Environ. Sci. Technol.* **8**, 657-663.

Tingey, D.T., M. Manning, L.C. Grothaus, and W. F. Burns (1979) The Influence of Light and Temperature on Isoprene Emission Rates from Live Oak, *Physiol. Plant* **47**, 112-118.

Tokarczyk, R., and R.M. Moore (1994) Production of volatile organohalogens by phytoplankton cultures, *Geophys. Res. Lett*. **21**, 285-288.

Toledo, G., B. Palenik, and B. Brahamsha (1999) Swimming Marine *Synechococcus* Strains with Widely Different Photosynthetic Pigment Ratios Form a Monophyletic Group, *Appl. and Environ. Microbiol*., **65(12)** 5247-5251.

Van Ginkel, C. G., E. De Jong, J. W. R. Tilanus, and H. A. M. De Bont (1987) Microbial oxidation of isorpene, a biogenic foliage volatile and of 1,3-butadiene, an anthropogenic gas, *FEMS Microbiol. Ecol.* **45**, 275-279.

Veldhuis, M.J.W., G.W. Kraay, W.W.C.Gieskes (1993) Growth and fluorescence characteristics of ultraplankton on a north-south transect in the eastern North Atlantic, *Deep-Sea Res. II* **40** (1/2), 609-626.

Verity, P.G., C.Y. Robertson, C.R. Tronzo, M.G. Andrews, J.R. Nelson, and M.E. Sieracki (1992) Relationships between cell volume and the carbon and nitrogen content of marine photosynthetic nanoplankton, *Limnol. Oceanogr.* **37**(7), 1434-1446.

Vors, N., K. R. Buck, F. P. Chavez, W. Eikrem, L. E. Hansen, H.B. Ostergaard, and H. A. Thomsen (1995) Nanoplankton of the equatorial Pacific with emphasis on the heterotrophic protists, *Deep-Sea Res. II* **42**(2-3), 585-602.

Wagner, W.P., M. Nemecek-Marshall, and R. Fall (1999) Three distinct phases of isoprene formation during the growth and sporulation of *Bacillus subtilis*, *J. Bacteriol.* **181**, 4700-4703.

Waterbury, J. B. & F. W. Valois (1993) Resistance to co-occurring phages enables marine *Synechococcus* communities to coexist with cyanophage abundant in seawater. *Appl. Environ. Microbiol.* **59**(10), 3393-3399.

Waterbury, J, S. W. Watson, F. W. Valois, and D. G. Franks (1986) Biological and Ecologica Characterization of the Marine Unicellular Cyanobacterium *Synechococcus, Can. Bull. Fish. Aq. Sci..*, 71-120.

Wever, R., M.G.M. Tromp, J.W.P.M. Van Schijndel, and E. G. M. Vollenbroek (1993) Bromoperoxidases, their role in the formation of HOBr and bromoform in seaweeds, in *Biogeochemistry of Global Change,* (R. S. Oremland, ed.) Chapman and Hall, New York.

Wiesse, T. (1993) Dynamics of autotrophic picoplankton in marine and freshwater ecosystems. *Adv. Microb. Ecol.* **13**, 327-369

Wildermuth, M.C. and Fall, R. (1996) Light-dependent isoprene emission. *Plant Physiol.*, **112**, 171-182.

Wilson, D.F., J.W. Swinnerton, and R.A. Lamontagne (1970) Production of Carbon Monoxide and Gaseous Hydrocarbons in Seawater: Relation to Dissolved Organic Carbon, *Science* **168**, 1577-1579.

Wolfe, G. V., and M. Steinke (1996) Grazing-activated production of dimethyl sulfide (DMS) by two clones of *Emiliania huxleyi*, *Limnol. and Oceanogr.* **41**(6), 1151-1160.

Wuosmaa, A. M, and L. P Hager (1990) Methyl Chloride Transferase: a carbocation route for biosynthesis of halometabolites, *Science* **249**, 160-162.

Yang, S.F., H.K. Pratt (1978) *The Physiology of Ethylene in Wounded Plant Tissues, Biochemistry of Wounded Plant Tissues,* G. Kohl, ed., Walter de Gruyter & Co., Berlin.

Yokouchi, Y., H. J. Li, T. Machida, S. Aoki, and H. Akimoto (1999) Isoprene in the marine boundary layer (Southeast Asian Sea, eastern Indian Ocean, and Southern Ocean): Comparison with dimethyl sulfide and bromoform. *J. Geophys. Res.* **104**(D7), 8067-8076.

Zafiriou, O.C., J. Joussot-Dubien, R.G. Zepp, and R.G. Zika (1984) Photochemistry of natural waters, *Environ. Sci. Technol*., **18**, 358A-371A.

Zingone, A., D. Sarno, and G. Forlani (1999) Seasonal dynamics in the abundance of *Micromonas pusilla* (Prasinophyceae) and its viruses in the Gulf of Naples (Mediterranean Sea), *J. Plankton Res.* , 2143-2159.

APPENDIX A

DIAGNOSTICS OF THE NMHC SAMPLING SYSTEM

A cryogenic method is used to pre-concentrate the sample. The cryogenic collection loop is a length of coiled stainless steel tubing that is cooled to subambient temperatures as a sample flows through. The loop is submerged in a liquid argon bath (-186 °C) which condenses the hydrocarbons of interest, but allows nitrogen and most oxygen in the air sample to pass through and be vented. This can be a reliable, quantitative process if water vapor and ozone concentrations can be controlled. Both of these compounds can also be condensed and concentrated within the loop. Ice plugs can form and block air flow though the trap, effectively reducing the available sample for collection. Additionally, as the loop is heated to induce re-volatilization, ozonolysis reactions can occur with the alkene hydrocarbon species. Fabrication materials for coil loop construction also need consideration as the interior surface structure can affect the condensation process and potentially destroy ozone. Characteristics of the sample drying system, ozone scrubbing method, and sampling loop construction are given below.

A.1. SAMPLE DRYING METHODS

The sealed nature of both the incubation flasks and purging technique used for sampling leads to gas aliquots with high humidity levels despite the inclusion of a Nafion® membrane counter-flow drying tube on the line. Sufficient moisture remains for condensation to occur in the GC injection system line during the cryogenic concentration process, which blocks sample flow. Several hygroscopic chemicals were tested as possible additional drying mechanisms; these include Aquasorb ™, Ascarite ™ (Thomas Scientific),

and magnesium perchlorate $Mg(ClO_4)_2$ (Sigma-Aldrich Co.). Aquasorb™ and $Mg(ClO_4)_2$ are intended to remove water vapor, while Ascarite™ (sodium hydroxide on an asbestos-based carrier) is efficient at removing CO_2 as well. Several grams of each were inserted into a ¼ inch outer diameter, 7 inch long glass tube equipped with Swagelock® compression fittings and Teflon ferrules. The chemicals were kept in place with plugs formed of glass wool, and the tubes individually installed on the line after the Nafion ® dryer, but before a mixing length of approximately 7 ft that leads to the cryogenic trap.

A.1.A Magnesium Perchlorate

Nitrogen blanks and representative humidified experimental samples were run with and without the magnesium perchlorate drying tube. The chemical contributes contamination peaks of only propene, and 2-me-propene to the nitrogen sample, which are present whenever the tube is installed. If a nitrogen blank is run directly after removal of the drying tube, no contamination peaks are found. These quantities of contaminants are significant because they are of the same order of magnitude as our experimental sample concentrations. If the (peak area) (sample volume)$^{-1}$ ratios of identified humidified sample peaks are compared with and without the magnesium perchlorate on the line, the percent differences range from -9% to 50% (see Table A1, column 1) where typical run-to-run difference on this GC system is < 10% for all compounds (e.g. precision > 90%). At this time we can only postulate that most increases in NMHC occurring when the drying tube is removed may be due to a possible scavenging by the magnesium perchlorate of an unknown agent that can degrade hydrocarbons. Other laboratories have also found NMHC losses to magnesium perchlorate (Schmidbauer & Oehmn, 1988).

Hydrocarbons were grouped by pi-bond content (e.g. alkanes, alkenes) as a check for possible ozonolysis effects. If the average percent change in the alkenes was much higher than for the alkanes with and without the dryer, it may be due to ozone removal by the

Table A1: Inline Results from Drying Tube and Ozone Scrubber Tests

	Humidity	**Ozone Scrubber**	
	Humid Sample, $Mg(ClO_4)_2$ n=3	Standard, $Na_2S_2O_3 \cdot 5H_2O$ n=1	Humid Sample, $Na_2S_2O_3 \cdot 5H_2O$ n=1
ethane	**38.7**	-0.4	0.6
ethene	4.4	0.7	**-18.5**
propane	5.3	5.6	**-11.9**
cyclopropane	**29.5** (n=2)	1.9	**-23**
propene	**50.6** (n=2)	**27.8**	**22.1**
2mepropane	**37**	0.81	**20.6**
butane	**33.3**	**-25.1**	**-15.4**
2mepropene	-8.8	-1.1	6.2
2mebutane	**44.9**	NA	NA
pentane	9.2	-1.6	**13.1**
hexane	**37.1**	-1.5	**14.7**
isoprene	**32.1**	-1	NA
alkanes	**29.4**	-2.9	0.2
alkenes	**19.6**	6.6	3.3

Mean % increase in NMHC (peak area) $(\text{sample volume})^{-1}$ ratio for tubes inline as compared to tubes removed. Boldface indicates a difference larger than the system precision (~10%).

$Mg(ClO_4)_2$. This is not the case. Additionally, the capacity of this chemical to remove water is only sufficient to reduce the rate of ice plug formation in the cryogenic collection loop, but not stop it. This is evidenced by the drop over time of the flow rate through the loop, as measured by a Model FC260 Tylan mass flowmeter (Millipore Corporation). On average there is a 20% drop in the slope of the sample flow rate versus time when the magnesium perchlorate is included.

A.1.2 Other Chemical Dryers

Detailed results for Aquasorb™ and Ascarite™ are not presented here because contamination peaks from these two chemicals were both significantly large in pure nitrogen blanks (particularly for 2-me-propene), and more numerous, than for the magnesium

perchlorate. Humidified samples through these traps were determined to have a memory effect. These two traps can also take up hydrocarbons. For most species this is < 5% of the sample, but for 2-me-propene and isoprene this number is closer to 50%. Additionally, if a nitrogen blank was run after a hydrocarbon-containing sample, additional contamination peaks would appear at significant levels (Kleiman, G., Graham, J., & Shaw, S.L., unpublished data). This indicates the Aquasorb™ and Ascarite™ retain not only water, but also hydrocarbons, which did not occur for magnesium perchlorate in our tests. Finally, the amount of water retained in these two dryers was once again enough to slow the rate of ice plug formation in the cryogenic collection loop, but not enough to stop it. Thus, none of the chemical dryers tested had performances worthy of justifying their installation on the line for experimental purposes.

A.1.3 Nafion® Counterflow Dryer

The counter-flow Nafion® membrane dryer also has the possibility of contaminating sample runs. It has been shown that Nafion® can cause rearrangement and possible loss for some terpene compounds (Gong & Demerjian 1995). Previous MIT testing by John Graham found no problem for C_2-C_5 compounds. Only benzene, heptane and various heavier terpenes seemed absorbed and possibly rearranged by the membrane (Graham, J., unpublished data) and they are of no interest in this current work. However, a thorough examination of the dryer under current experimental was performed, with positive results. Peak retention times, shapes, and resolution were all consistent whether or not the dryer was online; all variations were within our analytical precision (< 10% for all compounds). Any 'memory effects', or contamination left in the Nafion® membrane and re-emitted during further runs, were minimal (~1-2%) or nonexistent. These effects were most significant when high humidities were combined with high NMHC concentrations, as in an intentionally humidified standard run. This phenomenon is not likely to affect our experimental samples, as our standards typically have a much lower water content, and are run at the end of the day, just before the system is heated and flushed overnight. A final

note - we allow flushing of the entire injection system, including the Nafion® dryer, during sample elution on the GC to help keep it free of water or NMHC carryover. This is done at room temperature and appears to be sufficient, although others have shown that heating the length of the dryer while flushing would clean it even further (Pliel et al., 1987, McClenny et al., 1984).

A.2. OZONE SCRUBBER

To examine the possible ozonolysis effect, an ozone scrubber made of sodium thiosulfate $Na_2S_2O_3 \cdot 5H_2O$ (Mallinckrodt, Inc.) was constructed following Helmig (1997), installed on the line, and tested in a similar way as the drying tubes previously mentioned. The reaction between thiosulfate and ozone produces tetrathionate, oxygen, and water:

$$2\ S_2O_3^{-2} + O_3 + 2H^+ \rightarrow S_4O_6^{-2} + O_2 + H_2O$$

Approximately 51.8 g of sodium thiosulfate was dissolved in 100 mL of distilled, deionized water (Milli-Q system, Millipore Corp.) at room temperature. Sufficient glass wool to fill a 7 inch, ¼ inch outer diameter glass tube was soaked in the resulting liquid, and then placed in a 50 °C drying oven for 1 hour until dry.

Multiple nitrogen blanks run with and without the ozone scrubber showed no contamination from the tube or chemical, including possible humidity effects from water production in the reaction. If ozone was present in the loop during the normal run procedure, the (peak area)(sample volume)$^{-1}$ ratios for individual hydrocarbons, particularly unsaturated ones, would be expected to increase when the scrubber was installed online. There was also virtually no change in (peak area) (sample volume)$^{-1}$ ratios for most NMHC when the Tank 5138 hydrocarbon standard was tested with and without the scrubber (see Table A1, column 2). Most efficiencies were well within our run-to-run precision. However, this standard is very dry in comparison to experimental sample runs. To check if humidity affected potential ozonolysis, several representative experimental samples were also examined (see

Table A1, column 3). Significant variability among the hydrocarbons was found, most above the instrumental precision. In fact, several hydrocarbons showed a significant *decrease* in signal when the humid sample was sent through the scrubber, signifying loss. Hydrocarbons were again grouped by presence of pi-bonds as a check for possible ozone effects. The differences for alkenes were higher than for alkanes for both the standard and the sample, although well within the instrument precision. Unfortunately no ozone measurements were possible during this test, but the results are in accordance with previous work in the lab that such ozone effects did not occur with our sampling procedure. Donahue & Prinn (1990) showed that ozone mole fractions up to 100 ppb had no influence on alkene concentrations during cryotrapping on this system. Additionally, other laboratories report that the loss of reactive hydrocarbons to ozone during the thermal desorption process is on the order of 2-10% for ozone mole fractions up to 100 ppb. This is well within analytical precision for both their system and ours (Koppmann et al., 1995), although they did heat their stainless steel inlet line before sample collection and we do not. In conclusion, the ozone scrubber was deemed potentially mildly destructive to some hydrocarbons, and probably unnecessary, and thus not used for experimental sample analysis.

A.3. COLLECTION LOOP FABRICATION

The interior surface quality and area of the cryogenic loop itself can also significantly affect sample integrity. Ideally, a maximum surface area is desirable to allow for a large number of nucleation sites, and thus more efficient condensation. This is often achieved by packing a larger diameter loop with small glass beads. However, increasing the internal surface area and roughness can create potential new nucleation sites from which the sample may be difficult to completely re-volatilize. This can be altered with the use of a smoothed, electroformed tubing material instead of typical Type 316 stainless steel.

Three different loop constructions were examined to determine if the maximum amount of sample hydrocarbons were being condensed and re-volatilized to GC injection. Loop A was

the 1.02 cc volume, 1/16 inch diameter, stainless steel construction loop made in-house and previously used on the system. Loop B was the reference 1/16 inch diameter stainless steel construction, 0.50 cc volume made by Supelco (Sigma-Aldrich Co.) currently used on this system. Loop C was a similar construction, except for the electroformed nickel material (Supelco, Sigma-Aldrich Co.) Loop D was an 1/8 inch diameter construction filled with 250 μm diameter silanized glass beads. Because the internal porosity of this loop was not known, it was impossible to directly calculate the available internal volume for gas flow. Larger diameter tubing was required to allow for the appropriate sample flow through the packing material at a sufficiently low head pressure.

Hydrocarbon standards (Tank 5138) and representative experimental samples (taken from incubation flasks containing only media blanks) were examined with the various loops. Loop B as compared to loop A is shown in Figure A1 as "Supelco/in-house". The (peak area)(sample volume)$^{-1}$ ratios for runs on the two collection loops are ratioed {R = [(peak area) (sample volume)$^{-1}$ for loop A, C, or D] / [(peak area) (sample volume)$^{-1}$ for loop B]}. This is done for each NMHC, which are represented by an index. There is an excellent match (R~1) for virtually all hydrocarbons between the two loops, almost all well within our 10% precision ($0.9 < R < 1.1$). Ethene (index 2) is the one exception, but is still within 20% of our expected value. However, tracking this back to the original chromatograms, the peak area for one of the loop A runs has a notably small (peak area) (sample volume)$^{-1}$ for ethene, although all other NMHC look fine. Additionally, all loop B chromatograms look fine for all NMHC. Dropping this anomalous peak brings the ratio for ethene down to 1.02, and highlights the point that these two loops are virtually interchangeable.

Loop C as compared to loop A is designated "ELFNi/in-house" in Figure A1. The ratios of the (peak area)(sample volume)$^{-1}$ for these two loops are similar for most NMHC, but at a much higher value (all NMHC average ~118%). This is far above our day-to-day precision and represents a real effect of the electroformed nickel surface. We postulate that the smoothed nickel surface allows for more complete sample desorbtion than the stainless

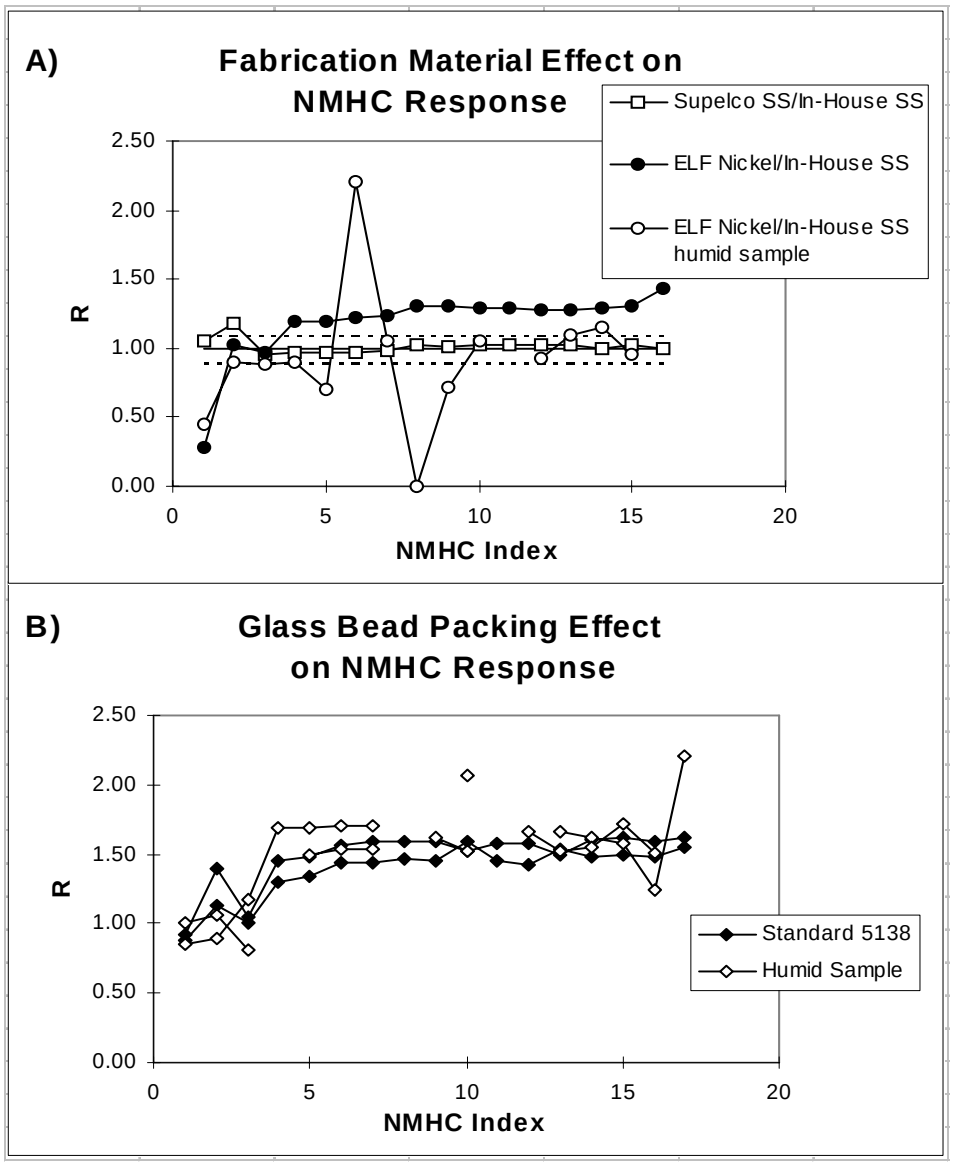

Figure A1: Various Loop Configurations Tested for Accuracy R = [(peak area) (sample volume)$^{-1}$ for Loop A,C, or D]/[(peak area) (sample volume)$^{-1}$ for Loop B]. NMHC Indices are: ethane-1, ethene-2, propane-3, cyclopropane-4, propene-5, 2mepropane-6, butane-7, t2butene-8, 1butene-9, 2mepropene-10, c2butene-11, cyclopentane-12, 2mebutane-13, pentane-14, hexane-15, isoprene-16, and 3mehexane-17. A) The R = 1 line is plotted (solid line), as well as the 10% precision limits (dashed lines). Average R over all NMHC for the Supelco/In-House SS (loop B), ELF Ni/In-House SS (loop C), and ELF Ni/In-House SS (loop C) humid samples are 1.01, 1.18, and 0.93, respectively. B) Loop D/Loop B. Average R over all NMHC for the two standards are 1.38, 1.48, and for the humid samples 1.48, 1.48.

steel. However, if the effect is the same for the sample and the standard it will cancel in the calibration process. The humid sample results are shown in Figure A1 (R=0.93); the effects

are not the same and can not be ignored. Additionally, ethane, ethene, propane, and 3-me-hexane appear to have anomalous ratios. Nickel is known to be a catalytic surface for many reactions involving hydrocarbons; thus, the possibility of sample loss to the tubing walls exists. Unfortunately, it was the only electroformed tubing available. This effect may be heightened for the lighter molecular weight hydrocarbons and explain why their ratios are much less than the all-NMHC average ratio of 118%. These complicating effects render loop C unreliable. The stainless steel loops are preferred, even though the absolute amount of hydrocarbon they trap and release is not optimal.

Loop D as compared to loop B is shown in Figure A1B. Once again, the effect for the standard 5138 is fairly consistent over the various NMHC, but the absolute difference between the glass bead-filled loop and our typical loop is almost 50%. This effect is likely due to the large amount of additional surface area in Loop D. More available surfaces increase the probability of nucleation sites for condensation, allowing more hydrocarbon to be trapped out of the original air sample and later desorbed into the column. Exceptions are ethane, propane, and to a lesser extent ethene, possibly due to their larger volatility as compared to the other NMHC. Their trapping/desorbtion efficiencies were already quite high for loop B, and perhaps could not be increased with the additional surface area in loop D as much as for the other NMHC. The ratios for a humid sample are is also shown in Figure A1B. The values for sample and standard are indistinguishable for almost all chemicals, despite up to an order of magnitude different concentrations. Exceptions are isoprene (index 16), which is slightly lower in the samples, and 2-me-propene (index 10) and 3-me-hexane (index 17), which are significantly higher. Previous work in the lab indicates that the Nafion® membrane may be a significant source of 2-me-propene under humid conditions (Graham, pers. comm.), although we never detected this. We currently have no explanation for these anomalies. Since the ratios for the humid sample and the standards are similar for most NMHC, we can make the assumption that runs performed with the different loops are comparable, as long as the standards used to calibrate them were also performed with the same methods. (e.g. Hydrocarbon concentrations in a sample run on loop D must be calculated by calibration against a standard run on loop D. These numbers could then be compared against a sample both run and calibrated on loop B.)

Thus, because the absolute concentrations with loop D are more accurate, we could choose to use it as typical protocol. However, since the results for isoprene, a chemical of great importance for this work, aren't completely understood, we chose to remain with loop B. Future workers should take these results into consideration during the establishment of their protocols.

APPENDIX B

PHOTOGRAPHS

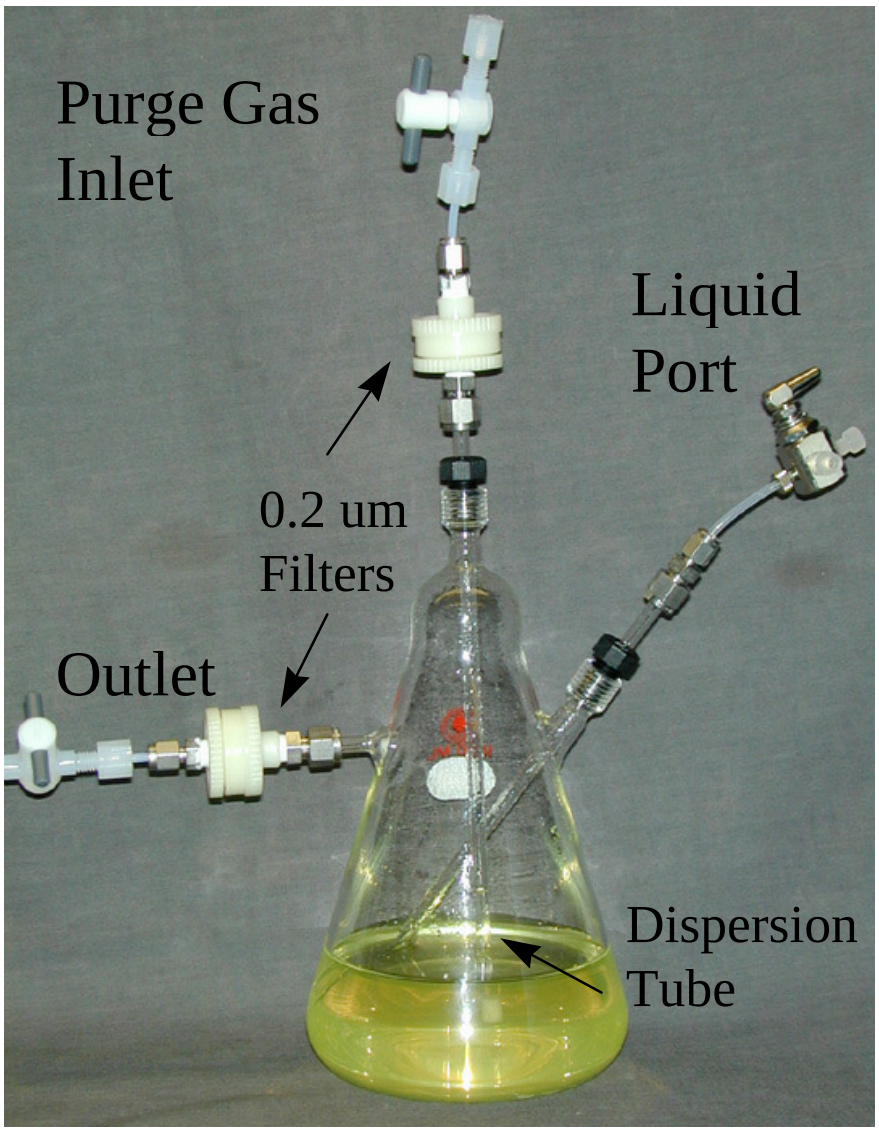

Figure B1: Experimental Incubation Flasks Typical setup with a mid-exponential culture of *Prochlorococcus marinus*. See Chapter 2 for a detailed description of the apparatus and sampling technique.

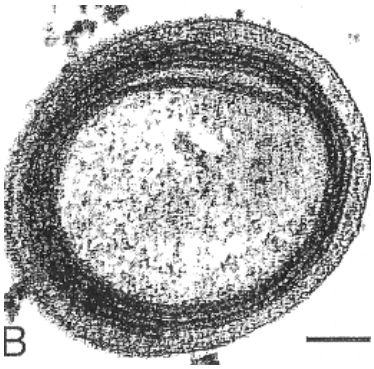

Figure B2: *Prochlorococcus marinus* A thin section TEM image taken by C. Ting. Scale bar is 500 nm. Intracytoplasmic membranes, the site of important metabolic processes such as photosynthesis and respiration, are clearly visible.

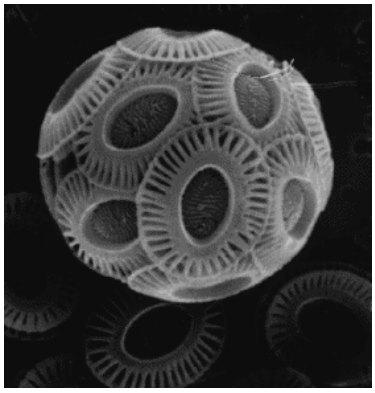

Figure B3: *Emiliania huxleyi* SEM image taken by Jeremy R. Young, NHM, London. (http://www.soc.soton.ac.uk/SOES/STAFF/tt/eh/pics/cocco5.gif) Calcium carbonate coccoliths cover the ~ 5 μm diameter cell.

Figure B4: *Micromonas pusilla* SEM image Copyright 1996-2000 by Mats Kuylenstierna & Bengt Karlson (http://www.marbot.gu.se/sss/others/Micromonas_pusilla.htm). These pear shaped cells are approximately 1.5 μm in length, not including the flagella.

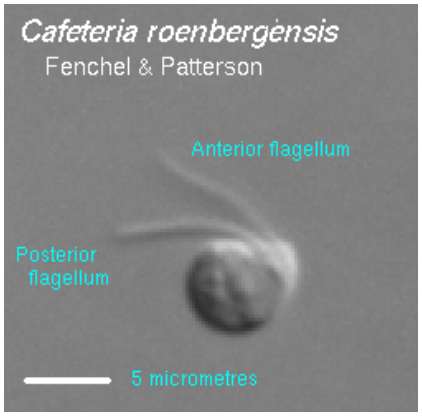

Figure B5: *Cafeteria roenbergensis* A typical bactiverous marine nanoflagellate. Image taken by Charles J. O' Kelly. (http://megasun.bch.umontreal.ca/protists/cafe/appearance.html)

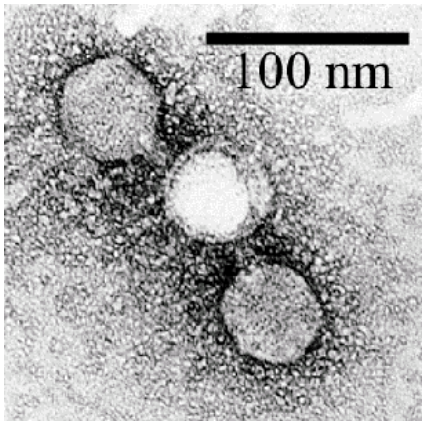

Figure B6: *Typical cyanophage of the Podoviridae family* TEM image taken by Matthew B. Sullivan (2000) with a uranyl acetate staining process. These phage have an 40 nm icosahedral head with a short 10 nm tail.

APPENDIX C

PROTOCOLS

C.1 TYPICAL SAMPLING PROTOCOL

The protocol that has been developed for sampling at each time point is outlined in detail below. It assumes that preparatory work for each experiment has already been done (e.g. thorough cleaning and sterilization of all incubation flask incidentals, acclimation of cells to appropriate light, temperature, or nutrient conditions, and an initial overnight purge of the media broth in all incubation flasks to remove background VOC before cellular inoculation).

1) Allow gas lines, including hydrocarbon traps, to flush for ~ 20 minutes at 8 psig. Meanwhile, swirl each flask for homogeneity, and remove ~ 7 mL liquid sample through syringe port. (The resulting volume change in the initial ~500 mL in the incubation flask is accounted for in the production rate calculations.)

2) Dispense 1 mL sample from each flask in 1 mL Marine Purity Test Broth (see Appendix C.4) to test for contamination by heterotrophic bacteria. Dispense 1 mL sample from each flask into cryovial for later enumeration, incubate in the dark for 10 minutes, then freeze in liquid nitrogen with 5 mL 25% glutaraldehyde.

3) Dispense 5 mL sample from each flask to sterile test tubes for fluorometry reading on Turner Model 10-AU Fluorometer, then transfer to larger sterile tubes for pH measurement.

4) Remove additional aliquots as needed (~20 mL) for chlorophyll or slide samples as per Appendix C.2.

5) Differential Pressure Method: Re-attach purge gas lines and take gas samples one flask at a time, randomizing the order. Attach gas sample cylinder evacuated to - 27 psig with pressure gauge to outlet line of incubation flasks, then open inlet and outlet valves. Allow gas to flow for 4 minutes, during which pressure in gas cylinders rises to ~ 8 psig, and flow decreases as pressure differential decreases. Close sample cylinder and inlet valve, and remove cylinder from line, allowing incubation flask to vent pressure. Reseal all flasks for next time step.

6) Run all hydrocarbon samples on the GC system as soon as possible.

7) Run all biological samples (e.g. flow cytometry, slides) in one batch at end of experiment.

C.2 CELLULAR DNA STAINING

This method was developed by Claire Ting in the Chisholm Laboratory.

1) Prepare a stock solution of DAPI at 1 mg/mL, and filter through a 0.22 um filter. Store at 4 °C, in dark.

2) Add the following to a 1.5 mL Eppendorf tube, vortex, and incubate in the dark at room temperature for 15 minutes.
   1 mL diluted culture
   10 mL DAPI
   50 mL 10% Formalin

3) Vortex again, and carefully filter onto a 0.2 mm Poretics black membrane filter (on top) and a 0.45 mm membrane filter (on bottom) using a low vacuum. Don't allow filters to dry through.

4) Transfer black filter to a slide, and cover with coverslip.

5) Use the Zeiss Axiscope 2 epifluorescence microscope with a UV filter to count cells in at least 20 grids.

C.3 PIGMENT EXTRACTION METHOD

This method was developed by Lisa Moore in the Chisholm Laboratory (Moore, 1995).

30 min extraction

1) Filter cells under low vacuum (<5 in. Hg) onto Whatman GF/F filter.
2) Immediately put filter into 3 mL 90% acetone in a centrifuge tube, and let extract in 4 °C in dark for 30 minutes

Grinding

1) Transfer acetone and filter to grinding tube, and grind into tiny pieces.
2) Rinse pestle and grinding tube with 90% acetone, and transfer back to centrifuge tube.
3) Note total volume of extract.

30 min extraction

1) Allow to extract at 4 °C, in dark for another 30 minutes.
2) Centrifuge to pellet filter fragments, transfer supernatant to another centrifuge tube, and put on ice until measuring absorption.
3) Extract rest of pigment from pellet: add 4 mL 90% acetone, resuspend pellet, and let extract for 30 minutes at 4 °C in the dark.
4) Centrifuge the mixture, transfer supernatant out, and measure absorption.

Absorption

1) Using 90% acetone as a blank, measure absorption at 647 nm, 664 nm, and 750 nm.
2) Use spectrophotometric equations from Jeffrey and Humphrey (1975) to calculate chlorophyll quantities.
3) For divinyl chlorophyll-a, use 650 nm instead of 647 nm, as the absorption peak is shifted slightly.

C.4 MARINE PURITY TEST BROTH

Recipe from Mak Saito and John Waterbury, Woods Hole Oceanographic Institute.

Chemicals necessary for Marine Purity Test Broth (MPTB):

Chemical	**Final Concentration**	**For 1 Liter**
NaCl	2 %	20 g
AC Difco Broth		17 g
$MgSO_4 \cdot 7 H_2O$	32 mM	8 g
$CaCl_2 \cdot 2H_2O$	10 mM	1.5 g

Dissolve $MgSO_4$ and $CaCl_2$ each in a separate beaker of Milli-Q water. Combine NaCl and AC Broth, and autoclave all solutions. When cool, combine all solutions with sterile technique.

To use, dispense 1-3 mL aliquots into small tubes with equivalent volumes of culture. Incubate in the dark for several days to 1 week. If heterotrophic organisms are present, they will grow up rapidly and turn the clear MPTB solution cloudy.

C.5 CELLULAR BIOMASS

For comparison of biological hydrocarbon production rates against as wide a range of published numbers as possible, it was necessary to obtain the cellular weights of *Prochlorococcus , Emiliania huxleyi,* and *Synechococcus.* This was of particular interest in comparing phytoplankton and cyanobacterial production rates to those of tree leaves and other higher plants. Additionally, knowledge of carbon content is necessary to assess a given organism's contribution to the total oceanic biomass. Typical values of total mass and cellular carbon content have been published for each organism, but for *Prochlorococcus* most of those published numbers were estimated and not directly measured (Partensky et al., 1999).

We used a dry-weight procedure to directly determine the cellular mass. A single batch of cells was grown at 23 °C and an irradiance of 85 μE m^{-2} s^{-1} (14:10 light:dark). Growth medium was either the Pro99 recipe (for *Prochlorococcus, Synechococcus*) or f/2 + Si formula from Sigma, Inc. (for *Emiliania huxleyi*). Subsamples of 1 mL were preserved with 5 μL of glutaraldehyde for later cell enumeration on the FACScan. Replicate 250 mL aliquots of culture from this batch were filtered through a 47 mm diameter Whatman GF/F filter, with a 47 mm diameter, 0.2 um pore diameter, Poretics polycarbonate backing filter at approximately 3 mm Hg vacuum. Replicate 250 mL aliquots of media were also filtered as a blank. All samples were weighed on a Mettler balance wet, and then stored in a 37 °C drying oven for several days. The samples were removed and weighed periodically until there was no significant change in mass. This was assumed to be the point when all water was removed from the filters. The biological mass, M, was calculated as

$$M = (M_C - T_C) - (M_B - T_B)$$

where M_C is the mass of the dried culture-containing filter, M_B is the mass of the dried blank-containing filter, T_C is the tare weight of the culture filter, and T_B is the tare weight of the blank filter. The differences between the tare-corrected blank and culture weights were

quite small compared to their values. For example, for *Synechococcus*, $(M_C - T_C) \sim 0.0252$ grams, and $(M_B - T_B) \sim 0.0207$ grams; for *Prochlorococcus*, $(M_C - T_C) \sim 0.0277$, and $(M_B - T_B) \sim 0.0242$. The biological mass, M, is then normalized by the culture cell count determined by average of duplicate preserved flow cytometry samples. The data is summarized in Table C1 and shows good agreement with the previously estimated values. We always used our measured results from Table C1 when available, and not those from the literature, in all aspects of this work.

Table C1: Biomass of Cultured Organisms

Prochlorococcus

author	method	fg C cell^{-1}	fg cell^{-1}*
Li et al. (1992)	0.8 um diameter, 220 fg C/um3††	59	118
Campbell et.al. (1994)	0.6 um diameter, 470 fg C/um^{3}**	53	106
Cailliau et al. (1996)	^{14}C pigment label†††	49	98
Moore (1997)	photosynthetic rate,‡‡	61, 94 §	122, 188
Durand et al. (2001)	CHN + calculation 325 fg C/μm^3	56	112
Bertilsson, S. (pers. comm.)	CHN analyzer	54	108
This work	dry weight	78	155
average			**126 fg cell^{-1}**

Synechococcus

author	method	fg C cell^{-1}	fg cell^{-1}*
Cuhel & Waterbury (1984)	^{14}C bicarbonate uptake	294***	588
Kana & Glibert(1987)	CHN analyzer	250	500
Campbell et al. (1994)	1 μm diameter, 470 fg C (μm)$^{-3}$**	470	940
Waterbury et al. (1986)	CHN analysis	220§§	420
Durand et al. (2001)	CHN + calculation 325 fg C (μm)$^{-3}$	112	224
This work	dry weight	160	320
average			**499 fg cell^{-1}**

Emiliania huxleyi

author	method	pg C cell^{-1}	pg cell^{-1*}
E. huxleyi. website†		10‡	20
average			**20 pg cell^{-1}**

Heterotrophic bacteria

author	method	fg C cell^{-1}	fg cell^{-1*}
Caron et al. (1991)	CHN analyzer	71 ± 3	142 ± 6
P. halodurans (rename: *H. halodurans*)			
average			**142 fg cell^{-1}**

Eukaryotic algae

author	method	pg C cell^{-1}	pg cell^{-1*}
Verity et al. (1992)	‡‡‡, sphere of 10 μm diameter	98	196
Veldhuis et al. (1993)	250 fg C (μm)$^{-3}$, sphere of 10 μm diameter	131	262
average			**229 pg cell^{-1}**

*Indicates calculated from approximation of carbon content as 50% of cell biomass on average (Atlas, 1988)
** Conversion factor from Verity et al.(1992)
*** Intended for all cyanobacteria
† http://www.soc.soton.ac.uk/SOES/STAFF/tt/eh/index.html
‡ Organic carbon only - no coccoliths
†† For small, non-diatomeaceous phytoplankton (< 4μm diameter)
‡‡ Respiration could not be accounted for with this method
§ Values vary per isolate, two larger strains average 250 fg C cell^{-1}
§§ Diel values range from 150-290 fg C cell^{-1}
††† Used non-axenic cultures, with a method of accounting for heterotrophic contributions
‡‡‡ Calculated as: pg C = 433(biovolume)$^{0.863}$; biovolume in μm^3 cell^{-1}

APPENDIX D

SUPPLEMENTARY DATA

D.1 CARBON SOURCES

All living cells have an inorganic carbon requirement necessary for proper structural and metabolic function. Carbon accounts for approximately 50% of phytoplanktonic cellular biomass (Atlas, 1988). In these incubations carbon is supplied to the cells as 350 ppm CO_2 in the purge air, since the system is sealed against laboratory air intrusion. During typical experiments using this carbon source methodology we observed a distinct rapid decrease in cell counts at stationary phase (as in Figure 11). After only 1-2 days in stationary phase, the cell counts dropped rapidly during the senescent phase. This is in contrast to observed growth in test tubes or other incubation flasks that were kept open to the laboratory atmosphere; in these cases cell numbers declined, but quite slowly, and to a constant level of approximately 70-80% of the maximum cell count (Shaw, original data lost due to computer crash). These numbers remained fairly steady for the order of a week or so, despite rapid declines in cellular fluorescence from stationary phase and beyond. We hypothesized that this difference may be due to carbon limitation during stationary phase in the sealed (but not the open) incubation flasks.

To test this idea we spiked one of two duplicate *Prochlorococcus* axenic MED4 cultures at 95 $\mu E\ m^{-2}\ s^{-1}$ with sodium bicarbonate just before stationary phase (Figure D1). We added 10 mL of sodium bicarbonate ($NaHCO_3$) solution (1.01 g (Sigma-Aldrich, Inc.) dissolved in 50 mL Milli-Q water (Millipore Corporation)) to ~460 mL of cell culture at hour 104. This resulted in a final concentration of 0.44 g $NaHCO_3\ L^{-1}$ above the natural levels in the media (~ 2.4 mM, or 0.23 g L^{-1}). After two days this kept the pH down by 0.5 (pH 8.7) compared to the reference (pH 9.2), allowing the cells to continue growing at the same exponential rate of 0.52 day^{-1} for an additional day. Forward scatter, side scatter, and chlorophyll fluorescence all maintained constant values in the bicarbonate-spiked culture during hours 104 to 150. Maximum cell densities reached in the bicarbonate-spiked cultures were 60%

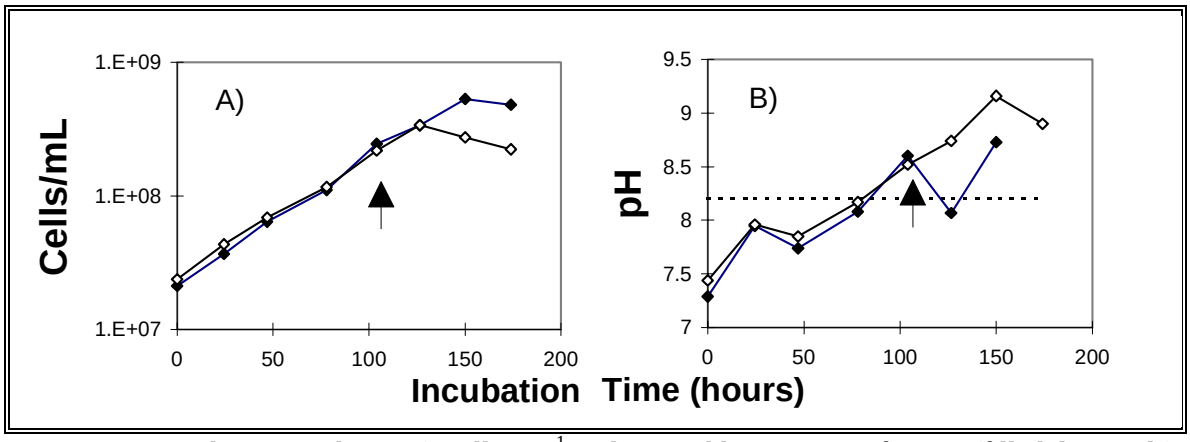

Figure D1: Bicarbonate Spiking A) Cells mL^{-1} in the *Prochlorococcus* reference (filled diamonds) and bicarbonate-spiked (open diamonds) cultures. Arrows mark the point of bicarbonate injection. B) Corresponding pH measurements. The dotted line indicates a typical bulk seawater pH of 8.2. Due to the ~ 12 hour purging time of the media at the beginning of each experiment, initial incubation pH measurements are much lower, ~ 7.2-7.4.

higher than for the reference, at $3.4x10^8$ and $5.3x10^8$ cells mL^{-1}, respectively. We determine from this experiment that a typical incubation does reach carbon limitation at stationary phase; this occurs with pH > 9.

Another way to avoid carbon limitation is to use much higher CO_2 concentrations in the purge gas. Scarratt & Moore (1996, 1998) used this method with 3000-5000 ppm CO_2. They detected carbon limitation (indicated by pH 9 and above; Riebesell et al., 1993) unless these high CO_2 concentrations were used in combination with low nitrate concentrations (< 50 μM). To determine if this had an effect in our incubations, we also attempted to use a purge air stream with 3500 ppm CO_2. Unfortunately our reference culture at the same light level (~63 μE m^{-2} s^{-1}), but with 350 ppm CO_2 , inexplicably died. However, we can compare our results from exponential phase to the trends produced by plotting growth rate and cellular chlorophyll content from other experiments versus growth irradiance in Figure D2. These plots indicate an expected range for growth rate, isoprene production rate, and cellular parameters for that approximate light level. While the cells in this incubation grew exponentially, the rate of 0.37 day^{-1} was a bit lower than expected from the growth rate trends (open symbols; Figure D2B). Additionally, the cellular chlorophyll content (a+b) is a bit higher than expected (Figure D2A).

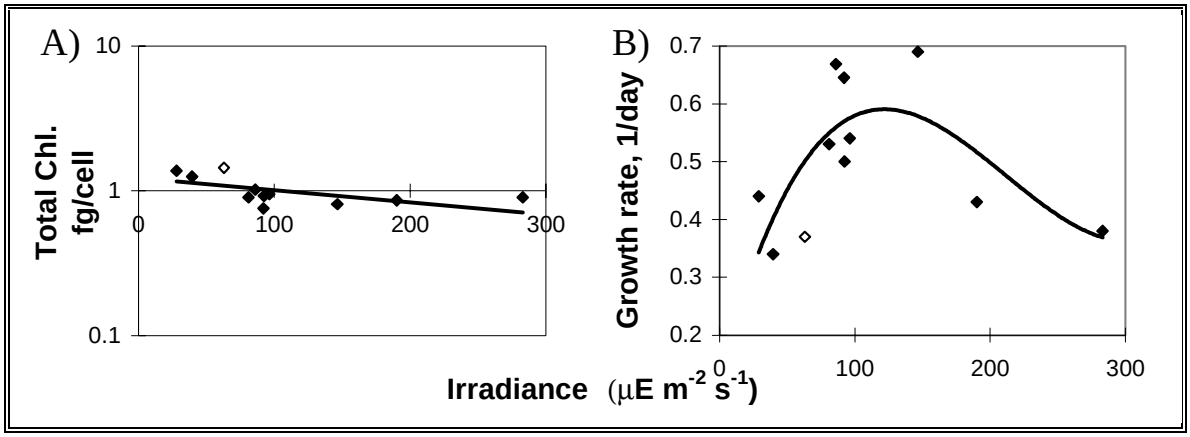

Figure D2: 3500 vs. 350 ppm CO_2 in Purge Air A) Cellular chlorophyll content (a+b) for cultures acclimated to a variety of irradiances using 350 ppm CO_2 in purge air. The open diamond is the data for the 63 μE m^{-2} s^{-1} incubation with 3500 ppm CO_2 in purge air. B) Corresponding specific growth rates. Fits for both A (linear) and B (cubic) were performed with all data points.

The expected range for cell-normalized isoprene production during exponential phase at ~63 μE m^{-2} s^{-1} is ~1.2-1.6x10^{-21} moles $cell^{-1}$ day^{-1} (Figure 11), but the measured rate was ~ 2.2x10^{-21} moles $cell^{-1}$ day^{-1}, ~ 50% higher than expected (Figure D3). The percent of fixed carbon lost to isoprene in this 3500 ppm CO_2 case is also significantly higher (factor of 5) than the usual ~1x10^{-4}%. Additionally, the cell counts decreased slowly and steadily after stationary phase in a similar manner to cultures grown in test tubes. However, isoprene production in the flasks still dropped during senescence, in the manner of cultures exposed to only 350 ppm CO_2. Sharkey et al. (1991) observed elevated isoprene production rates in oak leaves when supplied with excess CO_2, although these conditions tended to suppress isoprene production from aspen leaves. Unfortunately, due to the lack of a reference culture in our experiment we cannot be sure that the cause of these differences is due to the higher available CO_2.

For consistency throughout this work we chose to always use 350 ppm CO_2 in the purge air, and to not add bicarbonate to our liquid media. The former more accurately resembles in

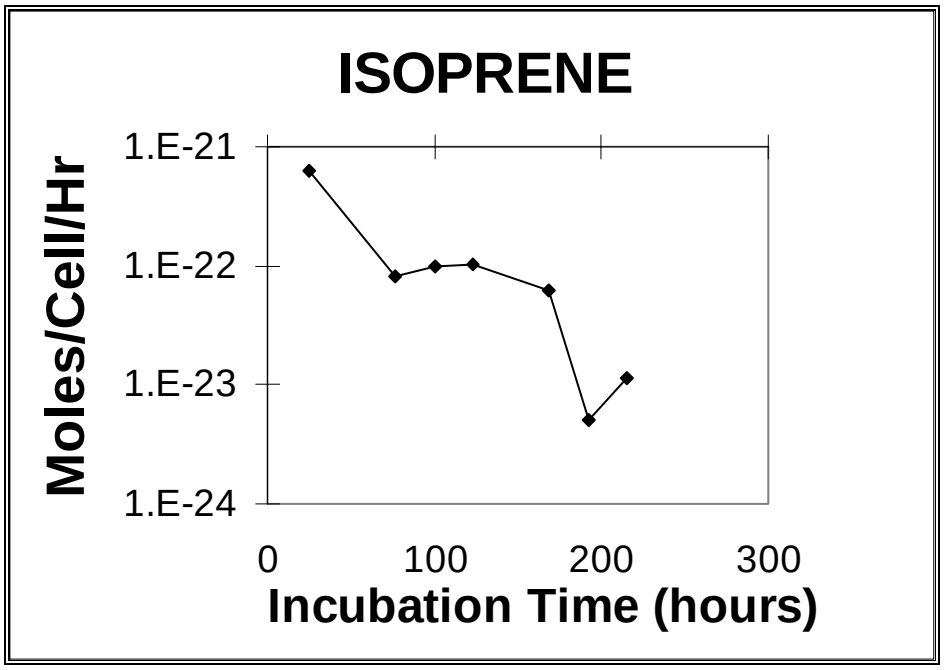

Figure D3: Isoprene Production with 3500 ppm CO_2 in Purge Air A *Prochloroccus* axenic MED4 strain was used for this experiment. Note that the high production rate at hour 26 is due to incomplete initial purging of the vessel before inoculation (see Section 2.3).

situ conditions, and we had no trouble obtaining consistent cellular growth sufficient for our purposes with either case. Additionally, all measurements used in subsequent analyses were taken from the pre-limited, exponential growth period. Thus, the nature of the limiting nutrient should be irrelevant.

D.2 ISOPRENE PRODUCTION BY EUKARYOTIC PHYTOPLANKTON

Figure D4 is referred to in Chapter 3, section 3.3.

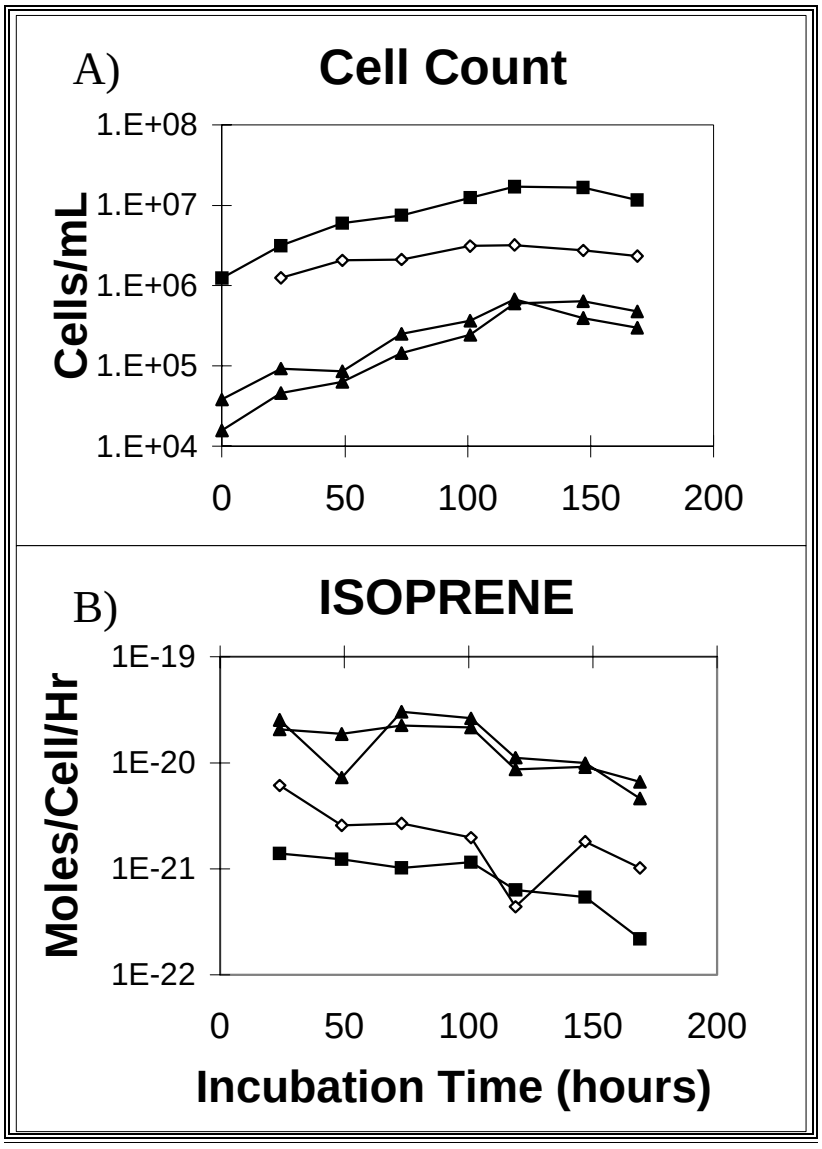

Figure D4: Isoprene Production by Eukaryotic Phytoplankton A) Cells mL^{-1} for four individual phytoplankton incubations. Filled squares represent *Micromonas pusilla*, open diamonds represent *Pelagomonas calceolata*, and filled triangles represent *Emiliania huxleyi*. B) Corresponding isoprene production in moles $cell^{-1}$ hr^{-1}.

D.3 EFFECT OF BACTERIA ON PHYTOPLANKTONIC ISOPRENE PRODUCTION

Isoprene production by phytoplankton occurs at statistically the same rates whether or not contaminant bacteria are present in the culture. Figure D5 is referred to in Chapter 3, Section 3.3.

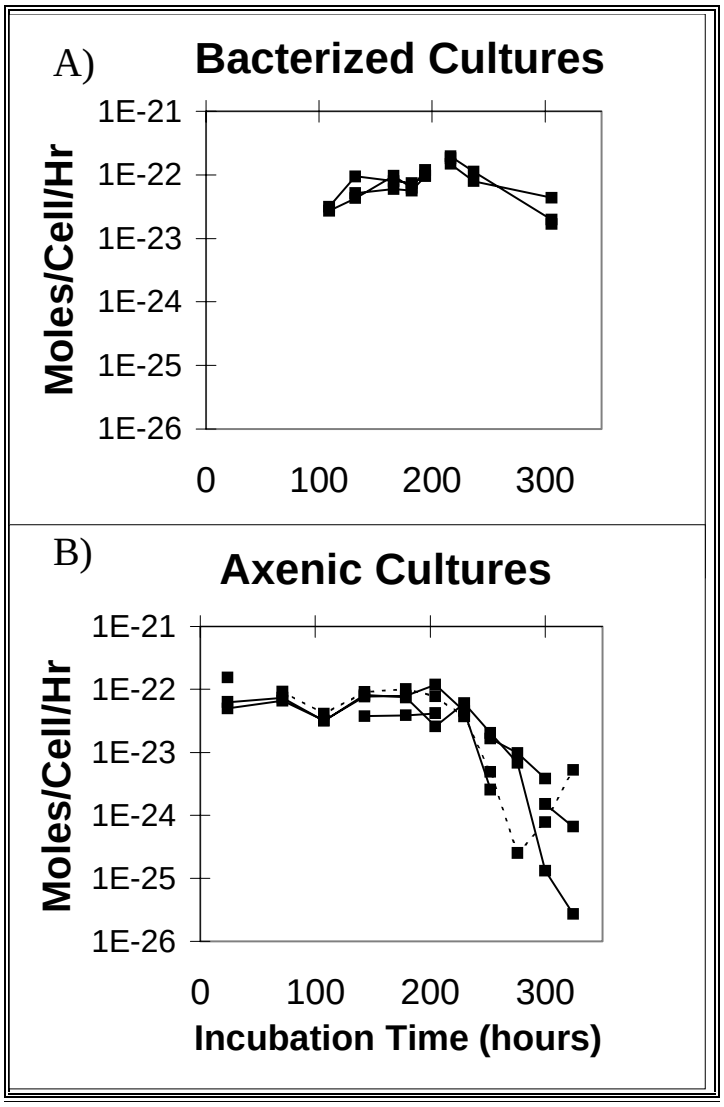

Figure D5: Bacterial Effect on Isoprene Production A) Isoprene production in moles cell^{-1} hour^{-1} in three replicate bacterized *Prochlorococcus* strain MIT 9401 incubations. All data shown in this panel is from the exponential phase of cell growth. B) Isoprene production in four originally replicate axenic *Prochlorococcus* strain MED4 incubations. The stationary phase of cell growth in this experiment was reached at approximately hour 250. Although x-axes have the same range, the data in the two separate panels are from separate experiments, done several months apart. Note that the incubation marked with a dotted line became bacterized at approximately hour 100. There is no difference between this incubation and the three axenic incubations throughout exponential and most of the senescent phase.

D.4 ISOPRENE PRODUCTION AND CELL GROWTH RATE

The rate of isoprene production by *Prochlorococcus* increased with increasing cell growth rate when the cells were grown under light-limited irradiances. Additionally, there appears to be a relationship between isoprene production rate and growth rate over the temperature range examined. These isoprene production rates are re-plotted versus growth rate in Figure D6, along with similar data from other experiments in this work.

The data from the temperature variation experiment (filled squares) shows indications of a positive linear relationship between isoprene production rate and cell growth rate despite the limited data points. Rates of all enzymatically-dependent cellular processes (which includes both of these) increase as temperature increases due to Arrhenius kinetics, so this general relationship is expected. The data from the light-limited regime of the light variation experiment (open squares) and other assorted experiments (see Figure D6) also exhibit a positive linear trend of increasing isoprene production rate with increasing growth rate, except for the point at 0.34 day^{-1}. However, when data from both the temperature and light variation experiments (e.g. all points in Figure D6) are lumped into one dataset, the point do not fit neatly to a single linear regression.

Changes in cell growth irradiance induce many intracellular changes in photosynthetic organisms, some of the most obvious being ATP (energy) and NADPH (reductant) content. However the relationship of irradiance to ATP and NADPH is a complex one. Isoprene production in terrestrial plants has been shown to be linked to photosynthetic electron transport, and requires both ATP and NADPH, although temporary production can continue even when there is no instantaneous net carbon assimilation (Monson & Fall, 1991; Loreto & Sharkey, 1990). The complex relationships between these photosynthetic parameters and cell growth and isoprene rates is in contrast to the straightforward relationships of cell growth and isoprene rate with temperature, and might imply that we would not expect to see the two groups of data in Figure D6 lie on a single line.

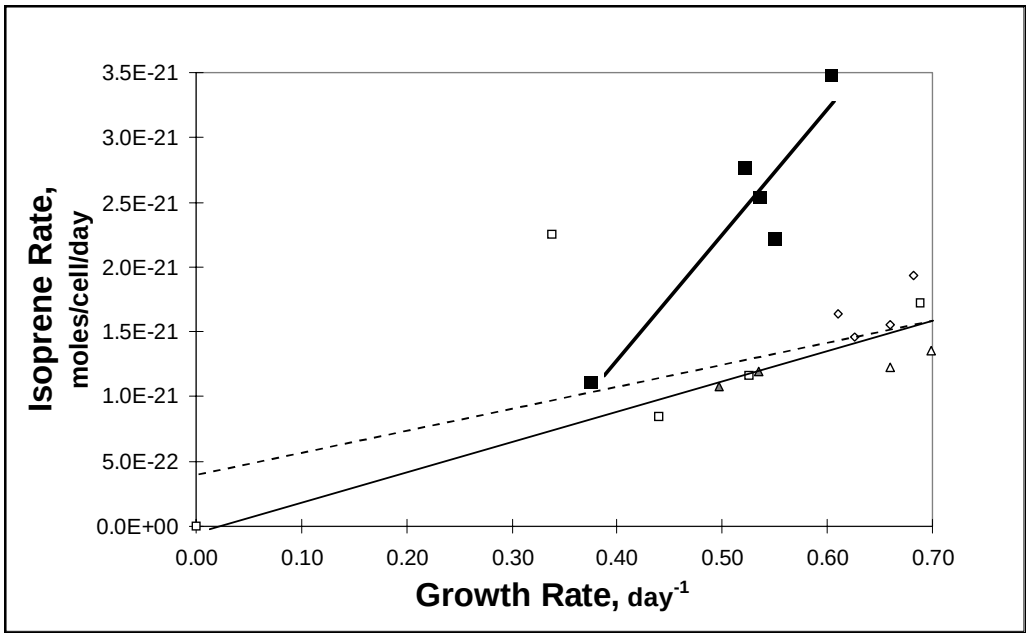

Figure D6: Isoprene Production and Cell Growth Rate Isoprene production rate in moles cell $^{-1}$ day $^{-1}$ from the exponential growth phase versus axenic *Prochlorococcus* MED4 growth rate, in day $^{-1}$, for a variety of experiments: filled squares - temperature variation experiment (all grown at 110 ± 10 μE m^{-2} s^{-1}), open squares - light variation experiment (includes all points in light-limited and light-saturated regimes, < 146 μE m^{-2} s^{-1}), open diamonds - from other MED4 experiments (all grown at 90 ± 5 μE m^{-2} s^{-1}), open triangles - reference cultures from grazing experiment (both grown at 87 μE m^{-2} s^{-1}), filled triangles - reference cultures from phage experiment (both grown at 95 μE m^{-2} s^{-1}). All cultures except those in the temperature variation experiment were grown at 23 °C. Linear regressions are shown for temperature experiment data (thick solid line), light experiment data with (dotted line), and light experiment data without (solid line) the point at 0.34 day^{-1}.

This phenomena implies that growth rate is not a better proxy to use for predicting isoprene production than cell count because both are function of at least light and temperature.

D.5 CELLULAR PARAMETERS OF PHAGE-INFECTED *PROCHLOROCOCCUS*

In Chapter 4 we report results from a culture of *Prochlorococcus* that was infected with a phage. Presented here are additional observations of the flow cytometric cellular parameters detected from this experiment (see Chapter 4.3.4).

We observed a distinct 'rain' pattern on the flow cytometric plots different from that of nutrient-limited senescing cells. For the latter, cellular chlorophyll fluorescence decreased, but the particle size did not change. For the phage-infected cells, both cellular chlorophyll fluorescence and size decreased. Chlorophyll fluorescence per cell steadily decreased during infection (Figure D7A). It increased again at and after hour 91 in one infected culture; this may signify regrowth of a *Prochlorococcus* population. Cellular chlorophyll-a content was also smaller at hour 78 for infected cells (0.4 fg cell^{-1}) as compared to healthy cells (0.9 fg cell^{-1}). Flow cytometric forward scatter intensity (FSC; Figure D7B) was not significantly different between the incubations, and flow cytometric side scatter intensity (SSC; Figure D7C) in infected cells dropped as compared to healthy cells. The exception for both FSC and SSC is the increase at and after hour 91.

Other researchers have reported similar types of changes in flow cytometric parameters due to phage infection (Brussard et al., 1999). However, our results are not conclusive as theirs are. Brussard et al. (1999) suggest SSC should be altered with infection, and also saw increased FSC which they attributed to cell 'swelling' due to phage content (as dying cells tend to have reduced FSC). We did not see a clear FSC increase in the infected *Prochlorococcus* population.

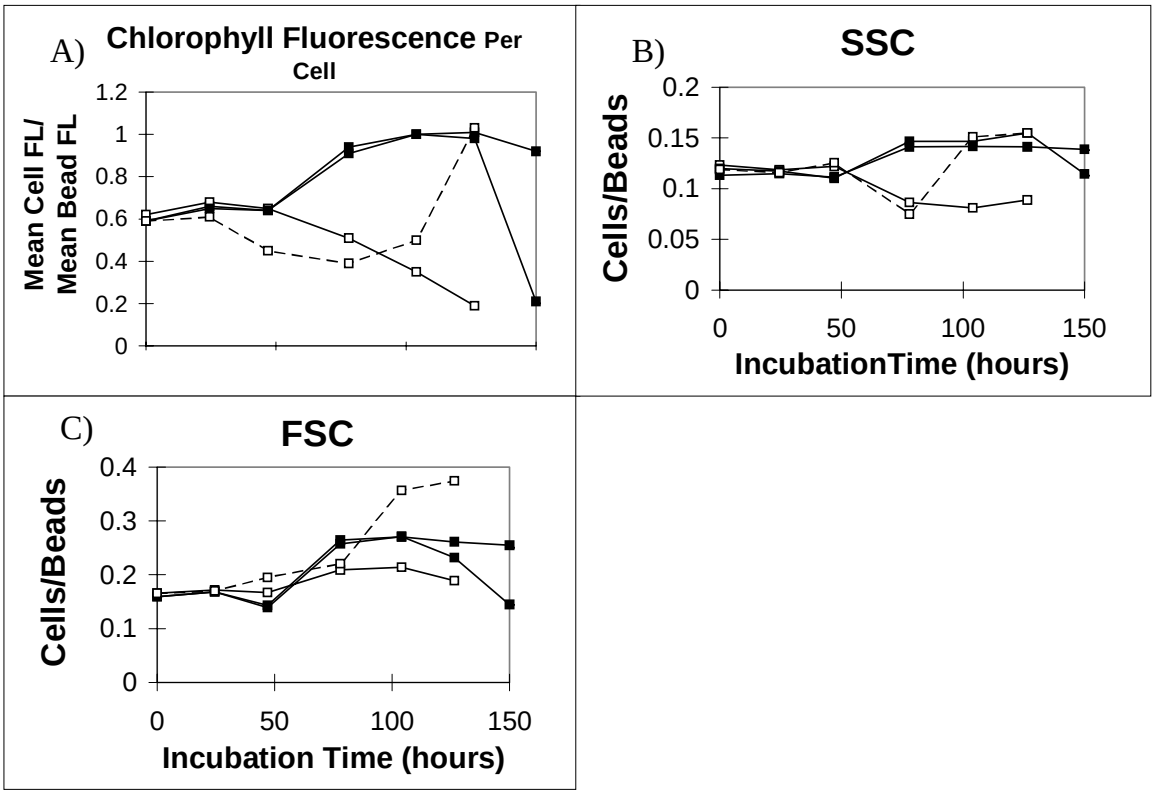

Figure D7: Cellular Parameters Due to Phage Infection A) Mean chlorophyll fluorescence per cell for the *Prochlorococcus* population. B) Mean side scatter intensity (SSC) for the same population. C) Mean forward scatter intensity (FSC) for the same population. Symbols represent various *Prochlorococcus* control and phage-infected cultures as described in Figure 19 (Chapter 4).

D.6 UVB EFFECT ON NMHC PRODUCTION BY *PROCHLOROCOCCUS*

Simply making more potential NMHC precursor available in the form of cell membrane fragments and released cytoplasmic materials did not appear to affect NMHC (see Chapter 4.3.5). To determine if photochemistry is also necessary for non-isoprene NMHC production in our biological incubations, cultures of both healthy and phage-infected *Prochlorococcus* were exposed to UVB light.

This experiment was intended only as a quick check of possible UVB-induced effects. Thus we did not establish a full experiment with multiple controls. Instead, we chose to simply compare the same incubation flask before and after irradiation. As isoprene production per cell is constant during exponential growth (see Chapter 3; with ± 1σ of ~ 30% for a single flask), if all samples are taken during that time period and we see an isoprene production rate after UVB irradiation that is significantly different from the pre-irradiation rate, we can attribute the difference to UVB. Previous experiments have shown production rates of other NMHC to be quite variable, often centered around zero over the exponential phase of cell growth. If all samples are taken during that time period, an average and standard deviation of these pre-irradiation data are calculated, and we see an isoprene production rate after UVB irradiation that is significantly different from the pre-irradiation rate, it is not unreasonable to potentially attribute the difference to UVB. However, we may not be capturing the true variability of NMHC production rates by only compiling three points. The best determination of whether or not UVB affects NMHC is through a more complete experimental design.

Samples were taken daily for three days to establish a "steady state" pre-irradiation NMHC production rate. For isoprene, this is the constant cell-normalized rate typical of exponential phase. For the alkanes and other alkenes, represented by ethane and ethene respectively, this allows the determination of a pre-irradiation production rate (moles mL^{-1} $hour^{-1}$) that is the average of those three samples. (An example of "steady state" production for ethane is

plotted in Figure D8B.) Conditions on the fourth day (sampled at hour 106) were identical as for the first three days except that the flasks were exposed to UVB light for either the last 5 or 30 minutes of the incubation period, just before sampling. This allowed potential NMHC precursors to accumulate for ~ 28 hours since the last sampling time. UVB irradiations were performed by exposing incubation flasks (pre-UVB irradiation at 35 $\mu E\ m^{-2}\ s^{-1}$) to the artificial light from a transilluminator with an emission peak at 312 nm (FOTO/UV 300, Fotodyne, Inc.) for 5, 30, or 60 minutes.

Microscopic observations with phase-contrast illumination (Zeiss Axiscope 2; Carl Zeiss, Inc.) demonstrated that five minutes of UVB exposure morphologically stressed the cells, resulting in elongation of their typical near-spherical shape. 30 minutes of UVB appeared to cause serious damage, resulting in smaller, shriveled cells whose populations subsequently collapsed within a day. Cell counts increased slightly in all incubations after UVB irradiation (Figure D8A); we currently have no explanation for this. Ethane and ethene production rates (Figure D8B, D8D) increased dramatically after either 5 (closed squares) or 30 minutes (open squares) of UVB irradiation on hour 106. In all cases the 'steady state' production changed from a net negative rate (e.g. higher in the media blank than the Prochlorococcus culture) to a net positive rate. The ethane increase is far greater than the pre-irradiation values for the *Prochlorococcus* cultures exposed to 5 and 30 minutes of UVB (e.g. ±78% for the example in Figure D8B), but not for the phage-infected culture. The ethene increase is far greater than the pre-irradiation value for the 5 minute *Prochlorococcus* culture only (Figure D8D). Isoprene production per cell decreased by approximately 50% (Figure D8C) after both the 5 and 30 minute exposures. This is greater than the pre-irradiation value. Isoprene production decreases during the latent period between infection and complete culture lysis as expected, but after UVB exposure it decreases further to a net negative rate.

A second exposure of 60 minutes was allowed for all flasks at the end of the next incubation period (hour 145). Ethane production dropped in all cases. Ethene production in the

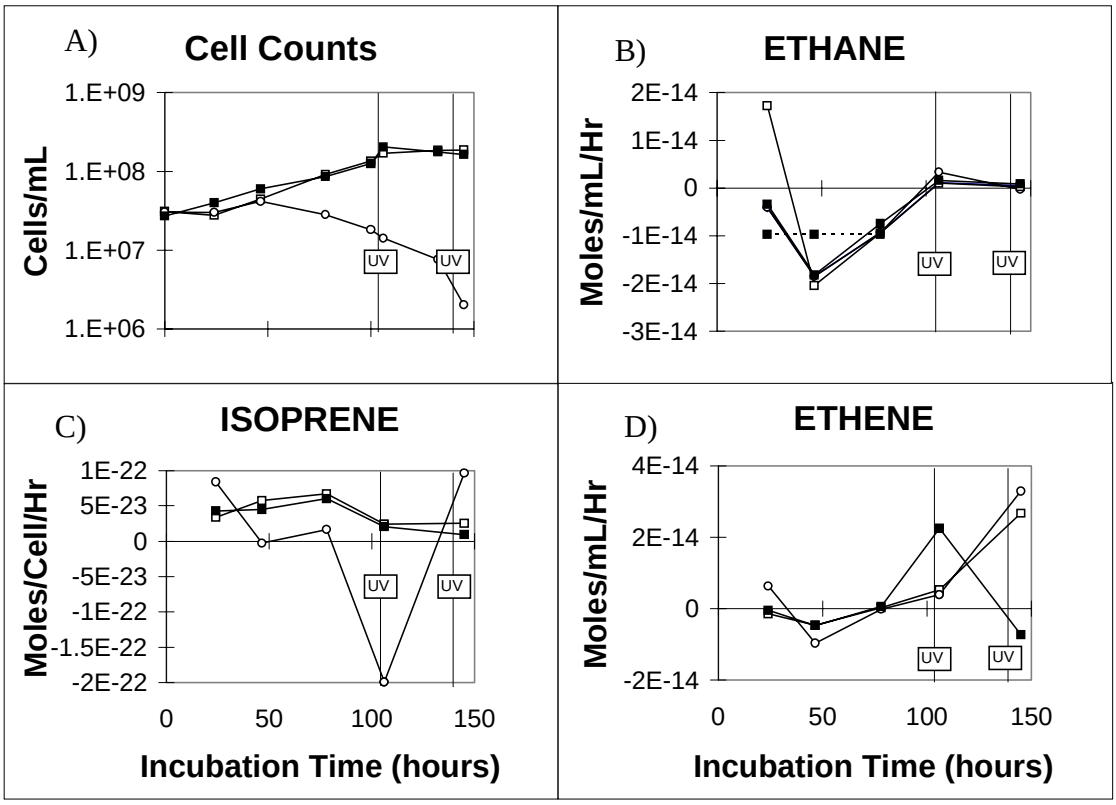

Figure D8. NMHC production rates as a function of time (B-D) over the growth cycle, in cells mL^{-1} (A). Filled squares represent *Prochlorococcus* undergoing a 5 minute UV-B exposure, open squares represent *Prochlorococcus* undergoing a 30 minute UV-B exposure, and open circles represent the phage-infected *Prochlorococcus* undergoing a 5 minute UV-B exposure, all at hour 106. A second irradiation was performed at hour 145, with all three cultures undergoing a 60 minute exposure. Lines labeled "UV" denote times of irradiation. The horizontal dotted line in panel B identifies an example of 'steadystate' production rate for ethane in the 30 minute UV-B exposure (at hour 106) *Prochlorococcus* incubation (filled squares).

phage-infected and one *Prochlorococcus*-only culture (open circles and open squares) increased more than for the 5 minute incubations on the previous day. Ethene production in the other *Prochlorococcus* culture (closed squares) dropped to a net negative rate. Isoprene (closed squares) dropped just slightly in the *Prochlorococcus* cultures, and returned to a small net positive rate in the infected culture. The ethane increase is far greater than the pre-irradiation values for the *Prochlorococcus* cultures exposed to 5 and 30 minutes of UVB, but not for the phage-infected culture. The ethene increase is far greater than the pre-irradiation values for the 5 minute irradiated *Prochlorococcus* culture and the phage-

infected culture, but not for the 30 minute irradiated *Prochlorococcus* culture. Total isoprene decreases for both irradiations, and the change is greater than the pre-irradiation values.

We define a UVB enhancement factor as the ratio of NMHC production rate (moles mL^{-1} $hour^{-1}$) after UVB exposure to the absolute value of the "steadystate" production rate (moles mL^{-1} $hour^{-1}$). Table D1 presents these UVB enhancement factors for the alkenes, as well as the ratios of these factors for the phage-infected and healthy cultures. The latter ratios represent any additional enhancement of NMHC production rate due to liberation of cytoplasmic or cell wall material by lysis.

Table D1: UV-B Enhancement Factors for Indicated UVB Exposure Times

Culture	**Irradiation Time (minutes)**	**Ethane**	**Propene**	**2-Methyl Propene**
***Prochlorococcus* UV-B Enhancement**	5	256	975	72
	30	1074	8850	868
(Phage-Infected *Pro.* UV-B Enhancement)/ (*Prochlorococcus* UV-B Enhancement)	5	134	24	235
	30	306	67	195

Enhancement factors are defined as in the text. For example, the *Prochlorococcus* incubation exposed to 30 minutes of UV-B produced 8850 times more propene than during its 'steadystate' period. The phage-infected *Prochlorococcus* incubation exposed to 30 minutes of UV-B produced 67 times as much propene as the *Prochlorococcus* incubation exposed to 30 minutes of UV-B, or 67*8850 times as much propene as the *Prochlorococcus* incubation in its 'steadystate' period.

In summary, when the *Prochlorococcus* incubations were exposed to UVB for varying lengths of time, the alkane and non-isoprene alkene production rates increased from net negative to net positive values. This is potentially due to photochemical transformations of

dissolved organic carbon (DOC) from phytoplankton as others have previously shown (Wilson, 1970; Lee & Baker, 1992; Ratte et al., 1993, 1998; Reimer et al., 2000). However, there was not a "no UVB" control in this experiment so we can not be sure that the irradiation was the source of the production rate differences. When cultures of phage-infected *Prochlorococcus* were exposed to UVB, enhanced NMHC production rates were seen, similar in magnitude to those in the healthy *Prochlorococcus* cultures exposed to UVB. This may imply that phage lysis does not change the amount of NMHC precursors available for photochemical production of NMHC, if this indeed is the process that is occuring. Isoprene production per cell dropped by ~ 50% after UVB exposure; this could be due to internal cellular damage (Buma et al., 1996). Harley et al. (1996) found no change in biomass-normalized isoprene production from several tree species when they were exposed to elevated UVB-B simulating 30% ozone depletion, but leaf morphologies were modified such that the leaves had higher mass densities.

65. The Production of Non-Methane Hydrocarbons by Marine Plankton, *S. Shaw, 9/01*

65. Optimal Determination of Global Tropospheric OH Concentrations Using Multiple Trace Gases, *J. Huang, 1/00*

64. Measurement and Deduction of Emissions of Short-lived Atmospheric Organo-chlorine Compounds, *G. Kleiman, 9/99*

63. Construction of the Adjoint MIT Ocean GCM and Application to Atlantic Heat Transport Sensitivity, *J. Marotzke et al., 5/99*

62. Terrestrial Sources and Sinks of Atmospheric Methyl Bromide: 3D Modeling of Tropospheric Abundance and Sensitivities, *C. Jensen, 4/99*

61. Inverse Modeling of Seasonal Variations in the North Atlantic Ocean, *L. Yu & P. Malanotte-Rizzoli, 8/98*

60. Interhemispheric Thermohaline Circulation in a Coupled Box Model, *J. Scott, J. Marotzke & P. Stone, 7/98*

59. Seasonal Measurements of Nonmethane Hydrocarbons in a Sub-tropical Evergreen Forest in Southern China, *J. Graham, 7/98*

58. Temporal Changes in Eddy Energy of the Oceans, *D. Stammer & C. Wunsch, 6/98*

57. On Convective Mixing and the Thermohaline Circulation, *J. Marotzke, 6/98*

56. The Importance of Open-Boundary Estimation for an Indian Ocean GCM-Data Synthesis, *Q. Zhang & J. Marotzke, 5/98*

55. Boundary Mixing and Equatorially Asymmetric Thermohaline Circulation, *J. Marotzke & B.A. Klinger, 4/98*

54. Impact of the Horizontal Wind Profile on the Convective Transport of Chemical Species, *C. Wang & R. Prinn, 3/98*

53. Adjusting to Policy Expectations in Climate Change Modeling, *S. Shackley, J. Risbey, P. Stone & B. Wynne, 3/98*

52. Open-Ocean Convection: Observations, Theory and Models, *J. Marshall & F. Schott, 1/98*

51. Global Thermohaline Circulation: Parts I and II, *X. Wang, P. Stone & J. Marotzke, 10/97*

50. Destabilization of the Thermohaline Circulation by Atmospheric Transports: An Analytic Solution, *Y. Krasovskiy & P. Stone, 7/97*

49. The Global Ocean Circulation Estimated from TOPEX/POSEIDON Altimetry and the MIT GCM, *D. Stammer, et al., 7/97*

48. Trapped Methane Volume and Potential Effects on Methane Ebullition in a Northern Peatland, *E. Fechner-Levy & H. Hemond, 5/97*

47. Seasonal Cycles of Meridional Overturning and Heat Transport of the Indian Ocean, *T. Lee & J. Marotzke, 3/97*

46. Analysis of the North Atlantic Climatologies Using a Combined OGCM/Adjoint Approach, *L. Yu & P. Malanotte-Rizzoli, 12/96*

45. Tracer Applications of Anthropogenic Iodine-129 in the North Atlantic Ocean, *H.N. Edmonds, 11/96*

44. Boundary Mixing and the Dynamics of 3-Dimensional Thermohaline Circulations, *J. Marotzke, 8/96*

43. The Role of Aerosols in the Troposphere: Radiative Forcing, Model Response, and Uncertainty Analysis, *W. Pan, 5/96*

42. Development of a 3D chemical transport model based on observed winds and use in inverse modeling of $CFCl_3F$ sources, *N. Mahowald, 4/96*

41. The Role of Vegetation in the Dynamics of West African Monsoons, *X. Zheng & E. Eltahir, 3/96*

40. Inferring meridional mass and heat transports of the Indian Ocean by fitting a GCM to climatological data, *T. Lee & J. Marotzke, 2/96*

39. Analysis of Thermohaline Feedbacks, *J. Marotzke, 12/95*

38. The Iron Hypothesis: Basic Research Meets Environmental Policy, *S.W. Chisholm, 12/95*

37. Hydrostatic, Quasi-Hydrostatic and Non-Hydrostatic Ocean Modeling, *J. Marshall, C. Hill, L. Perelman & A. Adcroft, 9/95*

36. A Finite-Volume, Incompressible Navier Stokes Model for Studies of the Ocean on Parallel Computers, *J. Marshall, et al., 9/95*

Copies are available by request from the Center office. See inside front cover for contact numbers.

35. A Case Study of the Adequacy of GCM Simulations for Assessing Regional Climate Changes, *J. Risbey & P. Stone, 3/95*

34. On the Role of Vegetation in Sustaining Large Scale Atmospheric Circulations in the Tropics, *E. Eltahir, 2/95*

33. Sprites, Q-Bursts and Positive Ground Strokes, *D. Boccippio, E. Williams, et al., 2/95*

32. Subduction of Carbon in the Subtropical Gyre of the North Atlantic, *M. Follows, R. Williams & J.C. Marshall, 10/94*

31. The Growth of Convective Plumes at Seafloor Hot Springs, *K. Speer & J. Marshall, 10/94*

30. The CMPO/MIT TOPEX/POSEIDON Altimetric Data Set, *C. King, D. Stammer & C.I. Wunsch, 8/94*

29. Atmospheric transports, the thermohaline circulation, and flux adjustments in a simple coupled model, *J. Marotzke & P. Stone, 4/94*

28. Climate Dynamics and Global Change, *R. Lindzen, 3/94*

27. Effects of Atmospheric Coupling on the Stability of the Thermohaline Circulation, *M. Nakamura, P. Stone & J Marotzke, 1/94*

26. Poleward Heat Transport in a Barotropic Ocean Model, *X. Wang, P.H. Stone & J. Marotzke, 12/93*

25. An EPV view of the zonal mean distribution of temperature and wind in the extra-tropical troposphere, *D. Sun & R. Lindzen, 12/93*

24. Laboratory Experiments of Chemical Reactions on Polar Stratospheric Cloud Particles, *K. Beyer, 11/93*

23. A Model of the Ion Chemistry of Electrified Convection, *R. Boldi, 5/93*

22. Destabilization of the Thermohaline Circulation by Atmospheric Feedback, *M. Nakamura, P.H. Stone & J. Marotzke, 3/93*

21. Global Circuit Response to Seasonal Variations in Global Surface Air Temperature, *E. Williams, 3/93*

20. Precipitation Recycling in the Amazon Basin, *E. Eltahir & R.L. Bras, 1/93*

19. On the Response of the Tropical Atmosphere to Large-Scale Deforestation, *E. Eltahir & R.L. Bras, 1/93*

18. On the feasibility of determining surface emissions of trace gases using an inverse method in a 3D transport model, *D. Hartley & R. Prinn, 11/92*

17. Deducing Trace Gas Emissions Using an Inverse Method in 3D Chemical Transport Models, *D. Hartley, 11/92*

16. An Active Titration Method for the Local Measurement of Tropospheric Hydroxyl Radical, *M. Sprengnether, 10/92*

15. A description of rainfall interception over large areas, & On the estimation of the coverage of rainfall in climate models, *E. Eltahir & R. Bras, 8/92*

14. The Schumann Resonance: A Global Tropical Thermometer, *E. Williams, 5/92*

13. The heterogeneous reaction HOCl $\rightarrow$ HCl_2 + H_2O on ice and nitric acid trihydrate, *J. Abbatt & M.J. Molina, 4/92*

12. Forecast Cloudy: The Limits of Global Warming Models, *Peter H. Stone, 3/92*

11. The implementation and validation of improved landsurface hydrology in an atmospheric GCM, *K. Johnson et al., 2/92*

10. Inferring the Annual-mean Subduction Rate Over the North Atlantic, *J.C. Marshall, A.J.G. Nurser & R.G. Williams, 1/92*

9. The Role of Ice in the Conditional Instability of the Tropical Atmosphere, *E. Williams & N. Renno, 11/91*

8. Nonmethane Hydrocarbon Chemistry in the Remote Marine Atmosphere, *N. Donahue, 7/91*

7. Global-Scale Sea Surface Variability from Combined Altimetric and Tide Gauge Measurements, *C.I. Wunsch, 1/91*

5/6. Non-linear dynamics of soil moisture at climate scales: Stochastic and chaotic analyses, *I. Rodriguez-Iturbe, D. Entekhabi & R. Bras, 11/90*

4. Atmospheric emissions and trends of nitrous oxide deduced from ten years of ALE-GAGE data, *R. Prinn, et al., 6/90*

3. A Scheme for Representing Cumulus Convection in Large-Scale Models, *K.A. Emanuel, 4/90*

2. On the Limitations of General Circulation Climate Models, *P.H. Stone & J. Risbey, 3/90*

1. An Annotated Bibliography on Greenhouse Effect Change, *M. Handel & J. Risbey, 4/92*

Copies are available by request from the Center office. See inside front cover for contact numbers.